NONLINEAR QUANTUM COSMOLOGY

MEER ASHWINKUMAR MUHYIDIN BIN MEER AHMAD

B.Sc.(Hons.)(Malaya)

A THESIS SUBMITTED

FOR THE DEGREE OF MASTER OF

SCIENCE

DEPARTMENT OF PHYSICS

NATIONAL UNIVERSITY OF SINGAPORE

2012

DECLARATION

I hereby declare that this thesis is my original work and it has been written by me in its entirety. I have duly acknowledged all the sources of information which have been used in the thesis.

This thesis has also not been submitted for any degree in any university previously.

.....

Meer Ashwinkumar Muhyidin bin Meer Ahmad

31st May 2012

Acknowledgements

I would like to thank my supervisor Dr. Rajesh Parwani for his guidance and mentorship throughout the duration of this research project, I have learnt a great deal in a wide range of fields as a result of undertaking this study under his able supervision.

I would also like to thank my mother Dr. Indra Sinnadurai, for her loving support and care, always a pillar of strength and a source of determination, never failing to raise my spirits in the toughest of times.

Finally, I would like to thank my family and friends who have supported me in one way or another. Thank you all.

Contents

Abstract

Quantum cosmology intends to explain our universe by imbibing our current, general relativistic ideas of cosmology with quantum theory, which is understood to be fundamental. One of the most important reasons for this is to explain our universe at time $t = 0$, at which quantum effects are expected to be large, and at which singularities occur for matter filled universes. However quantum cosmology, based on a canonical quantum formulation of general relativity, does not solve all singularities via the Wheeler-DeWitt equation. In order to model the fundamental theory of quantum gravity, whatever it may be, we resort to information-theoretic nonlinearisations of the Wheeler-DeWitt equation, in hope that the problem of singularities can be resolved. This work is divided into two parts. The first part is an extension of a previous work which studied the nonlinear Wheeler-DeWitt equation for a de Sitter universe, non-pertubatively. The generalisation here is that the cosmological constant is now a function of the scale factor. We find results similar to the previous study including a minimum and maximum size to the universe, in some cases further implying a cyclic universe via the effective classical dynamics. The second part is a non-pertubative study of the FLRW-ϕ universe, in which the only matter is a free massless scalar field, which can be used as an internal clock. The Wheeler-DeWitt equation is now used to describe the evolution of a wavepacket, and bounces at small and large sizes were found, leading to cyclic-type evolution, which is however not periodic nor everlasting.

List of Figures

List of Symbols

1. a - Modified scale factor
2. ψ - Wavefunction of the universe in minisuperspace
3. p - Probability density distribution
4. Λ - Cosmological constant
5. α - Logarithmic modified scale factor
6. ϕ - Scalar field
7. m - Parameter modulating variation of cosmological constant
8. L - Nonlinear length parameter
9. η - Nonlinear regularization parameter
10. $\zeta = \eta L$ - Lattice spacing/nonlinear parameter
11. $F(p)$ - Information theoretic nonlinearity

Chapter 1

Introduction

The subject of cosmology is in some sense one of the oldest known to man, never failing to leave in a state of astonishment the imaginations of both philosophers and scientists alike, throughout time. In its modern form, much of cosmology as we know it is based on Einstein's theory of general relativity, with the most important development being the Big Bang theory which postulated that the Universe expanded from an extremely hot and dense state, which appeared approximately 13.8 billion years ago; and continues to expand today. In recent years, the Lambda-Cold Dark Matter (Λ-CDM) model of the universe has come to be accepted as the standard model of Big Bang cosmology, incorporating an inflationary epoch, cold dark matter, and accelerating expansion, all of which are necessary to corroborate modern experimental evidence.

However, as versatile as it is in explaining various phenomena, the Λ-CDM model is still not complete in the sense that there are still some unsolved problems, which require us to look for a more fundamental and holistic theory; that is, of quantum cosmology. Even without these problems, the necessity for a quantum theory of cosmology would not be precluded, since it is the general belief of modern physics that nature is intrinsically quantum in its behaviour.

One of the most important questions left unanswered by all general relativistic

models of cosmology is that of the singularity of curvature invariants at the beginning of time, $t = 0$. This singularity arises as a consequence of having all the mass and energy of the universe at a single point, which is the point of infinite density known as the Big Bang. In fact, classical cosmology is inadequate in explaining our universe before the Planck time (10^{-44} seconds after the Big Bang), at which the universe was no larger than 10^{-35} m, with energies of the order 10^{19} GeV. At such scales, at which the Compton wavelength of a particle is approximately equal to its Schwarzschild radius [1], it would be difficult not to expect quantum effects to come into play, and quantum cosmology is expected to either properly explain this epoch, or do away with it altogether.

Many potential theories of quantum gravity have emerged in recent years, the main contenders being string theory and loop quantum gravity, together with many other potential theories such as Regge calculus, causal sets and topological quantization. Quantum cosmology however does not attempt to answer the question of what the fundamental theory of quantum gravity is, but rather relies on a canonical quantum formalism based on general relativity alone. The assumption in doing this is that whatever the exact fundamental theory of quantum gravity is, in its semiclassical limit it should agree with the semiclassical limit of the canonical quantum formalism based only on general relativity [1].

The defining equation of quantum cosmology is the Wheeler-DeWitt equation, which is obtained by directly quantizing Einstein's equations. However, in order to model the actual fundamental theory of spacetime, we shall resort to nonlinearising this equation. This is based on the idea that at small scales and high energies (as in our early universe), it is possible that quantum mechanics itself will change, and may not be a linear theory anymore. However, many different types of nonlinear quantum mechanics exist in the literature, and as such we must choose one which is best suited to quantum cosmology.

We shall choose to use information theoretically motivated nonlinearities, devel-

oped by Parwani [2]. The nonlinear equations we shall work with are derived via the maximum entropy/uncertainty principle, in a manner similar to how the canonical probability distribution is derived via the Gibbs-Shannon entropy in statistical mechanics. Such a method provides the most unbiased description of the system, since maximising the uncertainty measure acknowledges our ignorance of a more detailed structure [2], and which is appropriate in our case since our knowledge of physics at small scales is limited. Our subject of nonlinear quantum cosmology is thus concerned with solving information theoretically motivated nonlinear Wheeler-DeWitt equations.

In this thesis we shall generalise and extend on previous research in this field. Parwani and Nguyen [3] first studied the nonlinear Wheeler-DeWitt equation pertubatively, for a spatially flat, empty Friedmann-Lemaître-Robertson-Walker (FLRW) universe with a cosmological constant (also known as a de Sitter or FLRW-Λ universe) as well as for a spatially flat FLRW universe in which the only matter is a free massless scalar field (also known as a FLRW-ϕ universe), while Parwani and Tarih [4] studied the de Sitter universe via non-pertubative numerical methods.

In the first part of this work we shall generalise the non-pertubative study of a de Sitter universe to one where the cosmological constant varies slowly as a function of the scale factor. As we shall see, we find universes with minimum and maximum allowed sizes, which in some cases are proven to be cyclic universes. In the second part, we study the spatially flat FLRW-ϕ universe non-pertubatively. We treat the scalar field as an intrinsic time variable, enabling us to approximately understand the dynamics of this universe. We find different cyclic-type evolutions for different nonlinear parameter values, with bounces at small and large size in some instances. However, we do not see periodic nor everlasting cycles. As we shall see, in all these evolutions the universe begins and ends at a finite size, without ever reaching zero size at which a singularity would occur.

Chapter 2

Review on Classical Cosmology

In this chapter we shall briefly recapitulate the main ideas of general relativistic cosmology that will be used in our study of nonlinear quantum cosmology.

One of the basic assumptions of physical cosmology is that of the cosmological principle, which states that we do not occupy any special or privileged location in the universe. The physical consequences of this principle is that our universe is isotropic (meaning that it appears the same to us regardless of the direction in which we look) and homogeneous (it is identical at every point). Observationally, we find both of these requirements to be true at scales of more than a 100 million light years.

As noted previously, our universe is expanding, and does so according to Hubble's law, which says that the velocity, v at which interstellar bodies move away from Earth is directly proportional to their proper distance from us, d, or

$$v = Hd, \tag{2.1}$$

where H is the Hubble parameter, which is in general a function of time, t.

The proper distance is also a function of time, since the universe is expanding. It is however customary to use comoving coordinates in the study of physical cosmology. Comoving coordinates are coordinates that are independent of the expansion (and

thus independent of time), and to find the actual proper distance, $d(t)$ between any two points, we use

$$d(t) = a(t)\chi, \tag{2.2}$$

in which χ is the comoving distance, and $a(t)$ is the scale factor. The scale factor here is a measure of the expansion of the universe, and as such is a function of time.

In studying physical cosmology we have to resort to the laws of general relativity, which define gravitation as the curvature of spacetime occurring due to the presence of a certain mass-energy density distribution. This relationship is represented using the Einstein field equations, a set of 10 nonlinear partial differential equations, written succinctly as

$$R_{\mu\nu} - \frac{1}{2}g_{\mu\nu}R + g_{\mu\nu}\Lambda = \frac{8\pi G}{c^4}T_{\mu\nu}. \tag{2.3}$$

The left hand side of this equation contains information about the local geometry, or curvature, of a spacetime, in which $R_{\mu\nu}$ is the Ricci curvature tensor, R is the scalar curvature, $g_{\mu\nu}$ is the metric tensor and Λ is the cosmological constant. The right hand side contains information about the matter and energy content in the same spacetime via the energy-momentum tensor $T_{\mu\nu}$. The constant of proportionality contains G which is Newton's gravitational constant, and c which is the speed of light.

The entire local geometry of the spacetime is in fact encoded within the metric tensor, $g_{\mu\nu}$, since we can use it to obtain the Ricci curvature tensor, from which we can then obtain the scalar curvature. Thus, in order to study any spacetime we merely need to specify the metric tensor of that spacetime and the energy-momentum tensor of the mass-energy density within it. The metric tensor is related to the separation in between events, or points in spacetime (the line element), via

$$ds^2 = g_{\mu\nu}dx^\mu dx^\nu. \tag{2.4}$$

The local geometry of a homogeneous and isotropic universe can be represented

by the Friedmann-Lemaître-Robertson-Walker (FLRW) line element,

$$ds^2 = -c^2N^2dt^2 + a^2(t)\left(\frac{dr^2}{1-kr^2} + r^2(d\theta^2 + sin^2\theta\, d\phi^2)\right). \tag{2.5}$$

Here $a(t)$ is the scale factor, N is the lapse function (which relates coordinate time t and proper time τ), and k is a constant which represents the curvature of all space, and can take values -1, 0 or 1 depending on whether the universe has an open, flat or closed geometry respectively. We use comoving spherical spatial coordinates here, and the comoving coordinate distance, r, is related to the previously specified comoving distance, χ, by $\chi = r$ if $k = 0$, $\chi = \sin^{-1} r$ if $k = 1$, and $\chi = \sinh^{-1} r$ if $k = -1$.

The matter in our universe can be modelled as a perfect fluid, which is a fluid without viscosity, shear stresses, or heat conduction. The energy-momentum tensor for such a fluid is given by

$$T_{\mu\nu} = (\rho c^2 + p)u_\mu u_\nu - p g_{\mu\nu}, \tag{2.6}$$

where ρ is the mass-energy density, p is the pressure and u_μ is the four-velocity of the matter.

Using the FLRW metric implied by equation (2.5) and the energy-momentum tensor for a perfect fluid (equation (2.6)) in the expression (2.3), we obtain the Friedmann equation,

$$\dot{a}^2 = \frac{8\pi G\rho a^2}{3} - kc^2 + \frac{\Lambda c^2 a^2}{3}, \tag{2.7}$$

and the Friedmann acceleration equation,

$$\ddot{a} = -\frac{4\pi G}{3}\left(\rho + \frac{3p}{c^2}\right)a + \frac{\Lambda c^2 a}{3}. \tag{2.8}$$

These are the equations of motion that govern the expansion of space. However, in order to solve these equations , we need another equation, since we have 3 unknowns

($a(t)$, $\rho(a)$, $p(a)$) and only 2 equations relating them. This is equation is known as the equation of state,

$$p = w\rho c^2, \tag{2.9}$$

where w is a dimensionless parameter. Various types of fluids can be modelled by choosing different values for w, such as dust ($w = 0$), radiation ($w = 1/3$), and dark energy/cosmological constant ($w = -1$).

A scalar field, ϕ, can be understood to be a type of perfect fluid, with

$$w = \frac{\frac{1}{2}\dot{\phi}^2 - V(\phi)}{\frac{1}{2}\dot{\phi}^2 + V(\phi)} \tag{2.10}$$

(Here c has been set to 1). If the scalar field is constant in time, it has zero kinetic energy, and is thus equivalent to a cosmological constant, since w becomes -1. If the scalar field is free and massless ($V(\phi) = 0$), then $w = 1$. Likewise, with a proper choice of kinetic and potential energies, we are able to achieve any w between -1 and 1, and as such the scalar field is a useful tool for modelling various cosmological phenomena.

Chapter 3

Review on Quantum Cosmology

As mentioned previously, quantum cosmology does not try to answer the fundamental question of what the correct theory of quantum gravity is, but rather attempts to solve cosmological problems that occur at scales where both gravitational and quantum effects are strong (i.e. large mass and small size) by directly quantizing general relativity canonically. One hopes that in doing so one arrives at a theory which in its semiclassical limit agrees with the semiclassical limit of the actual quantum theory of gravity.

The foundations of quantum cosmology were first put in place by Bryce DeWitt in 1967 [5], who after developing the canonical theory of quantum gravity, applied canonical quantization to a closed FLRW universe with matter. Further contributions by Wheeler [6] (who had first suggested the use of a wavefunctional) and Misner [7] completed the canonical formalism. After a lull, the subject was revived with focus on boundary conditions, with the seminal paper by Hawking and Hartle [8] concerning the 'no-boundary' proposal, and Vilenkin [9] suggesting the 'tunnelling' proposal, in which the universe is born via quantum tunnelling to appear at a finite, non-zero size. Since then quantum cosmology has attempted to tackle the question of fixing the initial conditions for cosmic inflation, which are unanswered in classical inflationary cosmology. Other problems that quantum cosmology has attempted to answer is

the arrow of time, the origin of structure formation and how the transition from the quantum realm to the classical realm (quantum decoherence) occurs.

We shall review the main concepts of the subject as pertinent to our study of nonlinear quantum cosmology. Quantum mechanics is very different from general relativity in the sense that in general relativity, the field equations tell us how a source of mass-energy affects the curvature of spacetime; whereas in quantum mechanics, the wavefunction is a single mathematical object which contains all the information about a system. For example, we are able to find the expectation value of the momentum of a quantum particle by using just its wavefunction and an operator. Thus, in quantum cosmology we would require some sort of wavefunction which can contain the information of both the geometry and the matter content in the universe. This mathematical object is known as a wavefunctional,

$$\Psi[h_{ij}(\mathbf{x}), \phi(\mathbf{x})], \tag{3.1}$$

which can be interpreted as the probability amplitude of the universe being a spatial hypersurface, Σ, on which $h_{ij}(\mathbf{x})$ is the intrinsic 3-dimensional metric, and which contains a matter field, $\phi(\mathbf{x})$.

The wavefunctional is the solution of the Wheeler-DeWitt equation, and in order to derive this equation we have to use the Hamiltonian, or ADM formalism of general relativity, in which the 4-dimensional manifold, $\mathcal{M}$ that represents the evolution of our universe is foliated into spatial hypersurfaces, Σ_t, which are labelled by a global time function , t. The relevant action is called the Einstein-Hilbert action,

$$S = \frac{1}{16\pi G}\left[\int_{\mathcal{M}} d^4x\sqrt{-g}({}^4R - 2\Lambda) + 2\int_{\partial\mathcal{M}} d^3x\sqrt{h}K\right] + S_{matter}, \tag{3.2}$$

where

$$S_{matter} = \int_{\mathcal{M}} d^4x\sqrt{-g}\left(-\frac{1}{2}g^{\mu\nu}\partial_\mu\phi\partial_\nu\phi - V(\phi)\right) \tag{3.3}$$

is the usual action for a scalar field. Here g is the determinant of the metric tensor $g_{\mu\nu}$, h is the determinant of the 3-dimensional intrinsic metric h_{ij}, ${}^4R$ is the Ricci scalar, and K is the trace of the extrinsic curvature K_{ij}, which describes how the spatial hypersurfaces Σ_t curve with respect to the manifold, $\mathcal{M}$ within which they are embedded.

By obtaining the equation of motions, and then quantizing them via identification of the conjugate momenta, one equation we can find is the Wheeler-DeWitt equation [1] (hereon we only work in natural units, where $\hbar = c = 1$):

$$\hat{H}\Psi[h_{ij}, \phi] = \left[-(16\pi G) G_{ijkl} \frac{\delta^2}{\delta h_{ij} \delta h_{kl}} + \frac{\sqrt{h}}{16\pi G} (-{}^3R + 2\Lambda + 16\pi G \hat{T}^{\hat{0}\hat{0}}) \right] \Psi[h_{ij}, \phi] = 0 \tag{3.4}$$

where the 00-component of the energy-momentum tensor in an orthonormal frame,

$$\hat{T}^{\hat{0}\hat{0}} = \frac{-1}{2h} \frac{\delta^2}{\delta \phi^2} + \frac{1}{2} h^{ij} \partial_i \phi \partial_j \phi + V(\phi) \tag{3.5}$$

for a scalar field. Also, ${}^3R$ is the Ricci scalar of the intrinsic 3-geometry, and

$$G_{ijkl} = \frac{1}{2} \sqrt{h} (h_{ik} h_{jl} + h_{il} h_{jk} - h_{ij} h_{kl}) \tag{3.6}$$

is known as the DeWitt metric. The Wheeler-DeWitt equation is in fact not a single equation, but one equation at every point, $\mathbf{x}$, on the spatial hypersurface Σ_t.

We also find one other quantum equation, known as the momentum constraint [1], which can be used to show that the wavefunctional, $\Psi[h_{ij}, \phi]$ is the same for configurations $\{h_{ij}(\mathbf{x}), \phi(\mathbf{x})\}$ which are related by diffeomorphisms in the spatial hypersurface, Σ_t. However, we shall only consider the Wheeler-DeWitt equation hereon, since it will be argued later that the momentum constraint will be automatically satisfied under a symmetry restriction.

One may ask on what configuration space is the Wheeler-DeWitt equation defined. The answer to this is the space of all Riemannian 3-metrics $h_{ij}(\mathbf{x})$, and matter

configurations $\phi(\mathbf{x})$ on the spatial hypersurfaces, Σ_t, which is also known as superspace. This is an infinite-dimensional space, since it is essentially a space which has a 3-geometry at every one of its points [6].

Using the concept of superspace also gives us greater insight into the conceptual aspects of quantum cosmology, via the method of path integrals. In quantum mechanics, the propagator, which gives the probability amplitude of a particle initially at a point $\mathbf{x_a}$ to be found later at a certain point $\mathbf{x_b}$, can be defined as the sum of all possible paths that the particle can take between both points, with each path assigned a certain amplitude. Similarly one is able to define a path integral in canonical quantum gravity (as pioneered by Gibbons and Hawking [10, 11]) as giving us the probability amplitude for a spatial hypersurface, Σ_t, with intrinsic metric $h_{ij}(\mathbf{x})$ and matter configuration $\phi(\mathbf{x})$ to evolve into a spatial hypersurface, $\Sigma_{t'}$, with intrinsic metric $h'_{ij}(\mathbf{x})$ and matter configuration $\phi'(\mathbf{x})$. This is given by a functional integral of e^{iS} over all 4-geometries $g_{\mu\nu}$ and matter configurations $\phi(x)$ which can interpolate between the initial and final configurations, or

$$\langle h'_{ij}, \phi', \Sigma_{t'} | h_{ij}, \phi, \Sigma_t \rangle = \int \mathcal{D}\boldsymbol{g}\mathcal{D}\phi e^{iS[g_{\mu\nu},\phi]} \tag{3.7}$$

Thus, just like how via path integrals in quantum mechanics, we come to understand that because of quantum fluctuations in position and momentum due to the uncertainty principle, the classical trajectory of a particle becomes ill-defined, and non-classical trajectories close to the classical one gain a significant amplitude, likewise in quantum gravity the quantum fluctuations in the superspace coordinates $h_{ij}(\mathbf{x})$ and $\phi(\mathbf{x})$ and their respective conjugate momenta due to the uncertainty principle result in the classical evolution of a 3-geometry (according to Einstein's equations) becoming ill-defined, and now non-classical evolutions close to the classical one also gain a significant amplitude. In fact, the very idea of a precise evolution or trajectory loses its meaning, and we have to forgo the concept of a classical spacetime, and make

do with a 'spacetime foam' in which quantum fluctuations occur in the geometry of space and its rate of change [6, 12].

However in practice we do not actually work with the full infinite dimensions of superspace, as it is impossible. One instead makes some restrictions based on symmetry, which truncate the infinite dimensions of superspace to a finite dimensional configuration space, referred to as minisuperspace. The fact that we are able to do this bodes well for cosmology, since we are used to making the assumptions of homogeneity and isotropy there, as in the FLRW metric. In general the Wheeler-DeWitt equation is actually one equation for every point $\mathbf{x}$, of the spatial hypersurface at a certain point in time; but upon assuming that it is homogeneous we have just one Wheeler-DeWitt equation for the entire spatial hypersurface. The minisuperspace coordinates are now $\phi(\mathbf{x})$, and up to three coordinates that specify the 3-geometry. If we further assume isotropy on the spatial hypersurface, then the minisuperspace coordinates are only $\phi(\mathbf{x})$ and the scale factor, $a(t)$, which now completely specifies the 3-geometry. Furthermore, under the minisuperspace scheme, the momentum constraint equation mentioned earlier is automatically satisfied [13,14], since the diffeomorphisms it deals with are meaningless in a homogeneous space, allowing us to work only with the Wheeler-DeWitt equation. We shall use this minisuperspace approximation for our study of nonlinear quantum cosmology.

However before proceeding, it is important to note that the procedure of minisuperspace quantization itself has not been rigorously proven to be a valid approximation to superspace quantization, and critics have proven several instances in which it could be an incorrect one (Kuchař and Ryan [15], for example). The source of the possible invalidation has to do with the fact that if we perform a series expansion of a metric in terms of space-dependent modes, the uncertainty principle disallows the setting of the inhomogeneous modes to zero prior to quantization, which is exactly what we do in minisuperspace quantization. Nevertheless, the procedure is still important in that it provides us with verifiable results, which are impossible to retrieve using the full

superspace. Furthermore homogeneity and isotropy are both features observable in our own universe; and thus it is not unreasonable to expect that a rigorous truncation scheme to some minisuperspace models will be found in the future, and it is with this belief that we proceed.

The Wheeler-DeWitt equation in minisuperspace is much simpler than its superspace counterpart, as we shall see. The Einstein-Hilbert action (3.2) becomes

$$S \equiv \int dtL = \frac{1}{2}\int dtNa^3\left[-\frac{\dot{a}^2}{N^2a^2} + \frac{k}{a^2} + \frac{\dot{\phi}^2}{N^2} - V(\phi)\right] \tag{3.8}$$

for a FLRW universe, and we shall use this action to derive the Wheeler-DeWitt equation in minisuperspace. It should be noted that the scale factor, a, we use here is not the physical scale factor a_{phys}, which appears in the FLRW metric. They are related by the expression

$$a_{phys} = \sqrt{\frac{4\pi l_p^2}{3V_{a^3}}}a, \tag{3.9}$$

where l_p is the Planck length, and V_{a^3} is the volume of the spatial hypersurface divided by a^3. V_{a^3} depends on the curvature, k, and the topology of the hypersurface [16,17]. If the spatial hypersurface has a closed geometry $k = 1$ (i.e. a 3-sphere) and topology S^3 then $V_{a^3} = 2\pi^2$, whereas if the geometry of the hypersurface is flat ($k = 0$), V_{a^3} can take any value since the fundamental polyhedra of such hypersurfaces can have any arbitrary size [18].

We can further simplify the action (3.8) by assuming that we have a scalar field that varies very slowly, or is constant. In such a case we have a negligible kinetic energy term, and a potential energy term that can be taken to be constant ($V(\phi) = V$). We will then only have one minisuperspace coordinate, the scale factor, $a(t)$. The action then becomes

$$S \equiv \int dtL = \frac{1}{2}\int dtN\left[-\frac{\dot{a}^2a}{N^2} + a(k - \frac{a^2}{a_0^2})\right], \tag{3.10}$$

where $a_0^2 = 1/V$. If we vary the action with respect to the lapse function, N (which

measures the difference between coordinate time, t, and proper time, τ, on curves normal to the hypersurfaces Σ_t) and choose the gauge $N = 1$, we then obtain a Friedmann equation,

$$\dot{a}^2 + \left(k - \frac{a^2}{a_0^2}\right) = 0. \tag{3.11}$$

Upon comparison with the general form of the Friedmann equation (2.7), we see that this is just the Friedmann equation for an empty universe with a cosmological constant, $\Lambda = 3/a_0^2$ (a FLRW-Λ universe). The expanding solution to equation (3.11) for a flat ($k = 0$) geometry is

$$a = e^{\left(\frac{t}{a_0}\right)}. \tag{3.12}$$

This solution permits the existence of a universe of zero size, since $a \to 0$ as $t \to -\infty$.

We shall now obtain the Wheeler-DeWitt equation in minisuperspace for a FLRW-Λ universe by quantizing the Friedmann equation (3.11). We first find the momentum conjugate to the scale factor from the Lagrangian implied by the action (3.10),

$$p_a = \frac{\partial L}{\partial \dot{a}} = -\dot{a}a. \tag{3.13}$$

The Friedmann equation (3.11) then becomes

$$p_a^2 + a^2\left(k - \frac{a^2}{a_0^2}\right). \tag{3.14}$$

Next, we quantize via Dirac's quantization rule, promoting the canonical momentum p_a to an operator $\hat{p}_a = -i\frac{\partial}{\partial a}$ in equation (3.14), leading to

$$\left[-\frac{\partial^2}{\partial a^2} + a^2\left(k - \frac{a^2}{a_0^2}\right)\right]\psi(a) = 0, \tag{3.15}$$

the Wheeler-DeWitt equation in minisuperspace, for an empty FLRW universe with a cosmological constant. It is obvious that this equation is mathematically equivalent to a time-independent Schrödinger equation for a particle of mass $m = 1/2$ with zero

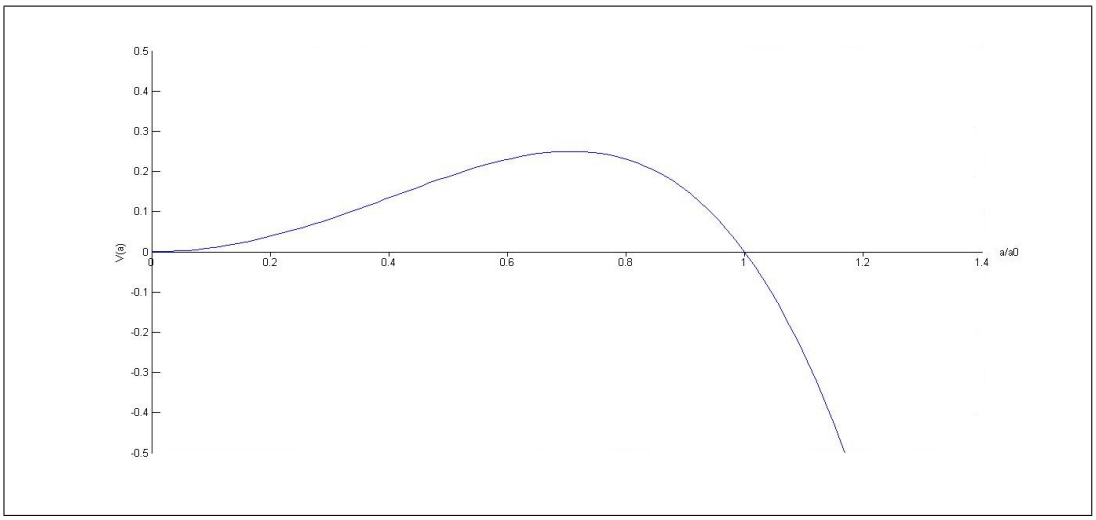

Figure 3.1: Plot of the potential energy for a closed, empty FLRW universe with a cosmological constant

energy, moving under the influence of a potential energy,

$$V(a) = a^2 \left(k - \frac{a^2}{a_0^2} \right). \tag{3.16}$$

For a closed universe ($k = 1$), we find that a potential barrier naturally occurs close to $a = 0$, as seen in Figure 3.1. This is desirable, as it implies that the universe can tunnel through the potential barrier to be born at $a = a_0$, thus avoiding zero size. Also, in the classical dynamics, a collapsing universe would experience a bounce when it reaches the barrier, thus preventing it from reaching zero size.

We are able to calculate a tunnelling probability for this universe from the potential energy using the WKB approximation:

$$P \approx \exp\left(-2 \int_0^{a_0} da \sqrt{V(a)} \right) = \exp\left(-2 \int_0^{a_0} da \sqrt{a^2 - \frac{a^4}{a_0^2}} \right) \tag{3.17}$$

$$= \exp\left(-2 \frac{a_0^2}{3} \right) \tag{3.18}$$

$$= \exp\left(-\frac{2}{\Lambda} \right) \tag{3.19}$$

One however has to be aware that this is not a traditional quantum system, in that

there is no classical observer separate from the quantum system since it encompasses the whole universe. We thus have to replace the usual Copenhagen interpretation of quantum mechanics with the idea of 'decoherent histories' proposed by Gell-Mann and Hartle [19], in which each possible history of the universe is assigned a certain probability. As such, equation (3.19) tells us that the most probable history in which a closed FLRW-Λ universe tunnels into existence at a finite size is one where the cosmological constant is at the maximum value it is allowed to take.

However, we do not see the kind of potential barrier seen in Figure 3.1 for the cases of $k = 0$, and $k = -1$, which is unfortunate, as much experimental data based on observations of the cosmic microwave background and observations of distant supernovae imply that our universe is spatially flat ($k = 0$). We thus study nonlinear quantum cosmology for spatially flat universes in order to see if the nonlinearities may cure the problem of zero size in a manner similar to that seen thus far, or in a different manner altogether. It is however imperative to note that we do not actually have a singularity of curvature invariants at zero size in the model we have been working with so far, as the only matter contained in a FLRW-Λ universe is a cosmological constant. Nevertheless, by studying this model we hope to find effects that will also hold true in more complicated models that do contain physical singularities.

Chapter 4

Review on Nonlinear Quantum Mechanics and Nonlinear Quantum Cosmology

It has been widely speculated in recent years that quantum mechanics could just be an approximate theory, and that the Schrödinger equation should actually contain additional, small, nonlinear terms. In fact, nonlinear Schrödinger equations are required to phenomenologically describe both quantum and classical systems, such as the Gross-Pitaevskii equation which describes the wavefunction of a Bose-Einstein condensate, and the cubic nonlinear Schrödinger equation that occurs in fiber optics and the description of water waves.

Thus, it would not be unreasonable to expect that under certain extreme conditions quantum mechanics in general will have to be modified, and nonlinearities that would otherwise be small might increase in magnitude to be comparable with the linear terms of the equation. One such condition could be the Planck scale, and this has been suggested by Svetlichny [20], who conjenctured that linear quantum mechanics is merely an emergent feature of the actual theory of quantum gravity,

which is probably nonlinear.

We thus shall attempt to solve our problem of understanding our universe at the Planck scale by resorting to nonlinear modifications to quantum mechanics. However many such modifications exist, with various motivations, and in this work we shall use an information theoretically motivated nonlinear Schrödinger equation introduced by Parwani [2]. Our basis for choosing this nonlinear equation over the others relies on the fact that it is based on the maximum uncertainty principle, which as we shall see is apt since we are attempting to model unknown new physics at the Planck scale, the form of which we do not know.

The maximum uncertainty principle here is the general principle of which the maximum entropy principle of statistical mechanics is an example. In statistical mechanics, the maximum entropy principle allows us to derive an unknown probability distribution for a statistical system under a given constraint. For example, if a statistical system has an unknown probability distribution, $p(x)$, but the mean energy is given as $E = \int \epsilon(x)p(x)dx$ (the constraint), we maximise the Gibbs entropy

$$I_{GS} = -\int p(x) \ln p(x) dx \tag{4.1}$$

subject to the constraint to give us the correct form of the probability distribution. In other words, by maximising $I_{GS} - \beta E$ (where β is a Lagrange multiplier) with respect to variations in $p(x)$ we obtain the canonical probability distribution $p(x) \propto \exp(-\beta\epsilon(x))$.

However an identical expression to that of (4.1) was derived by Shannon [21] as an information measure, which quantifies the information content, or conversely the uncertainty in a system. The maximum uncertainty principle is based on the idea that by maximising the uncertainty measure, one acknowledges our ignorance of a more detailed structure, thus giving us an unbiased description of the system.

The measure (4.1) is not the only uncertainty measure we may use when using

the maximum uncertainty principle; for example if one already has some information about the system in the form of a reference probability distribution $r(x)$, one may use the Kullback-Liebler information measure,

$$I_{KL} = -\int p(x) \ln \frac{p(x)}{r(x)} dx, \tag{4.2}$$

which reduces to the Shannon information measure (4.1) when we have no *a priori* information about the system, and are forced to take $r(x)$ to be a uniform distribution.

It was shown by Reginatto [22] that it is also possible to derive the Schrödinger equation via the maximum uncertainty principle by using another information measure, known as the Fisher information measure, as follows. By making the Madelung transformation $\psi = \sqrt{p} e^{\frac{iS}{\hbar}}$, the Schrödinger equation may be rewritten in terms of the hydrodynamical variables, p and S:

$$\frac{\partial S}{\partial t} + \frac{1}{2m}\left(\frac{\partial S}{\partial x}\right)^2 + V(x) + Q = 0 \tag{4.3}$$

$$\frac{\partial p}{\partial t} + \frac{1}{m}\frac{\partial}{\partial x}\left(p\frac{\partial S}{\partial x}\right) = 0 \tag{4.4}$$

where

$$Q = -\frac{\hbar^2}{2m}\frac{1}{\sqrt{p}}\frac{\partial^2 . \sqrt{p}}{\partial x^2} \tag{4.5}$$

Reginatto showed that it is possible to recover the Schrödinger equation in this form by minimising the combination $\Phi_A + \xi I_F$, where the action,

$$\Phi_A = \int p\left(\frac{\partial S}{\partial t} + \frac{1}{2m}\left(\frac{\partial S}{\partial x}\right)^2 + V(x)\right) dx\, dt, \tag{4.6}$$

the Fisher information measure,

$$I_F = \int \frac{1}{p}\left(\frac{\partial p}{\partial x}\right)^2 dx\, dt \tag{4.7}$$

and the Lagrange multiplier $\xi = \frac{\hbar^2}{8m}$.

It may at first seem apparent that both the information measures ((4.2) and (4.7)) used in statistical mechanics and quantum mechanics are different, however there is in fact a close relationship between both measures. If we choose the reference distribution in the Kullback-Liebler measure to be identical to $p(x)$ but with an infinitesimally shifted argument, or $r(x) = p(x + \Delta x)$, we see that, to lowest order [2]

$$I_{KL}(p(x), p(x + \Delta x)) = \frac{-(\Delta x)^2}{2} I_F(p(x)) + O(\Delta x)^3 \tag{4.8}$$

(It should be noted that for quantum mechanical applications, the probability distribution, p is not only a function of position, x, but a function of time, t as well, and as such in these cases the Kullback-Liebler measure should have an integral not only over position, but also over time). Thus one may speculate that a generalisation to the Schrödinger equation might arise if one uses the left hand side of (4.8) to derive it instead of just the Fisher information. This is indeed true, as was shown by Parwani [2], and we arrive at a nonlinear Schrödinger equation by minimising the combination $\Phi_A - \xi I_{KL}$. Here we need a negative sign in front of the term with the Kullback-Liebler measure, due to the negative sign that occurs in the leading order term in equation (4.8).

However the nonlinear Schrödinger equation we obtain is problematic, because singularities occur in it whenever either $p(x)$ or $p(x + \Delta x)$ vanishes. Thus in order to evade this, we shall modify our information measure. There is nothing wrong with doing this, as a relationship of the form (4.8) is satisfied by not only the Kullback-Liebler measure, but by many other information measures as well; that is they give us the Fisher measure multiplied by some factors to leading nontrivial order in Δx, when they are expanded in terms of Δx. However there are some further caveats that the information measure has to satisfy in order for it to give us a proper quantum mechanical equation. Firstly, the information measure should be positive definite,

and of the form

$$G(p(x,t);\Delta x) = \int p(x,t)H(p(x,t);\Delta x)dx\,dt, \tag{4.9}$$

in order for the superposition principle to hold for wavefunctions of negligible overlap. Also, we require that the function $H(p(x,t);\Delta x)$ in equation (4.9) should be invariant under scaling of the function $p(x,t)$, in order to ensure that the solutions are normalizable [2].

An information measure that satisfies all these assumptions, and does not lead to singularities is

$$I_{KL-R} = \frac{1}{\eta^4}\int p(x)\ln\left(\frac{p(x)}{(1-\eta)p(x)+\eta p(x+\eta L)}\right)dx\,dt, \tag{4.10}$$

which is a regularized Kullback-Liebler measure, where $L = \Delta x$, and η is a dimensionless parameter. The range of the parameter is $0 < \eta \leq 1$, and when $\eta = 1$ the measure reduces to the negative of the Kullback-Liebler measure (4.2).

Thus, minimising the combination $\Phi_A + \xi I_{KL-R}$ leads to the information theoretical nonlinear Schrödinger equation [2]

$$i\hbar\frac{\partial\Psi}{\partial t} = -\frac{\hbar^2}{2m}\frac{\partial^2\Psi}{\partial x^2} + V(x)\Psi + F(p)\Psi, \tag{4.11}$$

where the nonlinear term is

$$F(p) = Q_{NL} - Q, \tag{4.12}$$

where,

$$Q_{NL} = \frac{\hbar^2}{4mL^2\eta^4}\left[\ln\left(\frac{p}{(1-\eta)p+\eta p_+}\right) + \frac{\eta p_+}{(1-\eta)p+\eta p_+} - \frac{\eta p_-}{(1-\eta)p_- + \eta p}\right], \tag{4.13}$$

Q is the quantum potential, equation (4.5), $p(x) = \Psi(x,t)^*\Psi(x,t)$ is the probability density, and $p_\pm(x) = p(x \pm \eta L)$ is the probability density at two neighbouring points.

It can be shown that in the limit that the nonlinear length, L approaches zero, Q_{NL} reduces to Q, giving us the linear Schrödinger equation. The nonlinear length, L may be interpreted in various ways; it is possible that it is the Planck length, $l_p \sim 10^{-35}$, or perhaps related to the size of elementary particles, or it could just be the resolution at which spatial coordinates become distinguishable [2].

We now wish to nonlinearise the Wheeler-DeWitt equation in minisuperspace (3.15) in a similar manner to how the Schrödinger equation was nonlinearised. We first recall that the Wheeler-DeWitt equation in minisuperspace we saw in the last chapter is equivalent to a time-independent Schrödinger equation for a particle of mass, $m = 1/2$ and zero energy. Thus, factoring out the time-dependence of the wavefunction in equation (4.11) as usual, $\Psi(x,t) = \psi(x)e^{\frac{-iEt}{\hbar}}$, we find the time-independent nonlinear Schrödinger equation,

$$E\psi(x) = -\frac{\hbar^2}{2m}\frac{\partial^2\psi(x)}{\partial x^2} + V(x)\psi(x) + F(p)\psi(x) \tag{4.14}$$

Then, making the variable change $x \to a$, and setting $E = 0$, $m = 1/2$, and using natural units ($\hbar = c = 1$), we arrive at the nonlinear Wheeler-DeWitt equation in minisuperspace,

$$\left[-\frac{\partial^2}{\partial a^2} + V(a) + F(p)\right]\psi(a) = 0. \tag{4.15}$$

An alternative way of understanding the appearance of the nonlinearity is by taking Dirac's quantization rule to be modified to become $\hat{p}_a^2 = -\frac{\partial^2}{\partial a^2} + F(p)$. It is important to note that the nonlinear length, L is now rescaled just like how the scale factor, a was rescaled in equation (3.9), and we are working with L and not L_{phys}. In this case it is possible to interpret L as a minimal uncertainty in position, as seen in some suggested theories of quantum gravity, such as superstring theory [23].

It is the objective of nonlinear quantum mechanics to study the solutions to equations of the type (4.15). For a potential energy of the form (3.16), corresponding to

an empty FLRW universe with a cosmological constant, equation (4.15) becomes

$$\left[-\frac{\partial^2}{\partial a^2} + a^2\left(k - \frac{a^2}{a_0^2}\right) + F(p)\right]\psi(a) = 0. \tag{4.16}$$

Nonlinear equations such as this are difficult to solve exactly, and one may resort to pertubative approximations by assuming a small nonlinearity. As mentioned before we choose to focus on flat ($k = 0$) universes; and using a pertubative treatment, we are able study the effects of adding the nonlinearity to the Wheeler-DeWitt equation, as was shown by Nguyen and Parwani [3], and as we shall review here. Setting $k = 0$ and $a = lb$ in equation (4.16),with $l = a_0^{\frac{1}{3}}$, one obtains

$$\left[-\frac{\partial^2}{\partial b^2} - b^4 + l^2 F(p(lb))\right]\phi(b) = 0, \tag{4.17}$$

where $\phi(b) \equiv \psi(a)$. Next, assuming small nonlinearity at all times (even when the universe was of small size), we expand the nonlinear term F pertubatively in L to leading order,

$$F(b) = \frac{\eta(3-4\eta)L}{l^3} f(b) + O(L^2) \tag{4.18}$$

where

$$f(b) = \frac{q'}{12q^3}(2q'^2 - 3q''q). \tag{4.19}$$

Here $q(b) = \phi^*(b)\phi(b)$, and primes refer to derivatives with respect to b. Replacing this form of the nonlinearity into equation (4.17) gives us, to leading order,

$$\left[-\frac{\partial^2}{\partial b^2} - b^4 + \eta(3-4\eta)\epsilon f(b)\right]\phi(b) = 0, \tag{4.20}$$

where $\epsilon \equiv L/l$ is a parameter introduced to measure the strength of the nonlinearity. We may then iterate about the solution to the unperturbed equation by assuming $\epsilon \ll 1$, to solve the equation, as follows. The expanding solution to equation (4.20),

with $\epsilon = 0$ (no perturbation), is a Hankel function,

$$\phi_0(b) \propto \sqrt{b} H^{(2)}_{\frac{1}{6}}(\frac{b^3}{3}) \tag{4.21}$$

$$\approx \sqrt{\frac{6}{\pi b^2}} \exp\left[-\frac{i(b^3-\pi)}{3}\right] \text{ as } b \to \infty. \tag{4.22}$$

Using the asymptotic form (4.22), we may find $q_0(b)$ and thus $f_0(b)$, giving us an effective potential

$$V_{eff} = -b^4 + \eta(3-4\eta)\epsilon f_0(b). \tag{4.23}$$

In order to avoid zero-size, as was discussed at the end of the last chapter, we would need the potential (4.23) to form a potential barrier close to $b = 0$. This is indeed seen, since for small b, it can be shown that

$$f_0 \approx 0.1b, \tag{4.24}$$

and thus for $\eta < 3/4$, we see an effective potential barrier close to $b = 0$, through which the quantum universe tunnels into existence.

Applying the WKB formula as before, it can be shown that the tunnelling probability,

$$P \approx \exp(-0.1\eta(3-4\eta)\epsilon)). \tag{4.25}$$

Therefore for fixed η, as long as it is less than $3/4$, the probability can be interpreted as implying that smaller values of ϵ are 'preferred', which is consistent with our previous assumption $\epsilon \ll 1$. Thus, we have shown that for a flat ($k = 0$) universe, using a nonlinear Wheeler-DeWitt equation results in a universe tunnelling into existence at a finite size, and which is classically prevented from shrinking to zero size via a bounce, just as in the case for a closed ($k = 1$) universe using the linear equation.

However, we have only used approximate pertubative methods thus far, assuming small nonlinearity throughout time, and a more general study should allow for larger

nonlinearities via non-pertubative methods, and we shall do just this in the next chapter.

Chapter 5

Non-pertubative Study of a Spatially Flat FLRW Universe with a Cosmological Constant as a Function of the Scale Factor

5.1 Motivation

As we have seen, FLRW-Λ universes with positive curvature ($k = 1$) are allowed to be born at a finite size due to quantum tunneling, as was first described by Atkatz and Pagels [24] as well as Vilenkin [25]. Also, as shown in the previous chapter, if we introduce information theoretically motivated nonlinearities into the Wheeler-DeWitt equation in minisuperspace, we can similarly avoid a zero size universe at $t = 0$ for flat universes ($k = 0$) as well, as long as the parameter $\eta < 3/4$.

However we have only treated the nonlinear Wheeler-DeWitt equation pertubatively thus far, for a non-varying cosmological constant in a de Sitter universe. In Parwani and Tarih [4], the same case was treated non-pertubatively, leading to a numerically soluble difference equation. Our motivation for this section is to extend the

non-pertubative treatment to the case of a flat FLRW universe in which the only matter is a cosmological constant which varies as a function of the scale factor. We shall first review the non-pertubative treatment for the case of a non-varying cosmological constant.

5.2 Review of the Non-Pertubative Study of a Flat FLRW Universe with a Non-varying Cosmological Constant

As we have seen in the previous chapter, for our case of the flat FLRW-Λ universe, we may attempt to model new physics at the quantum gravity scale using the framework of information theory by using the following nonlinear Wheeler-DeWitt equation:

$$\left[-\frac{\partial^2}{\partial a^2} - \frac{a^4}{a_0^2} + F(p)\right]\psi(a) = 0. \tag{5.1}$$

To study it non-pertubatively we need to express the wavefunction of the universe in terms of its amplitude and phase:

$$\psi = \sqrt{p}e^{iS}. \tag{5.2}$$

Using this form of the solution, the Wheeler-DeWitt equation will have an imaginary part and a real part. The imaginary part of the equation is then a continuity equation,

$$\frac{\partial}{\partial a}\left(p\frac{\partial S}{\partial a}\right) = 0, \tag{5.3}$$

which is solved to give us the constant current, σ:

$$p\frac{\partial S}{\partial a} = \sigma. \tag{5.4}$$

This constant current can be fixed by requiring that the non-pertubative solution approaches the asymptotic form of the Hankel function solution to the linear Wheeler-

DeWitt equation (with a_0 set to 1),

$$\left[-\frac{\partial^2}{\partial a^2} - a^4\right]\psi(a) = 0, \tag{5.5}$$

for some large a. The asymptotic form of the solution is

$$\psi_0(a) \approx \sqrt{\frac{6}{\pi a^2}}\,\exp\left[-\frac{i(a^3-\pi)}{3}\right] \text{ as } a \to \infty. \tag{5.6}$$

Thus, using the amplitude and the phase of the asymptotic form, we obtain:

$$\sigma = \frac{-6}{\pi}. \tag{5.7}$$

The derivatives of S in the real part of the nonlinear Wheeler-DeWitt equation,

$$\left(\frac{\partial S}{\partial a}\right)^2 - \frac{a^4}{a_0^2} + Q_{NL} = 0, \tag{5.8}$$

can then be eliminated using equation (5.4), giving us a pure difference equation for the probability density (the detailed derivation can be found in Appendix A):

$$\left(\frac{\sigma}{p}\right)^2 = \frac{a^4}{a_0^2} - \frac{1}{2\zeta^2\eta^2}\left[\ln\left(\frac{p}{(1-\eta)p+\eta p_+}\right) + \frac{\eta p_+}{(1-\eta)p+\eta p_+} - \frac{\eta p_-}{(1-\eta)p_- + \eta p}\right] \tag{5.9}$$

This equation relates the probability density $p(a)$ at equally spaced lattice points, which are separated by a step size $\zeta = \eta L$, which is also a measure of the nonlinearity. However it is imperative to note that the variable a, and thus $p(a)$ are both still continuous. All that equation (5.9) implies is that the value of $p(a)$ at any point is now non-local, in that it depends on the values of $p(a+\zeta)$ and $p(a-\zeta)$. Thus, it should be understood that the region between any two lattice points is continuously connected.

The difference equation can easily be solved numerically, first, by specifying two initial values for p_+ and p, and finding p_-. Then we refer to the original p as p_+, and

the original p_- as p, and find the next lattice point. Iterating this process, we are able to find p as a function of a. However, this is only possible since, using the difference equation (5.9), we are able to write p_- in terms of p and p_+. It is unfortunately impossible to write p_+ explicitly in terms of p and p_-, and as such we have to resort to Newton's method to find values of the probability density forward from the two initial points specified earlier.

For the backward evolution a variable change has to be made in the difference equation, namely $a \to a + \zeta$, which leads to a relabelling of the probability density terms:

$$p_-(a) \to p(a) \tag{5.10}$$

$$p(a) \to p_+(a) \tag{5.11}$$

$$p_+(a) \to p_{++}(a) \tag{5.12}$$

As before $p_\pm(a) = p(a \pm \zeta)$, and $p_{++}(a) = p(a + 2\zeta)$. We may then rearrange the difference equation into an explicit form for $p(a)$:

$$p(a) = \frac{\eta p_+(a)}{(1-\eta)} \left[\frac{1}{1 - (\frac{1-\eta}{\eta})D} - 1 \right], \tag{5.13}$$

where (with the constant a_0 set to 1),

$$D = \ln\left(\frac{p_+}{(1-\eta)p_+ + \eta p_{++}}\right) + \frac{\eta p_{++}}{(1-\eta)p_+ + \eta p_{++}} - 2\zeta^2\eta^2\left((a+\zeta)^4 - \frac{\sigma^2}{p_+^2}\right). \tag{5.14}$$

Using equation (5.13) we may evolve the equation backwards from two starting lattice points.

These two initial values are obtained by assuming that about a certain size (which we shall assume to be $a = 5$), the nonlinearity is small, and that the wavefunction of the universe will be close to the solution of the linear Wheeler-DeWitt equation (5.5) that represents an expanding universe, which, as before, is given by the following

Hankel function:

$$\psi_0(a) \propto \sqrt{a} H^{(2)}_{\frac{1}{6}}(\frac{a^3}{3}) \tag{5.15}$$

$$\approx \sqrt{\frac{6}{\pi a^2}} \exp\left[-\frac{i(a^3-\pi)}{3}\right] \text{ as } a \to \infty. \tag{5.16}$$

In fact one can choose any initial starting point besides $a = 5$ as long as it is not too close to $a = 0$ (since it was conjenctured that when the universe is close to zero size the nonlinearities would be large in magnitude), and this will not qualitatively affect the numerical results obtained. We use the asymptotic form of the solution given by equation (5.16) to find the values of the probability density $p = \psi_0^* \psi_0$ at $a = 5$ and $a = 5 - \zeta$, which gives us the values of p_{++} and p_+ respectively for the backward evolution, or the values of p and p_- respectively for the forward evolution.

In Parwani and Tarih [4] many interesting properties were found for this cosmological model for various values of ζ and η. Firstly, it was found that a maximum size for the universe, a_{max}, existed for all values of ζ and η (Figures 5.1 and 5.2). This maximum size occurs because in the forward evolution, after several iterations, a lattice point which is negative or complex is found. Such a point denotes the beginning of an unphysical region, and as such constrains the range of scale factors within which the quantum universe can be found. It was also found that as ζ increases, the value of a_{max} decreases.

Also, as ζ is increased while η is kept constant, there is a certain critical ζ value (ζ_c) beyond which we find the occurrence of a minimum size to the universe, a_{min} (Figure 5.3). This occurs in a similar manner to the occurrence of the point a_{max}, that is, a negative/complex lattice point is encountered in the backward evolution, and is considered to be the beginning of an unphysical region.

The trend for a_{max} values also changes once ζ_c is encountered, that is, a_{max} increases as ζ increases, for $\zeta \geq \zeta_c$. Also the trend for a_{min} is that it decreases as ζ is increased. Thus, we find that the range of allowable scale factor values increases as

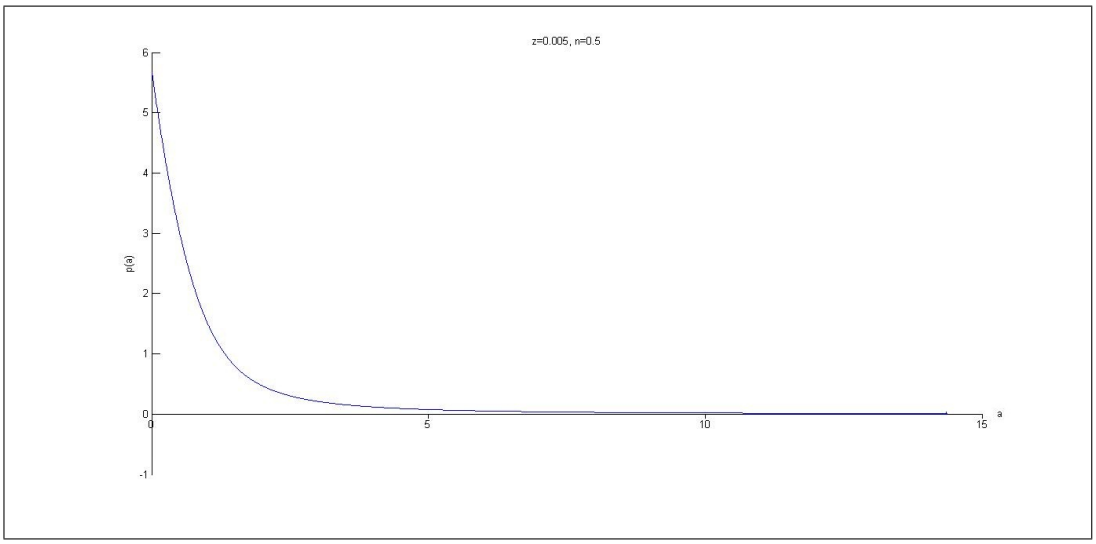

Figure 5.1: Plot of the probability density function $p(a)$ as a function of the scale factor a, for $\zeta = 0.005$ and $\eta = 0.5$.

ζ is increased, as long as $\zeta \geq \zeta_c$. Also, the probability density implying a minimum and maximum allowable size to the universe also allows for the existence of cyclic universes, with bounces at a_{min} and a_{max}. We may confirm such behaviour if the effective potential forms real barriers at a_{min} and a_{max}. A minimum size to the quantum universe is ideal because it allows us to avoid the problem of a singularity at $a = 0$. But what about the quantum universes which have $\zeta < \zeta_c$? Fortunately,

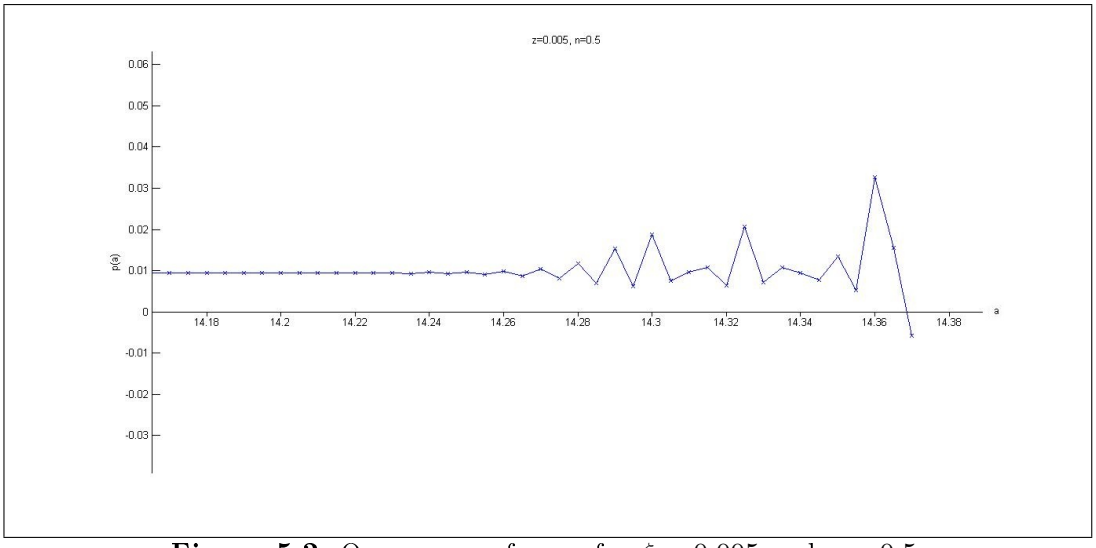

Figure 5.2: Occurrence of a_{max} for $\zeta = 0.005$ and $\eta = 0.5$.

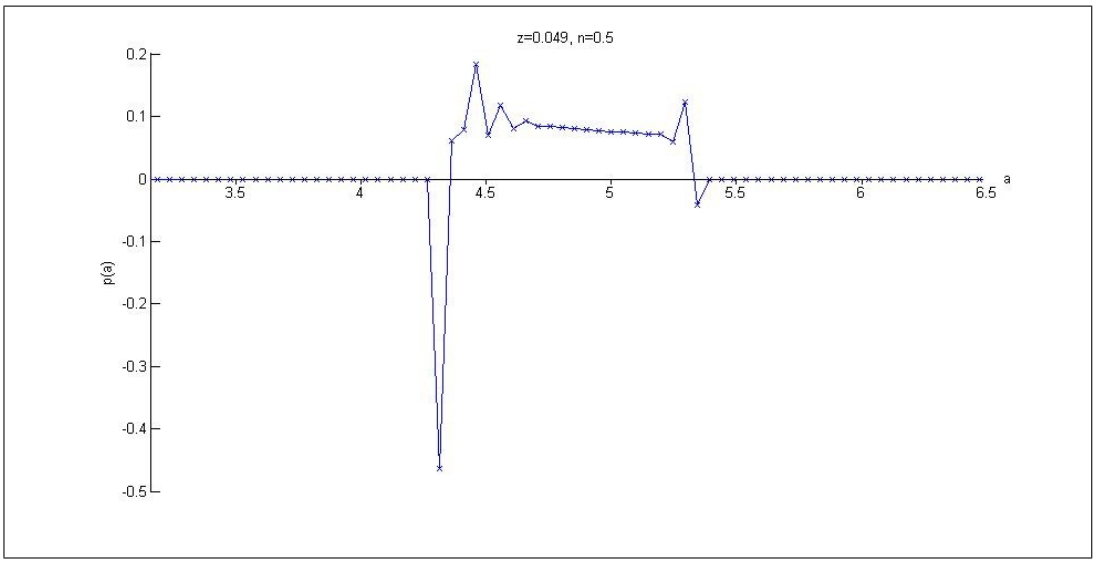

Figure 5.3: Plot of the probability density function $p(a)$ as a function of the scale factor a, for $\zeta = 0.049$ and $\eta = 0.5$.

when we study the effective potential $V_{eff} \equiv -a^4 + F(p)$, we find a real potential barrier close to $a = 0$, as seen in Figure 5.4, as long as $\eta < 3/4$, which is in agreement with the pertubative treatment. This type of potential barrier occurs for all low values of ζ, as long as $\eta < 3/4$, and possibly higher values of ζ, but this cannot be determined accurately since when generating the potential numerically, we need to

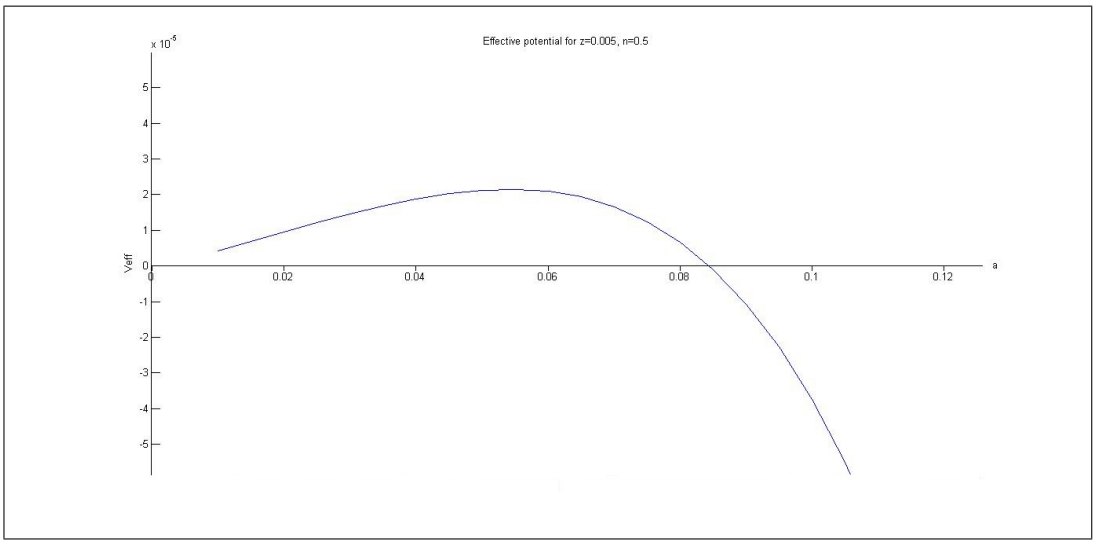

Figure 5.4: Plot of the effective potential V_{eff} as a function of the scale factor a, for $\zeta = 0.005$ and $\eta = 0.5$.

use the central difference approximation (to calculate the term Q), which is not an accurate approximation for large lattice spacing.

5.3 The Scale Factor Varying Cosmological Constant

We now extend the work done by Parwani and Tarih to a more general case, that is a model in which we replace the non-varying cosmological constant by one that is a function of the scale factor, $\Lambda(a)$.

The Einstein-Hilbert action for a FLRW universe is:

$$S = \int dtL = \frac{1}{2}\int dtNa^3\left[-\frac{\dot{a}^2}{N^2a^2} + \frac{\dot{\phi}^2}{N^2} - V(\phi) + \frac{k}{a^2}\right]. \tag{5.17}$$

For a slowly varying scalar field the action reduces to:

$$S = \int dtL = \frac{1}{2}\int dtN\left[-\frac{\dot{a}^2 a}{N^2} + a\left(k - \frac{a^2}{a_0^2}\right)\right], \tag{5.18}$$

where the kinetic energy term has been ignored, and,

$$\frac{1}{a_0^2} = V(\phi) = \frac{\Lambda}{3}. \tag{5.19}$$

Now in Parwani and Tarih, the cosmological constant was treated as being both a constant of time, t and the scale factor, a. In that case setting the kinetic energy term to zero was not an approximation. However when one chooses to vary the cosmological constant, Λ, one has a varying potential $V(\phi)$, and as such the kinetic energy term will not be zero. We shall ignore the kinetic energy term by assuming that the variation is slow, in order to simplify the analysis. Because of this simplification, the following analysis of the varying cosmological constant case should be considered as an approximation.

We shall now make the cosmological constant a function of the scale factor, a, by setting,

$$a_0 = \frac{(1 + a^{2m})}{(1 + 5^{2m})}, \tag{5.20}$$

which in turn gives us a cosmological constant of the form:

$$\Lambda(a) = \frac{3}{a_0^2} = 3\frac{(1 + 5^{2m})^2}{(1 + a^{2m})^2}, \tag{5.21}$$

where m is a parameter that can only take values $0 < m \leq 1$ (the $m = 0$ case corresponds to a non-varying cosmological constant). m is constrained to these values since it can be shown that when $m > 1$, our previous assumption that the kinetic energy term is small at all times is violated.

The factor of $(1 + 5^{2m})^2$ is a convenient normalisation used to simplify our numerical calculations, as will be explained later in this chapter. Figure 5.5 shows how the cosmological constant in equation (5.21) varies as a function of a for various m values. It is obvious from the figure that the cosmological constant is large when the universe is small, and drops in magnitude as the universe expands. The magnitude of the cosmological constant when the universe is small depends on the parameter m.

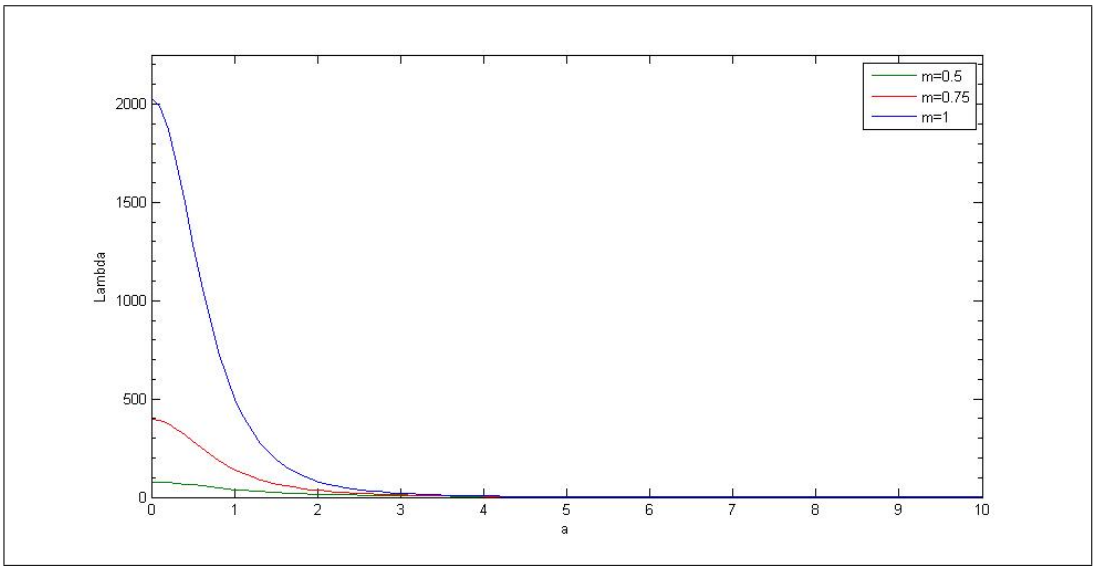

Figure 5.5: The cosmological constant, $\Lambda(a)$ as a function of the scale factor a, for m=0.5, 0.75 and 1. Though not obvious from the diagram, all three functions are equal at $a = 5$, as expected.

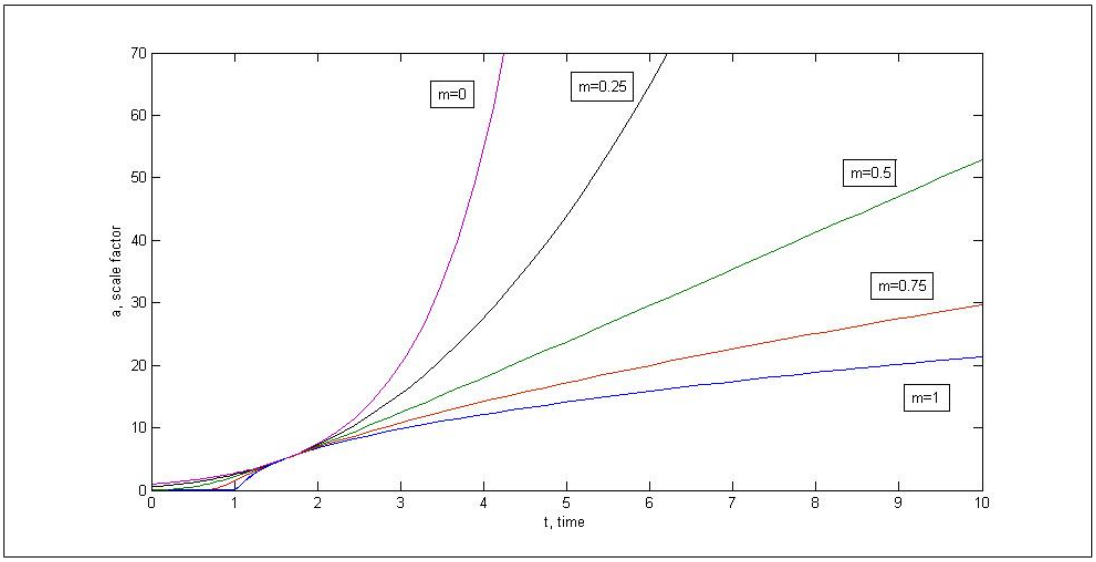

Figure 5.6: The classical evolution of universes with m=0, m=0.25, m=0.5, m=0.75 and m=1. Note that although not shown here, t can be negative, since for the $m = 0$ case $a = 0$ when $t = -\infty$. Also, as expected, $a = 5$ at the same time for all five universes.

We are still able to find the Friedmann equation as before, by varying the action with respect to the lapse function, N and choosing the gauge $N = 1$, giving us:

$$\dot{a}^2 + \left(k - a^2 \frac{(1+5^{2m})^2}{(1+a^{2m})^2} \right) = 0. \tag{5.22}$$

We wish to study only flat universes, and thus we set $k = 0$. This equation can then be solved numerically in terms of a. Figure 5.6 shows the classical evolution of the scale factor, a with time, t, for various values of the parameter m. It is clear that as m is increased, there is decreasing acceleration for the classical universe. For $m = 0.5$ linear expansion occurs after a certain point in time, and for any $m > 0.5$ we find deceleration in the universe after a certain point in time.

We may once again perform minisuperspace quantization as before, replacing the canonical momentum $p_a = \frac{\partial L}{\partial \dot{a}} = -\dot{a}a$ by the operator $\hat{p} = -i\frac{\partial}{\partial a}$, giving us the

following Wheeler-DeWitt equation.

$$\left[-\frac{\partial^2}{\partial a^2} - a^4\frac{(1+5^{2m})^2}{(1+a^{2m})^2}\right]\psi(a) = 0 \tag{5.23}$$

We may solve this equation numerically for $\psi(a)$, from which we can obtain the probability density distribution, $p(a)$ for various values of m. Examples of these are shown in Figures 5.7-5.10.

Next, we nonlinearise within the information theory framework (references [2,26]), giving rise to the following nonlinear Wheeler-DeWitt equation,

$$\left[-\frac{\partial^2}{\partial a^2} - a^4\frac{(1+5^{2m})^2}{(1+a^{2m})^2} + F(p)\right]\psi(a) = 0. \tag{5.24}$$

We shall avoid studying this equation pertubatively, since in the study involving the non-varying cosmological constant, it was found that the non-pertubative treatment provided more information, and therefore we shall proceed with such a treatment, which shall give us a difference equation. As usual we make the Madelung transformation $\psi = \sqrt{p}e^{iS}$, giving us an equation with a real and imaginary part. In fact, the derivation of the difference equation for this case is identical to that of the case of a non-varying cosmological constant, as shown in Appendix A, since the only difference

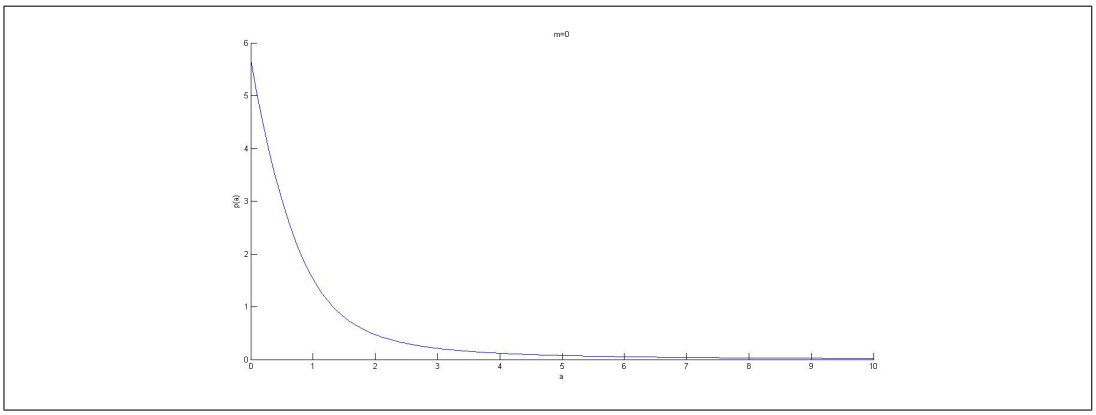

Figure 5.7: Probability density distribution for $m = 0$. This is equivalent to the non-varying cosmological constant case, and should be used for comparison with the following figures.

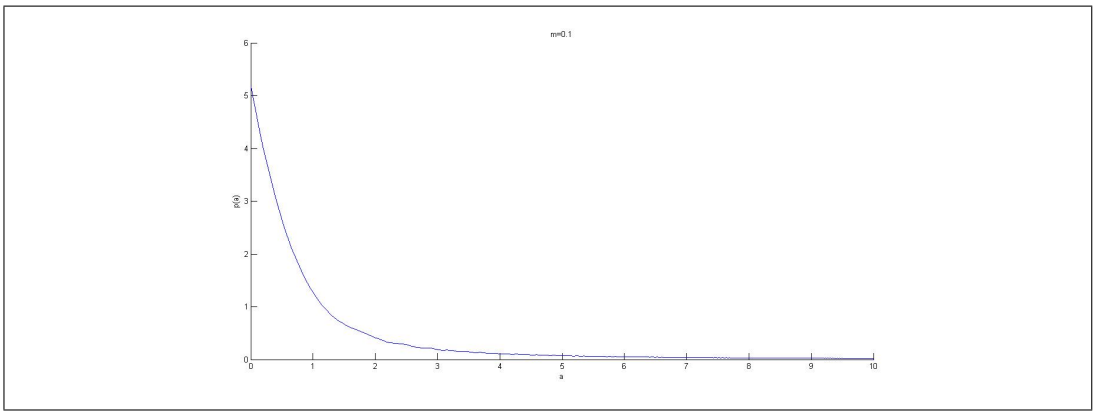

Figure 5.8: Probability density distribution for $m = 0.1$. There are small-amplitude oscillations along this curve, which are too small to be seen here.

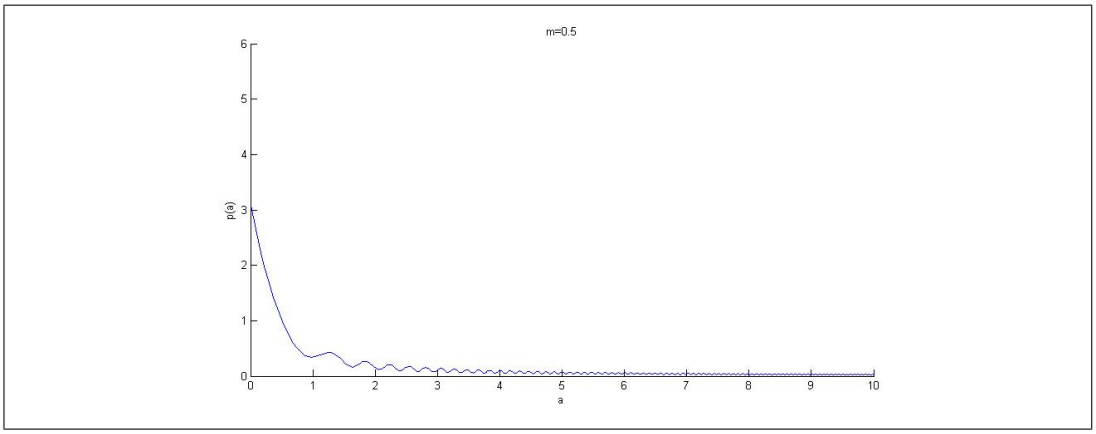

Figure 5.9: Probability density distribution for $m = 0.5$. Here we see oscillations that decrease in both amplitude and wavelength as a increases.

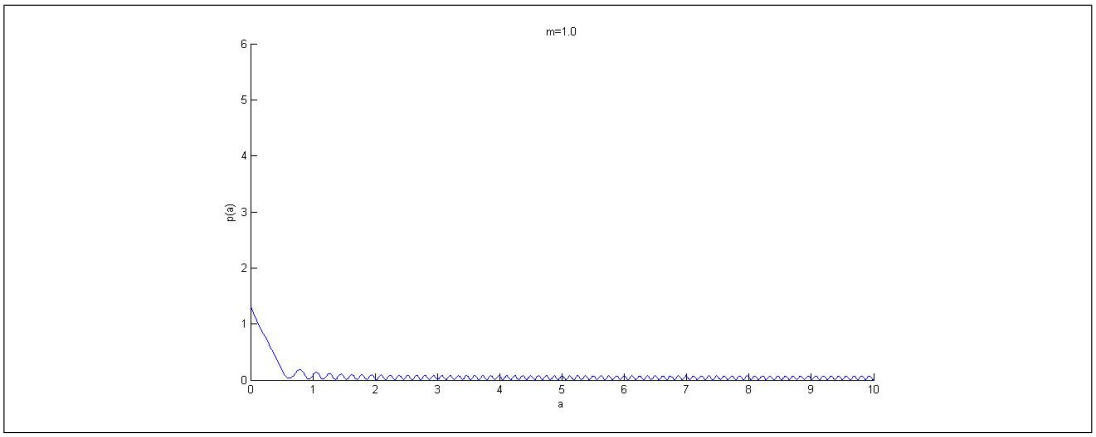

Figure 5.10: Probability density distribution for $m = 1$. In this case the oscillations are constant in amplitude and wavelength after a certain value of a.

is that now a_0 is not a constant but a variable (equation (5.20)). Thus we can just replace the new form of a_0 into the difference equation (equation (5.9)), giving us:

$$\left(\frac{\sigma}{p}\right)^2 = a^4\frac{(1+5^{2m})^2}{(1+a^{2m})^2} - \frac{1}{2\zeta^2\eta^2}\left[\ln\left(\frac{p}{(1-\eta)p+\eta p_+}\right) + \frac{\eta p_+}{(1-\eta)p+\eta p_+} - \frac{\eta p_-}{(1-\eta)p_- + \eta p}\right] \tag{5.25}$$

We shall study this difference equation numerically for $m = 0.1$, $m = 0.5$ and $m = 1$, since this should be sufficient to understand the change in behaviour in the probability density, $p(a)$ as m is increased from 0 to 1. The parameter ζ will be varied in the range $0 > \zeta > 1$, whereas for the parameter η we shall concentrate mainly on $\eta = 0.5$, since varying η does not provide us with much new behaviour.

5.4 Numerical Analysis

In our numerical analysis, we follow the method of Parwani and Tarih [4], where we use the solution to the linear Wheeler-DeWitt equation to find the values of the two initial lattice points, and evolve backward as well as forward from those points. We have once again assumed that at a certain size, $a = 5$, the solution of the nonlinear Wheeler-DeWitt equation approaches that of the linear one. Here we are able to understand why the factor of $(1 + 5^{2m})$ was included when defining the cosmological constant in equation (5.21), as follows. At $a = 5$, the factor allows our nonlinear Wheeler-DeWitt equation for a scale factor-varying cosmological constant, equation (5.24) to become the nonlinear Wheeler-DeWitt equation for a non-varying cosmological constant,

$$\left[-\frac{\partial^2}{\partial a^2} - a^4 + F(p)\right]\psi(a) = 0. \tag{5.26}$$

Then by assuming that the nonlinearity is small/zero at this size, this equation becomes the linear equation (5.5), and as such we are still able to use the linear solution (5.16) for our initial value of $p(a)$ at the lattice point $a = 5$ when solving the difference equation. For the other initial lattice point at $a = 5 - \zeta$ we do not exactly retrieve

equation (5.26), but since we are constrained to small ζ values, using equation (5.26) with zero nonlinearity to find the initial value at that point is a good approximation.

For the backward evolution, we once again have to make the same variable change as in the previous case ($a \to a + \zeta$), in order to obtain an explicit form for $p(a)$ in terms of two other lattice points. This variable change causes the same relabelling of the probability density terms as before (eqs. (5.10) to (5.12)), and thus we have:

$$p(a) = \frac{\eta p_+(a)}{(1-\eta)} \left[\frac{1}{1 - (\frac{1-\eta}{\eta})D} - 1 \right], \tag{5.27}$$

where,

$$D = \ln\left(\frac{p_+}{(1-\eta)p_+ + \eta p_{++}}\right) + \frac{\eta p_{++}}{(1-\eta)p_+ + \eta p_{++}} - 2\zeta^2\eta^2 \left((a+\zeta)^4 \frac{(1+5^{2m})^2}{(1+(a+\zeta)^{2m})^2} - \frac{\sigma^2}{p_+^2} \right). \tag{5.28}$$

We use the linear solution (5.16) to calculate the two initial lattice points p_{++} and p_+ and use them to find p. Next we refer to p_+ as p_{++}, and p as p_+, and find the next lattice point value. Iterating this process several times, we are able to find the probability density $p(a)$ for lattice points at smaller scale factor values than the two initial points. Similarly, for the forward evolution, we call the same two initial points p_- and p, and use the discrete difference equation as a function of p_+ in Newton's method, which is then used to obtain p_+. Renaming the points and iterating the process in a manner similar to the backward evolution, we are able to generate the entire profile of the probability density $p(a)$ as a function of a.

5.5 Results

5.5.1 m=1

For the case of $m = 1$, we vary the parameter ζ, while the parameter η is kept equal to 0.5, in order to obtain various probability density distributions, $p(a)$. The first major difference from the non-varying cosmological constant case that is immediately

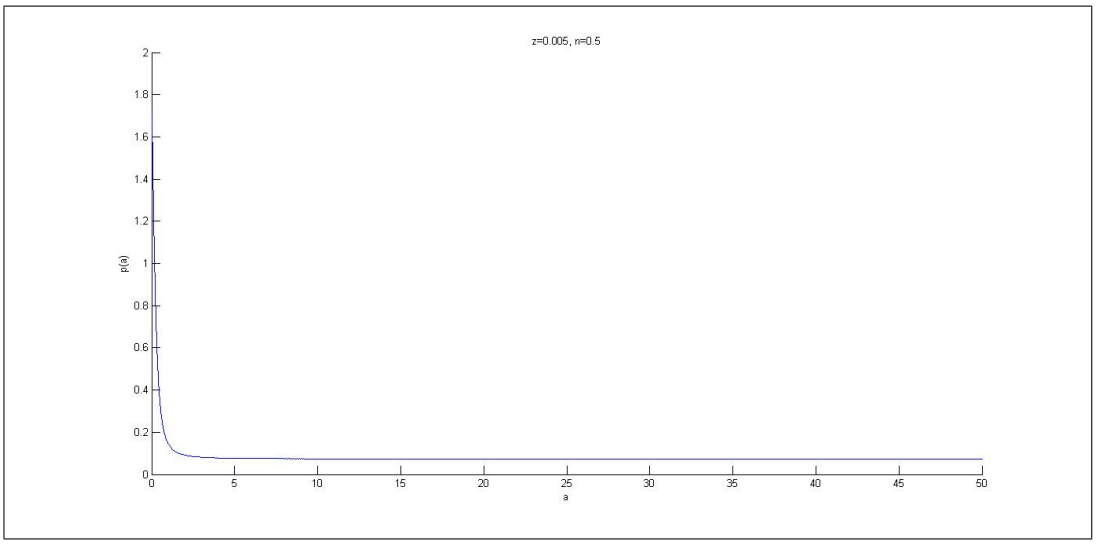

Figure 5.11: Plot of the probability density function $p(a)$ as a function of the scale factor a, for $m = 1$, $\zeta = 0.005$ and $\eta = 0.5$.

apparent is that for low values of ζ there is no a_{max}, as seen in the plot of the probability density function, $p(a)$ for $\zeta = 0.005$ (Figure 5.11). This however immediately poses a problem: since $p(a)$ does not seem to vanish as $a \to \infty$, it is not normalizable. This could be an effect of our analysis being an approximate one, since we have ignored the kinetic energy term in the Einstein-Hilbert action, equation (5.17). It

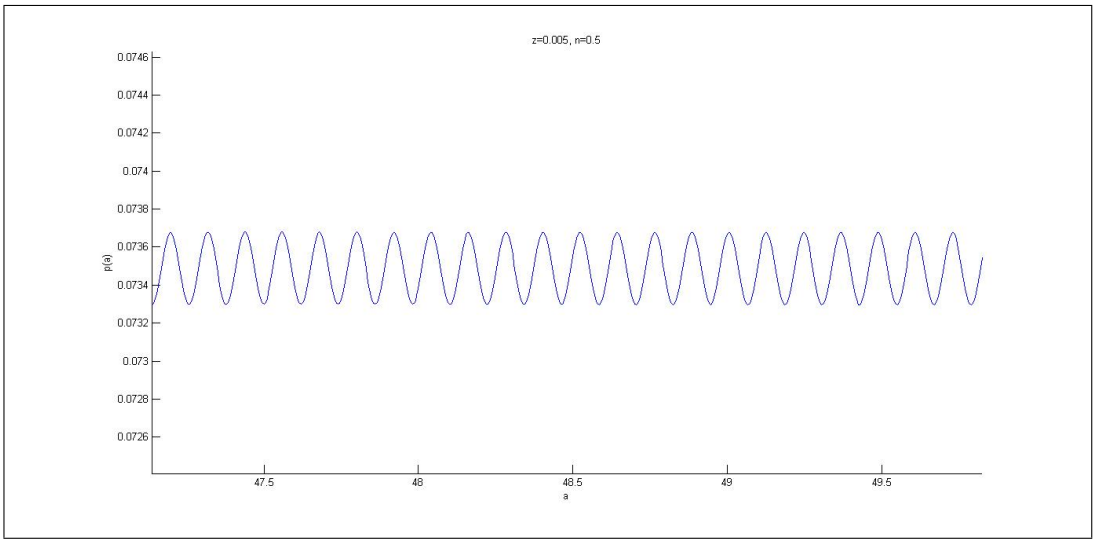

Figure 5.12: Oscillations in the probability density function $p(a)$ for $m = 1$, $\zeta = 0.005$ and $\eta = 0.5$.

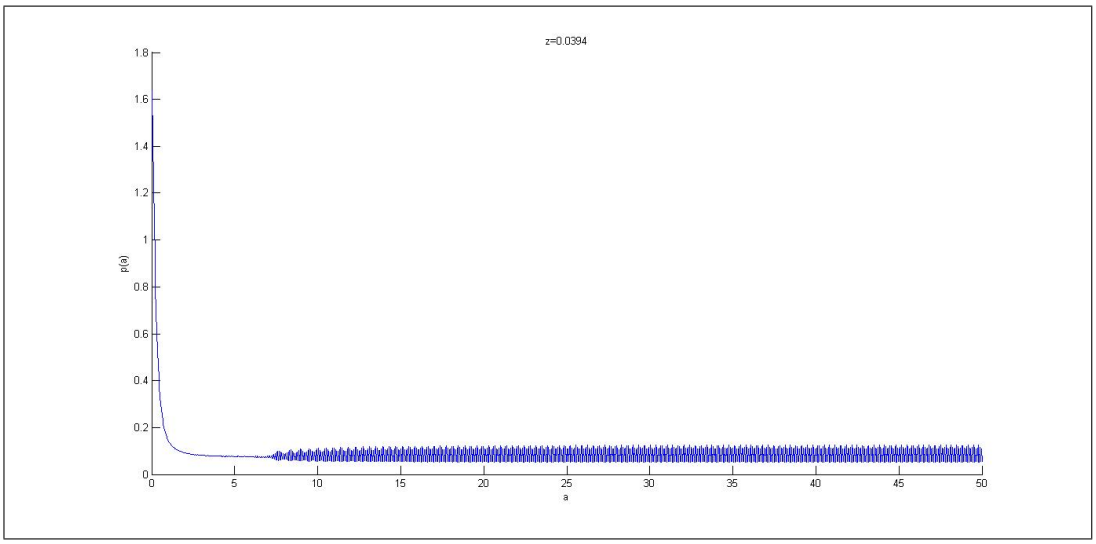

Figure 5.13: Plot of the probability density function $p(a)$ as a function of the scale factor a, for $m = 1$, $\zeta = 0.0394$ and $\eta = 0.5$.

should be noted that in the $m = 0$ case studied by Parwani and Tarih [4], oscillations of small amplitude, which tend to decrease in wavelength and increase in amplitude as a is increased, were found in the probability density curves. Though not obvious from Figure 5.11, similar oscillations were also found for $m = 1$, but with much larger amplitude and wavelength for identical values of ζ, as seen in Figure 5.12.

As ζ is increased, we find that the oscillations slowly increase in amplitude, and decrease in wavelength, eventually giving us a profile as seen in Figures 5.13 and 5.14, which are for $\zeta = 0.0394$. As we increase ζ further, we eventually encounter a critical value, ζ_c^{max}, at which we find an a_{max} in the probability density function. For the $m = 1$ case, we find that $\zeta_c^{max} = 0.0397$, and the occurrence of a_{max} for this ζ value can be seen in Figure 5.15.

It can easily be seen that the oscillations that are seen in Figure 5.14 and Figure 5.15 have amplitudes that seem to be modulated periodically. However, this is probably an effect of the larger lattice spacing (due to the higher values of ζ) causing the actual shape of the oscillations to be distorted.

As we increase ζ even further, there will be a value, ζ_c^{min}, at which we find an a_{min}. For $m = 1$, we have $\zeta_c^{min} = 0.0407$. Figure 5.16 shows an example of an a_{min}

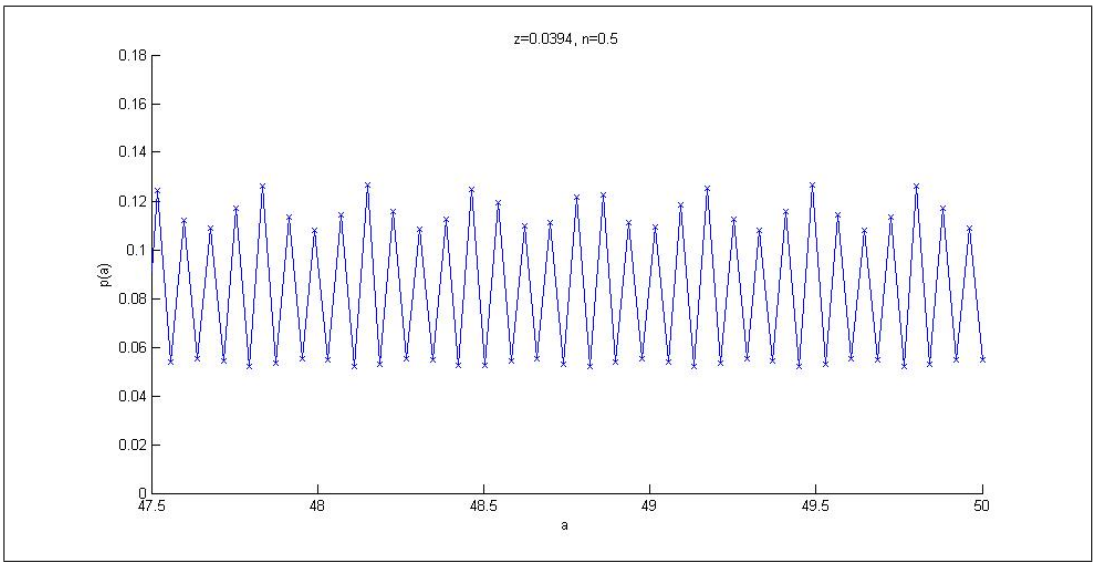

Figure 5.14: Oscillations in the probability density function $p(a)$ for $m = 1$, $\zeta = 0.0394$ and $\eta = 0.5$. Here the lattice points are denoted, in order to show that the larger spacings between them have distorted the profile slightly.

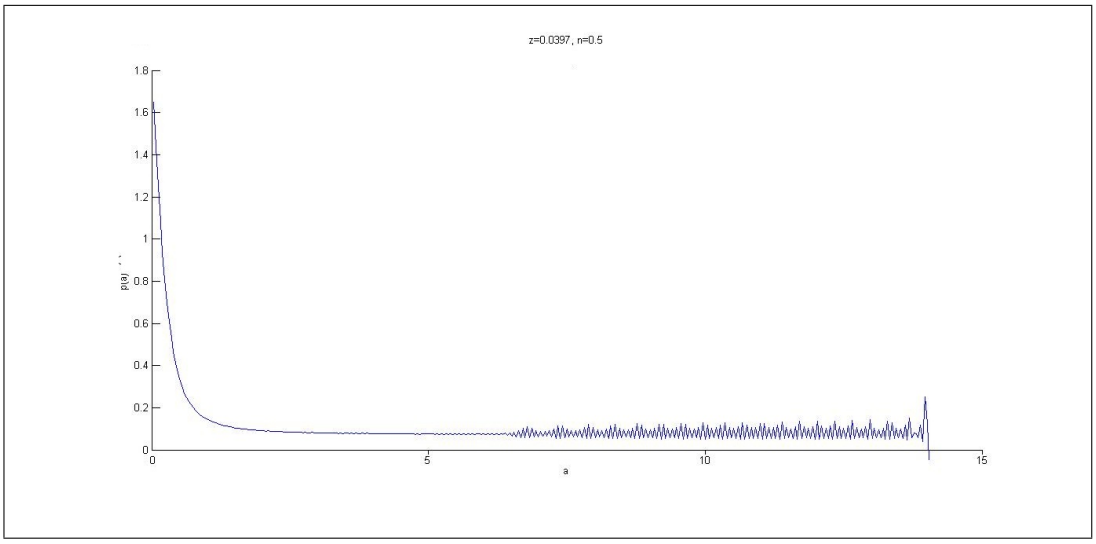

Figure 5.15: Plot of the probability density function $p(a)$ as a function of the scale factor a, for $m = 1$, $\zeta = 0.0397$ and $\eta = 0.5$. Here $a_{max} = 14.037$

occurring for $\zeta > \zeta_c^{min}$.

Increasing ζ above the two critical values does not give us much new features. The only notable feature is the slight change in trend for the values of a_{min} as ζ is increased. Whereas for the $m = 0$ case, a_{min} in general decreases as ζ is increased, here we see that for low ζ values a_{min} in general increases for increasing ζ, before

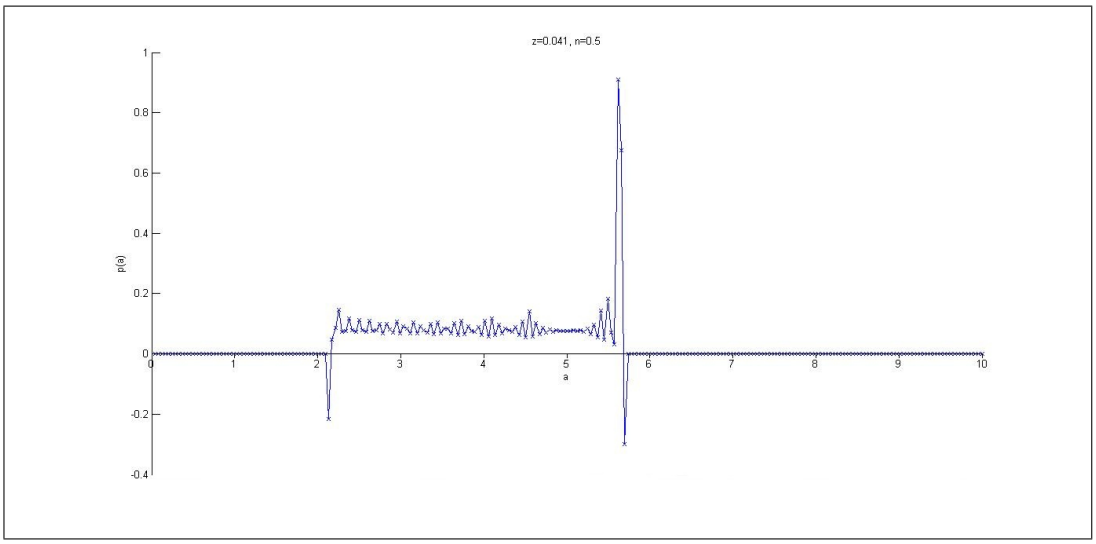

Figure 5.16: Plot of the probability density function $p(a)$ as a function of the scale factor a, for $m = 1$, $\zeta = 0.041$ and $\eta = 0.5$.

giving way to the typical decreament seen in the $m = 0$ case, as seen in Figure 5.17. The behaviour of a_{max} however is similar to the $m = 0$ case, where a_{max} in general decreases, before beginning to increase again about ζ_c^{min} onwards. In other words, the range of allowed scale factor, a, values increases with increasing ζ. However these are only a general trends, and there are occasionally sudden jumps from this behaviour.

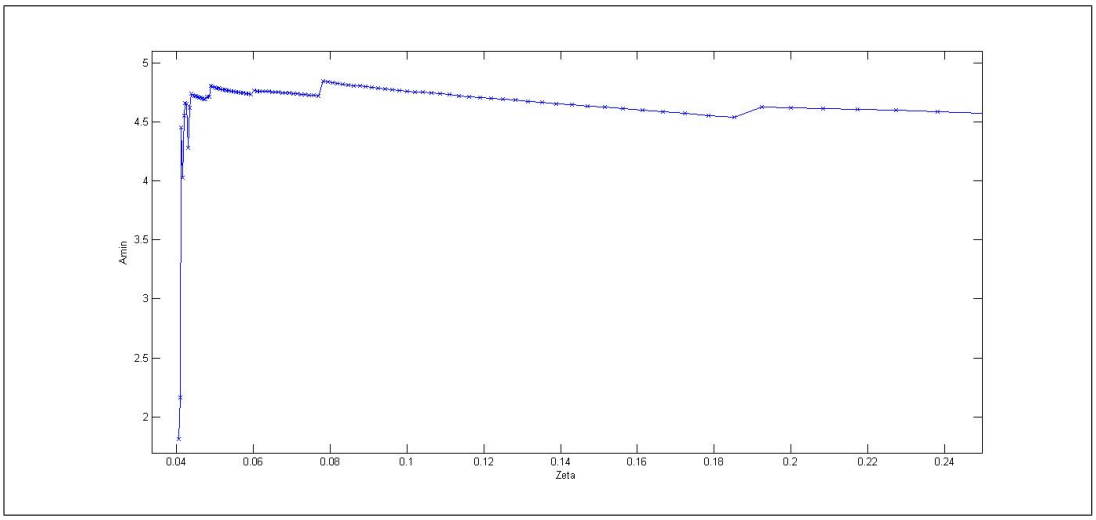

Figure 5.17: Plot of the variation of a_{min} values with ζ, for $m = 1$. Though not shown in this plot, a_{min} decreases monotonically for $\zeta > 0.24$.

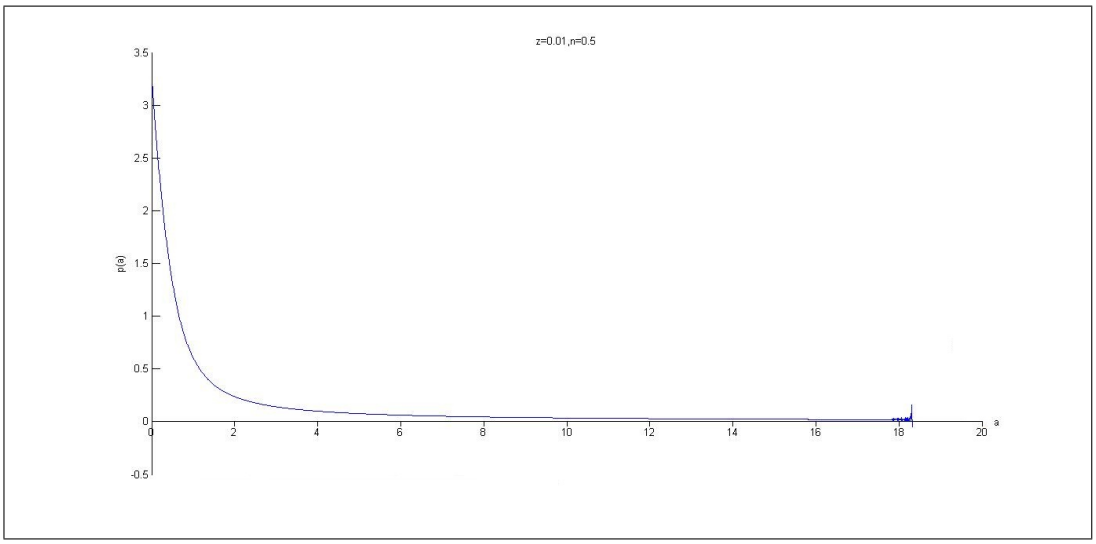

Figure 5.18: Plot of the probability density function $p(a)$ as a function of the scale factor a, for $m = 0.5$, $\zeta = 0.01$ and $\eta = 0.5$. Here $a_{max} = 18.317$.

5.5.2 m=0.5

For the case of $m = 0.5$ we find results that are closer in behaviour to the $m = 0$ case. For all ζ, even as low as 0.0005, we always find the occurrence of an a_{max}. The critical ζ value beyond which the occurrence of a_{min} is found (ζ_c^{min}) is 0.0438.

The probability density distributions found for low ζ were similar to Figure 5.15, except that the oscillations in the curve were much less obvious, as in Figure 5.18. As ζ is increased, we find that the oscillations behave differently from the $m = 1$ case, in that they now increase in both wavelength and amplitude, thus becoming increasingly less apparent. This trend continues until ζ is close to ζ_c^{min}, where the amplitude of the oscillations suddenly grow, giving us a profile as in Figure 5.19.

Beyond ζ_c^{min}, the probability density distributions exhibited both a_{min} and a_{max}, as in Figure 5.16. Unlike the $m = 1$ case, we find that a_{min} in general only decreases as ζ is increased (for ζ values at which it occurs). The trend in the variation of a_{max} however, is similar to that of the $m = 0$ and $m = 1$ case, that is it decreases as ζ is increased, but only until $\zeta = \zeta_c^{min}$, beyond which it generally increases. There are again, however, some instances where jumps from monotonic behaviour are noted in

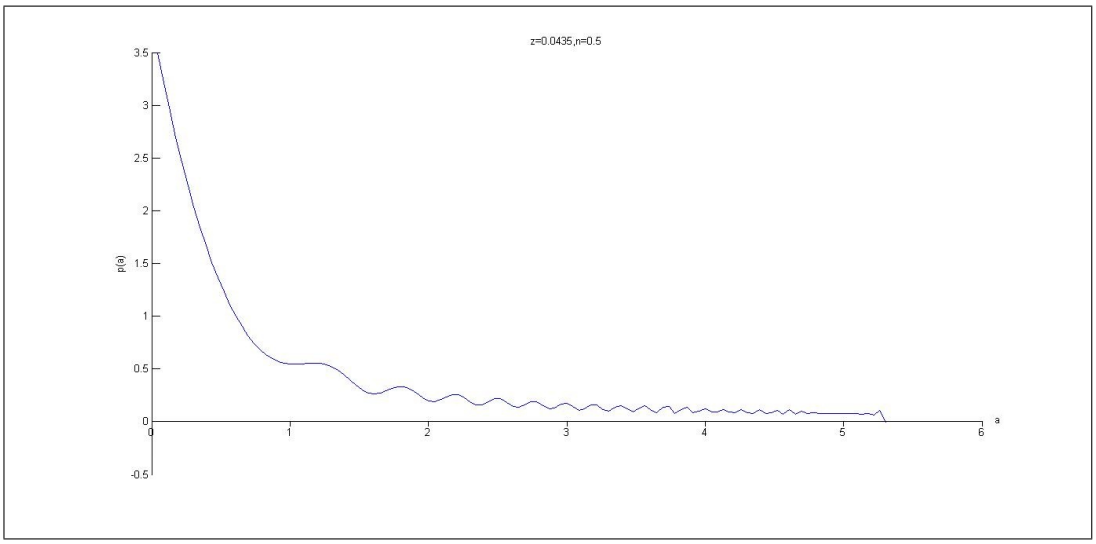

Figure 5.19: Plot of the probability density function $p(a)$ as a function of the scale factor a, for $m = 0.5$, $\zeta = 0.0435$ and $\eta = 0.5$. Here $a_{max} = 5.302$

these trends, as before. Also, the oscillations seen in the profiles for $\zeta < \zeta_c^{min}$ also seem to be of smaller amplitude, when compared to those seen in profiles with $m = 1$ for the same value of the parameter ζ. We also find that, for low ζ, a_{max} ($\zeta \leq 0.04237$) and a_{min} ($\zeta \leq 0.0463$) tend to be lower for $m = 0.5$ when compared to $m = 1$, for equal values of ζ.

5.5.3 m=0.1

For $m = 0.1$, we find behaviour that is even closer to the $m = 0$ case. a_{max} occurs for all values of ζ, and as ζ is increased, a_{min} occurs for all $\zeta > \zeta_c^{min} = 0.0462963$.

For low values of ζ the a_{max} ($\zeta \leq 0.04065$) and a_{min} ($\zeta \leq 0.0641$) values tend to be even lower when compared to the previous cases, for equal values of ζ. The oscillations are also of even smaller amplitude in comparison to the previous cases, for equal values of ζ, and behave in a similar fashion to the oscillations found for $m = 0.5$ as we increase ζ.

The trends associated with the variation of a_{max} and a_{min} are similar to that found for $m = 0.5$. Here we find that as ζ is increased, a_{max} decreases until $\zeta = \zeta_c^{min}$, beyond which it increases. This behaviour is similar to that of all the previous cases.

a_{min} unsurprisingly varies like how it did for $m = 0.5$ and $m = 0$, that is it decreases as ζ is increased. Once again, there are some values of ζ for which the values of a_{max} and a_{min} do not follow these trends.

It should be noted that using the linear Wheeler-DeWitt equation (5.23), the probability density curves for all three values of m (Figures 5.8-5.10) already exhibit oscillations, and as such the oscillations we have seen thus far are probably not due to the effects of adding the nonlinear term to the equation alone.

5.6 Analytical Study of a_{min}, a_{max} and the Difference Equation

In the previous section we see the occurrence of minimum and maximum scale factor values beyond which the probability density distribution, $p(a)$ takes on negative/complex values, which are considered unphysical. These occurrences can be understood by noticing that the difference equation does not guarantee that $p(a)$ will remain positive when we evolve it backward or forward from two initial points. This can be easily seen by studying the form of the difference equation used for the backward evolution, equation (5.27).

We first intend to understand why we do not see an a_{max} for $m = 1$ at low values of ζ. Using the difference equation (5.25), we first set $p_+ = p(a_{max}) = 0$, which then requires that $p = p(a_{max} - \zeta)$ and $p_- = p(a_{max} - 2\zeta)$. We then assume that for $\zeta \to 0$, the slope of the wavefunction, $\psi'(a)$ is a constant close to the point a_{max}. This is a valid assumption, as long as the wavefunction, $\psi(a)$ is smooth near the point a_{max}. Also since $p(a_{max}) = 0$, $\psi(a_{max}) = 0$. Thus, using a Taylor's series approximation, we have:

$$\psi(a_{max} - \zeta) \approx \psi(a_{max}) - \zeta\psi'(a_{max}) \tag{5.29}$$

$$= -\zeta\gamma \tag{5.30}$$

Here γ is the constant slope of the wavefunction, $\psi'(a)$, for any a close to a_{max}.

Likewise,

$$\psi(a_{max} - 2\zeta) \approx \psi(a_{max}) - 2\zeta\psi'(a_{max}) \tag{5.31}$$

$$= -2\zeta\gamma \tag{5.32}$$

The following expressions for p and p_- then immediately follow:

$$p = (\zeta\gamma)^2 \tag{5.33}$$

$$p_- = (2\zeta\gamma)^2 \tag{5.34}$$

Using these expressions, together with $p_+ = 0$ in the difference equation (5.25), we obtain the following expression (with $a = a_{max} - \zeta$):

$$\left(\frac{\sigma}{(\zeta\gamma)^2}\right)^2 = (a_{max}-\zeta)^4 \frac{(1+5^{2m})^2}{(1+(a_{max}-\zeta)^{2m})^2} - \frac{1}{2\zeta^2\eta^2}\left(\ln\left(\frac{1}{1-\eta}\right) - \frac{\eta(2\zeta\gamma)^2}{(1-\eta)(2\zeta\gamma)^2 + \eta(\zeta\gamma)^2}\right) \tag{5.35}$$

or,

$$(a_{max}-\zeta)^4 \frac{(1+5^{2m})^2}{(1+(a_{max}-\zeta)^{2m})^2} = \frac{1}{\zeta^2}\left(\frac{\sigma^2}{\gamma^4\zeta^2} - \frac{1}{2\eta^2}\left(\ln(1-\eta) + \frac{4\eta}{4-3\eta}\right)\right). \tag{5.36}$$

Now we know from our numerical results that for low values of ζ and for $m = 1$, a_{max} is very large, and possibly infinite. It is thus safe to assume that $1 + (a_{max} - \zeta)^{2m} \approx (a_{max} - \zeta)^{2m}$, and $\zeta \approx 0$. This gives us

$$a_{max} \approx \left(\frac{1}{(\zeta^2)(1+5^{2m})^2}\left(\frac{\sigma^2}{\gamma^4\zeta^2} - \frac{1}{2\eta^2}\left(\ln(1-\eta) + \frac{4\eta}{4-3\eta}\right)\right)\right)^{\frac{1}{4-4m}} \tag{5.37}$$

From this expression we see that when we set $m = 1$, a_{max} is approximately infinity.

So far we have investigated the behaviour close to the point a_{max}, by setting $p_+ = 0$. However, we see that setting $p = 0$ in the difference equation (5.25) leads to a divergence via the logarithmic term. However, if we rearrange the difference

equation and take the limit $p \to 0$, we obtain

$$2\zeta^2\eta^2\sigma^2 = -\lim_{p\to 0} p^2 \left(\ln\left(\frac{p}{(1-\eta)p + \eta p_+} \right) + \frac{\eta p_+}{(1-\eta)p + \eta p_+} - \frac{\eta p_-}{(1-\eta)p_- + \eta p} \right). \tag{5.38}$$

Since

$$\lim_{p\to 0} p^2 \left(\ln\left(\frac{p}{(1-\eta)p + \eta p_+} \right) \right) = 0, \tag{5.39}$$

we can then obtain the consistency relation

$$-2\zeta^2\eta^2\sigma^2 = \lim_{p\to 0} p^2 \left(\frac{\eta p_+}{(1-\eta)p + \eta p_+} - \frac{\eta p_-}{(1-\eta)p_- + \eta p} \right). \tag{5.40}$$

Thus, in order for the right hand side to remain constant, the coefficient of p^2 in the expression above must develop a $1/p^2$ divergence, which must occur through either p_+ or p_- becoming negative. In other words we have proven that as $p \to 0$ at a point, either one of its adjacent points must enter an unphysical region. This relationship is obviously identical for all values of m, including the $m = 0$ case, as was shown in Parwani and Tarih [4].

Next we find an exact solution to the difference equation (5.25) using just three lattice points. Setting p_- and p_+ equal to 0, and letting p take some positive value at the mid-point, $a = a_m$, the difference equation becomes

$$\left(\frac{\sigma}{p} \right)^2 = a_m^4 \frac{(1+5^{2m})^2}{(1+a_m^{2m})^2} - \frac{1}{2\zeta^2\eta^2} \left(\ln\left(\frac{1}{1-\eta} \right) \right). \tag{5.41}$$

The first constraint is that the right side of this equation is positive definite. Next, assuming that $a_{min} \neq 0$, we obtain the second constraint, $a_m = a_{min} + \zeta$. Using these constraints gives us the expression

$$(a_{min} + \zeta)^4 \frac{(1+5^{2m})^2}{(1+(a_{min}+\zeta)^{2m})^2} \zeta^2 > \frac{1}{2\eta^2} \left(\ln\left(\frac{1}{1-\eta} \right) \right) \tag{5.42}$$

If we take $\eta \to 0^+$ or $\eta \to 1^-$, the right hand side of this expression blows up. For

constant ζ and m, this then implies that we have a large a_{min}, which in turn implies that we can have large universes, with sizes as large as $a_{min} + 2\zeta$.

5.7 Effective Classical Dynamics

The Wheeler-DeWitt equation is independent of time, and therefore does not give us any ideas about the time evolution of a universe. The wavefunction merely gives us the probability of observing a universe in an ensemble of universes with a certain scale factor value. In the numerical analysis we have seen how only a certain range of scale factors was allowed for certain universes, due to occurrences of maximum and minimum scale factor values for these universes. However we would like to understand the behaviour of only a single universe, and not only of the allowed scale factors it can take, but of its dynamics. The arguments we shall use in this section are based on those in Parwani and Tarih [4].

To understand the dynamics of a single universe we return the nonlinear Wheeler-DeWitt equation (5.24) to the classical regime, resulting in a modified Friedmann equation:

$$a^2\dot{a}^2 + V_{eff} = 0, \tag{5.43}$$

where the effective potential

$$V_{eff} = -a^4\frac{(1+5^{2m})^2}{(1+a^{2m})^2} + F(p). \tag{5.44}$$

This Friedmann equation describes the classical dynamics of a single universe. However one must be aware that we are only able to do this since dS/da blows up near the nodes a_{max} and a_{min}, due to equation (5.4), enabling us to make a semiclassical approximation of the wavefunction; and since, as argued by Halliwell [27], dS/da has a correlation with the classical momentum for any oscillatory wavefunction of the form e^{iS}. Then, as in Atkatz [12], such a semiclassical approximation of the oscillatory

wavefunction will give rise to a Friedmann equation as in equation (5.43).

As long as the term $F(p)$ is small, then it cannot overcome the other term in V_{eff} (especially when a is large), and as such V_{eff} remains negative, and the expansion of the universe is unbounded. However $F(p)$ does not always remain small. Near one of the nodes (which we shall refer to as a_*), where the wavefunction, and thus p goes to zero, we find that $p \equiv |\psi|^2 \sim (a - a_*)^2$, by making a linear approximation in a manner similar to that done in the previous section. Equation (5.40) then tells us that $Q_{NL} \sim -1/p^2$, and we also notice that Q (equation (4.5), with $\hbar = 1$ and $m = 1/2$) is also possibly large and diverging. There is thus a possibility that $F(p) = Q_{NL} - Q$ is positive and large near the nodes. It is worth mentioning that the enhancement of the nonlinearity near nodes is found for simpler quantum mechanical problems as well, as in reference [26].

V_{eff} was found to be negative between the nodes a_{min} and a_{max}, for cases where both occur. In some cases we see a complex or real potential barrier developing close to a_{min} or a_{max}. For example, for $m = 0.1$, $\zeta = 0.0467$ and $\eta = 0.5$ we find a real potential barrier occurring close to a_{min}; and for $m = 0.2$, $\zeta = 0.02$, and $\eta = 0.8$, we see a real potential barrier close to a_{max}. We also see cases where real barriers occur close to both a_{min} and a_{max}, such as for $m = 1$, $\zeta = 0.042$ and $\eta = 0.5$ (Figure 5.20). It should however be noted that these potential barriers do not occur exactly at the nodes, and $p(a)$ can still be nonzero in regions where the potential is positive. This is not surprising as we are dealing with a quantum system.

A real potential barrier indicates that the region beyond it is classically inaccessible, and is desirable because it would imply that a bounce could possibly occur at the barrier in the effective classical dynamics of the system, and this shall be analytically proven to be indeed true shortly. Likewise, if we have potential barriers at small and large size, it can be shown that bounces occur at both these barriers, leading to a cyclic evolution for this universe. However the possibility of a cyclic universe is not precluded for all universes for which an a_{min} does not exist. Numerically, we find

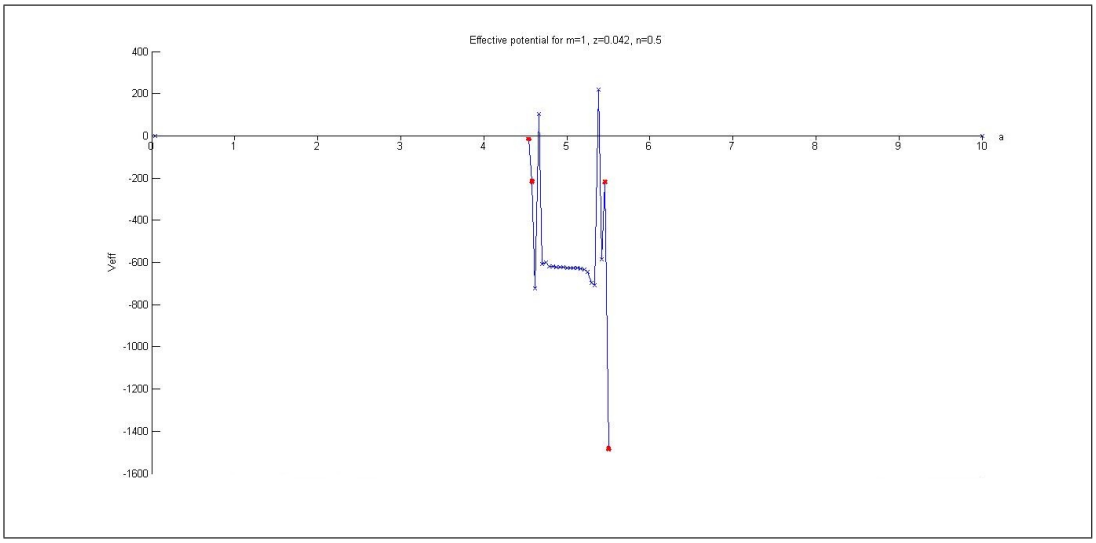

Figure 5.20: Plot of the effective potential for $m = 1$, $\zeta = 0.042$ and $\eta = 0.5$. The blank parts of the plot indicate regions where the effective potential is undetermined, which is due to $F(p)$ becoming undetermined whenever two adjacent lattice points in $p(a)$ are zero. The red squares indicate points where the potential has become complex.

that as long as $\eta < 3/4$, we see a small but finite potential barrier close to $a = 0$, which will prevent a collapsing universe from reaching zero size. Thus, whenever we have a real potential barrier at a_{max} for any $\eta < 3/4$, a cyclic universe will occur. An example of this is for $m = 0.5$, $\zeta = 0.0167$, and $\eta = 0.5$ as seen in Figure 5.21 and Figure 5.22.

We now proceed to show that the real potential barriers near a_{max} and a_{min} are indeed classical turning points at which bounces occur. We rearrange equation (5.43) and equate it to a new 'modified' potential function $V(a)$,

$$\dot{a}^2 = -\frac{V_{eff}}{a^2} = V(a), \tag{5.45}$$

on which we can then perform a Taylor expansion about the node a_*, giving us,

$$\dot{a}^2 \approx V(a_*) + (a - a_*)V'(a_*). \tag{5.46}$$

The prime here denotes differentiation with respect to a. In our numerical analysis

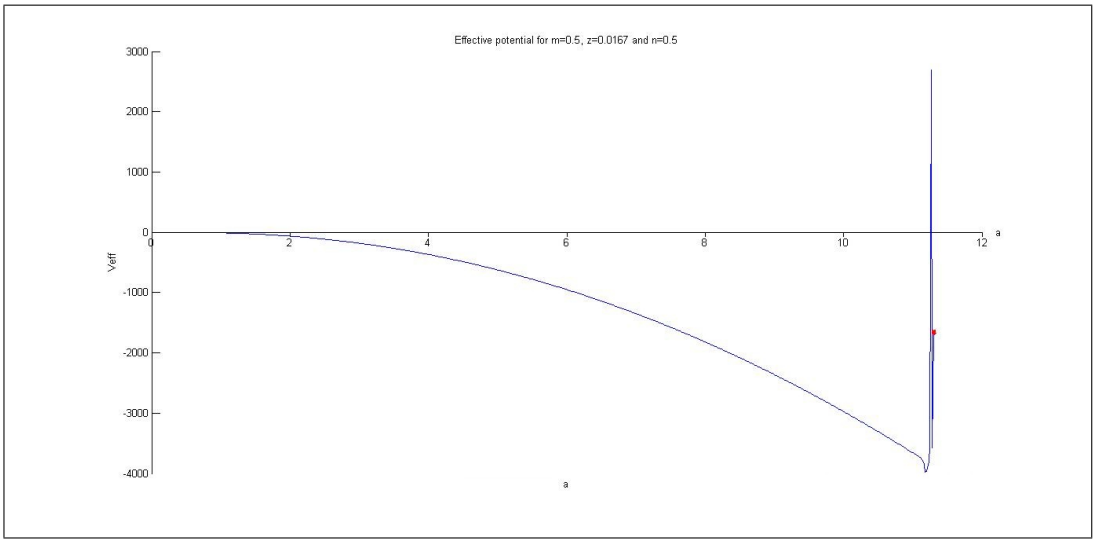

Figure 5.21: Plot of the effective potential for $m = 0.5$, $\zeta = 0.0167$ and $\eta = 0.5$. The red square indicates a point where the potential has become complex.

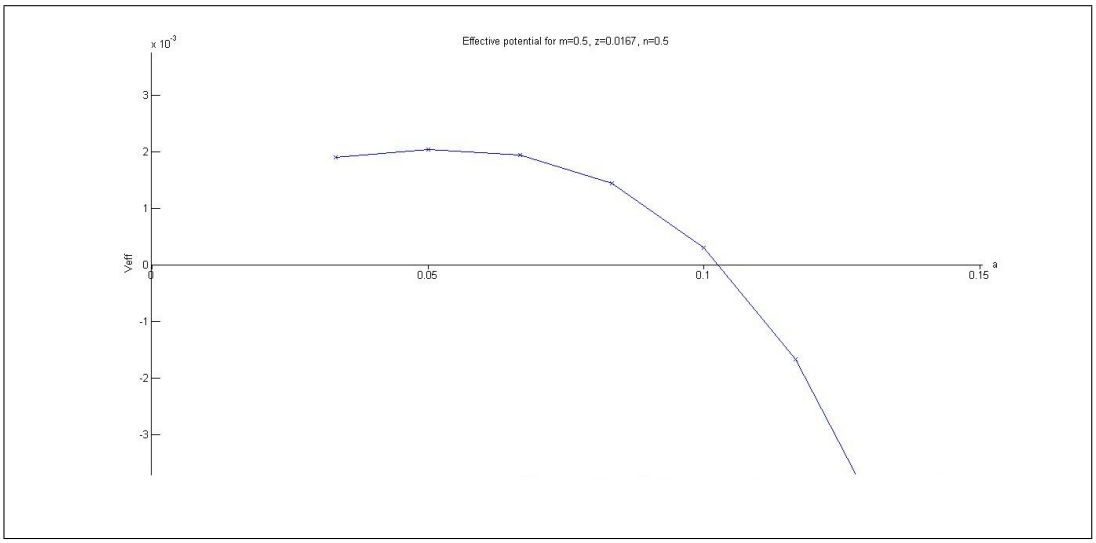

Figure 5.22: Plot of the effective potential for $m = 0.5$, $\zeta = 0.0167$ and $\eta = 0.5$. Here we see the small but nonzero potential barrier close to $a = 0$. The plot seems to end abruptly near $a = 0$, and this is because V_{eff} needs 3 lattice points of $p(a)$ to be defined and is only defined at the central lattice point, and as such V_{eff} is not defined at the first and last lattice points of $p(a)$.

we have seen that for a real potential barrier, V_{eff}=0 close to the node. Therefore we shall estimate that $V_{eff}(a_*) = 0$. It then follows from (5.45) that $V(a_*) = 0$.

Now if we concern ourselves with the node $a_* = a_{max}$, we see that $V'_{eff}(a_*)$ is a positive constant, since V_{eff} is shifting from a negative to a positive value at the node. By differentiating (5.45) we then see that $V'(a_*)$ is a negative constant. This proves that our approximation (5.46) is valid, because since $(a - a_{max})$ is always negative as we approach the node from the left, as long as $V'(a_*)$ is negative, the right hand side of (5.46) will remain positive , which is required since $\dot{a}^2$ is always positive. Thus, as we approach a_{max} from the left, we have

$$\dot{a} \approx K\sqrt{a_{max} - a}, \tag{5.47}$$

where K is some positive constant. We have chosen the positive square-root value for $\dot{a}$, because this indicates an expanding universe before a reaches a_{max}. Equation (5.47) indicates that $\dot{a} \to 0$ and $\ddot{a} < 0$ as $a \to a_{max}$.

Likewise, if we consider the node $a_* = a_{min}$, we now see that $V'_{eff}(a_*)$ is a negative constant, and therefore $V'(a_*)$ is a positive constant. $(a - a_*)$ is now always positive, since we are approaching the node from the right. Thus as we approach a_{min} from the right,

$$\dot{a} \approx -K\sqrt{a - a_{min}}, \tag{5.48}$$

where K is again some positive constant. This time we have chosen the negative square-root value for $\dot{a}$, since this universe is contracting before a reaches a_{min}. Equation (5.48) then indicates that $\dot{a} \to 0$ and $\ddot{a} > 0$ as $a \to a_{min}$.

Thus, we have proven that real potential barriers close to a_{min} and a_{max} are indeed turning points in the effective classical dynamics, by showing that contraction slows down at the barrier near a_{min} and that expansion slows down at the barrier near a_{max}. For universes with real potential barriers at small and large size, this analysis then concludes that they are indeed cyclic.

Chapter 6

Non-pertubative Study of a Spatially Flat FLRW Universe with a Free Massless Scalar Field

6.1 Motivation

So far we have studied a flat FLRW universe in which the only matter is a cosmological constant which varies slowly as a function of the scale factor; which is equivalent to a scalar field that has a potential which is a function of the scale factor and a negligible kinetic energy. In Parwani and Tarih [4], only the case of a flat FLRW universe with a non-varying cosmological constant (which is equivalent to a scalar field with a constant potential energy and no kinetic energy) was treated non-pertubatively. However Parwani and Nguyen [3] also studied the case of a spatially flat FLRW universe with a free massless scalar field pertubatively. This case is in some sense the other extreme to the case in Parwani and Tarih [4], since it is equivalent to a scalar field that has significant kinetic energy but no potential energy. In this chapter we shall study the free massless scalar field case non-pertubatively, after a brief review of the pertubative treatment. The motivation for studying this case is to attempt

to model the dynamics of the universe, using the scalar field as an 'intrinsic' time coordinate. However, before proceeding we shall first find the classical solutions for a flat FLRW universe with a free massless scalar field.

We transform the Einstein-Hilbert action as below, where $\alpha = \ln(a)$:

$$S = \frac{1}{2}\int dt N e^{3\alpha}\left[-\frac{\dot{\alpha}^2}{N^2} + \frac{\dot{\phi}^2}{N^2} + V(\phi) + ke^{-2\alpha}\right]. \tag{6.1}$$

We vary the action with respect to α, ϕ and N, in the gauge N=1, to give us the following classical equations:

$$\ddot{\phi} + 3\dot{\phi}\dot{\alpha} + \frac{1}{2}\frac{dV}{d\phi} = 0, \tag{6.2}$$

$$2\ddot{\alpha} + 3\dot{\alpha}^2 + 3\dot{\phi}^2 - 3V(\phi) + ke^{-2\alpha} = 0, \tag{6.3}$$

$$-\dot{\alpha}^2 + \dot{\phi}^2 + V(\phi) - ke^{-2\alpha} = 0. \tag{6.4}$$

Next, assuming a flat universe ($k = 0$) and a free massless scalar field ($V(\phi) = 0$); and scaling the time variable, we can find the following classical solutions:

$$\alpha = \frac{1}{3}\ln t + C, \tag{6.5}$$

$$\phi = \frac{1}{3}\ln t. \tag{6.6}$$

Here C is an arbitrary constant. From equation (6.5) it is obvious that as $t \to 0$ we have $\alpha \to -\infty$, and therefore $a \to 0$. Thus, we have the problem of a singularity of curvature invariants. We will apply nonlinear quantization to this model in the next section to see whether there is a means by which we can avoid this singularity, and also to study how the nonlinearities affect the evolution of the universe.

At this juncture it is instructive to note that the Wheeler-DeWitt equation contains no explicit time variable. As such, in quantum cosmology, we look at the correlations between variables to describe how the universe evolves in time [1,28,29].

A common method is to use a free massless scalar field as an internal clock to the universe [30–32] and this is exactly what we shall do in this chapter.

6.2 The Nonlinear Wheeler-DeWitt Equation for a spatially flat FLRW Universe with a Free Massless Scalar Field

To emphasize generality we shall reintroduce the potential $V(\phi)$ and the curvature, k. From the action (6.1) we may obtain the gravitational Hamiltonian [16,17,33]

$$H = \frac{N}{2e^{3\alpha}}\left[-p_\alpha^2 + p_\phi^2 + e^{6\alpha}V(\phi) - ke^{4\alpha}\right], \tag{6.7}$$

where

$$p_\alpha = \frac{-e^{3\alpha}\dot{\alpha}}{N} \tag{6.8}$$

and

$$p_\phi = \frac{e^{3\alpha}\dot{\phi}}{N} \tag{6.9}$$

are the canonical momenta. It can be easily shown that the Hamiltonian, equation (6.7) is a vanishing quantity using the constraint, equation (6.4); and thus we have

$$\frac{N}{2e^{3\alpha}}\left(-p_\alpha^2 + p_\phi^2 + e^{6\alpha}V(\phi) - ke^{4\alpha}\right) = 0. \tag{6.10}$$

Next we quantize this equation using Dirac's quantization rule, and obtain the Wheeler-DeWitt equation,

$$\left[\frac{\partial^2}{\partial\alpha^2} - \frac{\partial^2}{\partial\phi^2} + e^{6\alpha}V(\phi) - ke^{4\alpha}\right]\psi(\alpha,\phi) = 0. \tag{6.11}$$

This equation is equivalent to a time-independent Schröedinger equation in two dimensions. Since we are working with the case of a free massless scalar field in flat

space, the Wheeler-DeWitt equation thus reduces to

$$\left[\frac{\partial^2}{\partial\alpha^2} - \frac{\partial^2}{\partial\phi^2}\right]\psi(\alpha,\phi) = 0, \tag{6.12}$$

which is just a Klein-Gordon equation in terms of α and ϕ. The general solution of equation (6.12) can be obtained by separation of variables; i.e. using $\psi(\alpha,\phi) = f(\alpha)g(\phi)$. Doing this we may obtain the expressions

$$f(\alpha) = A_k(\alpha) = a_1 e^{ik\alpha} + a_2 e^{-ik\alpha}, \tag{6.13}$$

and

$$g(\phi) = B_k(\phi) = b_1 e^{ik\phi} + b_2 e^{-ik\phi}, \tag{6.14}$$

where a_1, a_2, b_1 and b_2 are arbitrary constants. In these expressions k is the separation constant, and should not be confused with the curvature. The general solution is a superposition of the eigensolutions $\psi_k(\alpha,\phi) = A_k(\alpha)B_k(\phi)$; i.e:

$$\psi(\alpha,\phi) = \int_{-\infty}^{\infty} w(k)A_k(\alpha)B_k(\phi)dk, \tag{6.15}$$

where $w(k)$ is an arbitrary function of k.

The eigensolution $\psi_k(\alpha,\phi) = A_k(\alpha)B_k(\phi)$ is itself not normalizable, but taking an approach similar to wavepacket construction in the free particle problem of quantum mechanics, we can normalize the general solution, equation (6.15), by choosing appropriate values for a_1, a_2, b_1 and b_2, and an appropriate function for $w(k)$.

We construct the wavepacket whilst keeping in mind that it should represent a large universe when the intrinsic time ϕ is large. To do so we take $a_2 = b_1 = 0$ and the function $w(k)$ to be a Gaussian weight,

$$w(k) = \exp\left[-\frac{(k^2 - g^2)^2}{\sigma^2}\right], \tag{6.16}$$

where σ and g are constants. Doing so, we may obtain the solution:

$$\psi(\alpha,\phi) = a_1 b_2 \sigma\sqrt{\pi}\exp\left[-\frac{(\alpha-\phi)^2}{4}\right]\exp(ig(\alpha-\phi)). \tag{6.17}$$

The corresponding probability density is

$$p(\alpha,\phi) \equiv \psi^*\psi = (a_1 b_2\sigma)^2\pi\,\exp\left[-\frac{(\alpha-\phi)^2}{2}\right]. \tag{6.18}$$

Since ϕ is being used as the internal clock of the system, and the probability density (6.18) is clearly localised near $\alpha \approx \phi$ for any ϕ, we can see that the wavefunction (6.17) we have derived represents a large universe at large time, as we required.

Next we shall nonlinearise the Wheeler-DeWitt equation (6.12), using the information-theoretic approach [2,26], to obtain

$$\left[\frac{\partial^2}{\partial\alpha^2} - \frac{\partial^2}{\partial\phi^2} - F_\alpha(p) + F_\phi(p)\right]\psi(\alpha,\phi) = 0, \tag{6.19}$$

where F_α and F_ϕ have the same form as F in (4.12), but with nonlinear parameters $L_\alpha > 0$ and $L_\phi > 0$ which are in general distinct from each other. Here L_α and L_ϕ correspond to the gravitational and matter degrees of freedom respectively.

6.3 Review of the Pertubative Study of a Flat Universe with a Free Massless Scalar Field

Now we shall briefly review the pertubative solution of equation (6.19) as demonstrated by Nguyen and Parwani [3]. Replacing the unperturbed probability density solution (equation (6.18)) in the nonlinear terms of equation (6.19), and keeping only the leading nontrivial terms in the series expansions of $F_\alpha(p)$ and $F_\phi(p)$, we obtain an effective linear equation,

$$\left[\frac{\partial^2}{\partial\alpha^2} - \frac{\partial^2}{\partial\phi^2} + V_{eff}\right]\psi(\alpha,\phi) = 0, \tag{6.20}$$

where

$$V_{eff} = u\left[\sigma^2(\phi-\alpha)^2 - 3\right](\phi-\alpha), \tag{6.21}$$

$$u \equiv \frac{\eta(3-4\eta)(L_\alpha + L_\phi)\sigma^4}{12}. \tag{6.22}$$

This equation approximately describes the quantum dynamics of wavepackets that are highly localised, to leading nontrivial order in perturbation theory. We do not calculate a tunneling probability here, but instead we shall work backwards to obtain the effective classical equations that should imply the modified quantum equation (6.20), via the correspondence principle [12]. It can easily be seen that the Hamiltonian that corresponds to equation (6.20) is

$$\hat{H} = \frac{N}{2e^{3\alpha}}\left[-\hat{p}_\alpha^2 + \hat{p}_\phi^2 + V_{eff}(\phi,\alpha)\right]. \tag{6.23}$$

This in turn arises from canonically quantising the classical action

$$S = \int dtL = \frac{1}{2}\int dt N e^{3\alpha}\left[-\frac{\dot{\alpha}^2}{N^2} + \frac{\dot{\phi}^2}{N^2} + e^{-6\alpha}V_{eff}(\phi)\right]. \tag{6.24}$$

Finally the classical action will give us the following modified classical evolution equations, in the gauge N=1:

$$\ddot{\phi} + 3\dot{\phi}\dot{\alpha} + \frac{1}{2}e^{-6\alpha}\frac{\partial V_{eff}}{\partial\phi} = 0, \tag{6.25}$$

$$2\ddot{\alpha} + 3\dot{\alpha}^2 + 3\dot{\phi}^2 + e^{-6\alpha}\left[3V_{eff} - \frac{\partial V_{eff}}{\partial\phi}\right] = 0, \tag{6.26}$$

$$-\dot{\alpha}^2 + \dot{\phi}^2 + e^{-6\alpha}V_{eff} = 0. \tag{6.27}$$

It is also instructive to note that

$$\frac{\partial V_{eff}}{\partial\phi} = -\frac{\partial V_{eff}}{\partial\alpha} = 3u\left[\sigma^2(\phi-\alpha)^2 - 1\right]. \tag{6.28}$$

The effective classicals equations (6.25)-(6.27) describe the mean dynamics of localized quantum states in a self consistent manner, since we used such states to obtain the effective potential, equation (6.21). It can be shown that the modified constraint, equation (6.27) combined with either one of the other two evolution equations (6.25) or (6.26) will imply the third remaining equation.

Perhaps the most important result which can be proven using the system of equations (6.25)-(6.27) is that if we assume the strong correlation condition $\alpha = \phi$ at all times, we find that a minimum size for the universe naturally occurs, thus replacing the Big Bang singularity with a bounce. It can be shown [3] using the modified classical equations that

$$\alpha \geq \frac{-C}{3u}, \tag{6.29}$$

and thus the minimum size of the universe is

$$a_{min} = \exp\left(\frac{-C}{3u}\right), \tag{6.30}$$

where C is a constant determined by the initial conditions.

This result has also been verified numerically by Nguyen and Parwani [3], wherein it was also shown that if $\alpha = \phi$ initially, it will remain so for all times. The more general initial condition of $\alpha \neq \phi$ was also studied, and was also shown to provide a bounce at some nonzero size, so long as the corrections due to V_{eff} remain within the regime of the pertubative approximation.

It is clear that in a pertubative study of the nonlinear Wheeler-DeWitt equation of a flat FLRW universe with a free massless scalar field taken to be the intrinsic time, one always encounters a minimum nonzero size for the universe, resolving the singularity problem. However we have so far only studied equation (6.19) assuming small nonlinearities, which is required of the pertubative treatment; and it is possible that we could find new predictions if the equation is studied non-pertubatively.

6.4 The Difference Equation

We shall study the nonlinear Wheeler-DeWitt equation for a flat FLRW universe with a free massless scalar field,

$$\left[\frac{\partial^2}{\partial\alpha^2} - \frac{\partial^2}{\partial\phi^2} - F_\alpha(p) + F_\phi(p)\right]\psi(\alpha,\phi) = 0, \tag{6.31}$$

in a manner similar to how the nonlinear Wheeler-DeWitt equation for flat FLRW-Λ universe with a cosmological constant was studied non-pertubatively by Parwani and Tarih [4], as well as earlier in this volume.

As before we write the wavefunction in terms of its amplitude and phase,

$$\psi(\alpha,\phi) = A(\alpha,\phi)e^{iS(\alpha,\phi)}. \tag{6.32}$$

Before using this form in equation (6.31), we should address a certain intricacy involving equations of the Klein-Gordon type, an example of which is equation (6.31). It is well known that the probability density of such equations is not positive definite. When using the Klein-Gordon equation to describe charged particles of zero spin, we have the luxury of multiplying the negative probability density by the charge, and interpreting the resulting quantity as a negative charge density. However in describing the state of the universe, we have no analogous quantity which can take both positive and negative values, and we thus need to find a way to show that the probability density is indeed positive definite.

The probability density associated with (6.31) is of the standard form,

$$p = i\left(\psi^*\frac{\partial\psi}{\partial\phi} - \psi\frac{\partial\psi^*}{\partial\phi}\right). \tag{6.33}$$

However if we substitute the form (6.32) into the probability density (6.33), it can be

shown that it reduces to

$$p = -2\frac{\partial S}{\partial \phi}|\psi|^2. \tag{6.34}$$

Since $|\psi|^2$ is positive definite, we can say that the probability density, p is positive definite, as long as

$$\frac{\partial S}{\partial \phi} < 0 \tag{6.35}$$

We shall use this constraint later when making an ansatz for the form of $S(\alpha, \phi)$.

Now we use the form of the wavefunction in equation (6.32) in the nonlinear Wheeler-DeWitt equation (6.31); the imaginary part of the resulting equation is given by

$$\frac{\partial}{\partial \phi}\left(A^2\frac{\partial S}{\partial \phi}\right) - \frac{\partial}{\partial \alpha}\left(A^2\frac{\partial S}{\partial \alpha}\right) = 0, \tag{6.36}$$

while the real part is given by

$$-\left(\frac{\partial S}{\partial \phi}\right)^2 + \left(\frac{\partial S}{\partial \alpha}\right)^2 - Q^{\alpha}_{NL} + Q^{\phi}_{NL} = 0 \tag{6.37}$$

(The full derivations of (6.36) and (6.37) can be found in Appendix B). Here Q^{α}_{NL} and Q^{ϕ}_{NL} are the generalised quantum potentials corresponding to α and ϕ respectively, and have the same form as Q_{NL} in equation (4.13).

Next we shall make an ansatz for the form of the phase S. We assume that

$$S(\alpha, \phi) = a\phi + b\alpha, \tag{6.38}$$

where a and b are constants. Invoking the constraint (6.35), we also see that we require

$$a < 0. \tag{6.39}$$

With the ansatz (6.38), equation (6.36) becomes

$$a\frac{\partial}{\partial \phi}\left(A^2\right) - b\frac{\partial}{\partial \alpha}\left(A^2\right) = 0 \tag{6.40}$$

Now we make the second ansatz, which is for the form of the amplitude $A(\alpha, \phi)$. We assume that

$$A(\alpha, \phi) = A(c\phi + d\alpha), \tag{6.41}$$

where c and d are constants. Now if we let $c\phi + d\alpha = z$,we have

$$\frac{\partial}{\partial \phi}\left(A(\alpha, \phi)\right)^2 = \frac{\partial A^2}{\partial z}\frac{\partial z}{\partial \phi} = \frac{\partial A^2}{\partial z}c, \text{and} \tag{6.42}$$

$$\frac{\partial}{\partial \alpha}\left(A(\alpha, \phi)\right)^2 = \frac{\partial A^2}{\partial z}\frac{\partial z}{\partial \alpha} = \frac{\partial A^2}{\partial z}d, \tag{6.43}$$

Then (6.40) becomes

$$a\left(\frac{\partial A^2}{\partial z}\right)c - b\left(\frac{\partial A^2}{\partial z}\right)d = 0, \tag{6.44}$$

or

$$ac = bd. \tag{6.45}$$

Equation (6.45) is a constraint, which can be automatically satisfied by setting $a = d$ and $b = c$.

Finally, equation (6.37) becomes

$$-a^2 + b^2 - Q^{\alpha}_{NL} + Q^{\phi}_{NL} = 0, \tag{6.46}$$

which is a difference equation describing the evolution of the universe in time, with the free massless scalar field playing the role of intrinsic time. Much of our remaining arguments in this volume shall concern the numerical study of this equation.

However before we proceed we would first like to justify the two choices of ansatz made in arriving at the difference equation (6.46) and the constraint (6.45). Both ansatzes (equations (6.38) and (6.41)) are justified if one observes the solution (6.17) to the linear Wheeler-DeWitt equation with a free massless scalar field.

The first ansatz (6.38) is justified if we study the phase of the linear solution, which is $-g\phi + g\alpha$. Comparing this phase with the first ansatz, which is $a\phi + b\alpha$

(remember a is negative due to constraint (6.35)), we may say that the effect of the nonlinearities is to make the coefficients of ϕ and α in the phase of the linear solution inequal, since in general $(-a) \neq b$.

The ansatz for the amplitude of the wavefunction can also be similarly justified. In the linear solution (6.17) the amplitude is given as

$$A_{linear}(\alpha, \phi) = a_1 b_2 \sigma \sqrt{\pi} \exp\left[-\frac{(\alpha - \phi)^2}{4}\right], \tag{6.47}$$

while the ansatz for the functional form of the amplitude of the nonlinear case is

$$A(\alpha, \phi) = A(b\phi + a\alpha) \tag{6.48}$$

(taking constraint (6.45) into account we have set $c = b$ and $d = a$, as before a is negative). We note that in the amplitude of the linear solution (6.47), the factor in the exponent can equivalently be

$$\exp\left[-\frac{(g\phi - g\alpha)^2}{4g^2}\right], \tag{6.49}$$

and the functional form of the amplitude of the linear solution would be

$$A_{linear}(\alpha, \phi) = A(g\phi - g\alpha). \tag{6.50}$$

It is then easy to see that the justification for the second ansatz is similar to the first one, that is we assume that the nonlinearities result in the coefficients of ϕ and α in the amplitude of the linear solution becoming inequal. It is obvious that in making both ansatzes, we are postulating that the effects of the nonlinear terms do not affect the linear form of the wavepacket (6.17) substantially.

6.5 Numerical Analysis

Before we explore the results of the numerical study of the difference equation (6.46), we shall first explore the properties of the equation a little further, before making some assumptions essential for the numerical calculations.

It is obvious that in the difference equation we have derived for a spatially flat FLRW-ϕ universe,

$$-a^2 + b^2 - Q^{\alpha}_{NL} + Q^{\phi}_{NL} = 0, \tag{6.51}$$

there are two generalised quantum potentials. The first,

$$Q^{\alpha}_{NL} = \frac{1}{2\zeta_{\alpha}^2\eta_{\alpha}^2}\left[\ln\left(\frac{p}{(1-\eta_{\alpha})p+\eta_{\alpha}p_{+}}\right) + \frac{\eta_{\alpha}p_{+}}{(1-\eta_{\alpha})p+\eta_{\alpha}p_{+}} - \frac{\eta_{\alpha}p_{-}}{(1-\eta_{\alpha})p_{-}+\eta_{\alpha}p}\right], \tag{6.52}$$

corresponds to the gravitational degree of freedom of the universe, or in other words the size of the universe as determined by the scale factor; and the second,

$$Q^{\phi}_{NL} = \frac{1}{2\zeta_{\phi}^2\eta_{\phi}^2}\left[\ln\left(\frac{p}{(1-\eta_{\phi})p+\eta_{\phi}p^{+}}\right) + \frac{\eta_{\phi}p^{+}}{(1-\eta_{\phi})p+\eta_{\phi}p^{+}} - \frac{\eta_{\phi}p^{-}}{(1-\eta_{\phi})p^{-}+\eta_{\phi}p}\right], \tag{6.53}$$

corresponds to the matter degree of freedom of the universe, or equivalently the intrinsic time for the evolution of the universe. Here $p(\alpha,\phi) = -2\frac{\partial S}{\partial\phi}|\psi|^2 = -2a|\psi|^2$ is the probability density (a is negative), $p_{\pm}(\alpha,\phi) \equiv p(\alpha\pm\zeta_{\alpha},\phi)$, $p^{\pm}(\alpha,\phi) \equiv p(\alpha,\phi\pm\zeta_{\phi})$, $\zeta_{\alpha} = \eta_{\alpha}L_{\alpha}$ and $\zeta_{\phi} = \eta_{\phi}L_{\phi}$ are positive dimensionless parameters which represent the nonlinearity scales corresponding to α and ϕ respectively, and finally $0 < \eta_{\alpha} < 1$ and $0 < \eta_{\phi} < 1$ are the regularization parameters that each label a family of nonlinearisations.

It is obvious that with the scalar field as an added temporal dimension, the difference equation now represents a two-dimensional lattice of points, each representing the probability density, p for a certain scale factor value and at a certain point in intrinsic time. As before it is important to note that both variables α and ϕ, as well

as the probability density $p(\alpha, \phi)$ are all still continuous.

The first assumption we make in order to simplify the numerical calculations will be that the two nonlinearity scales are equal, i.e. $\zeta_\alpha = \zeta_\phi = \zeta$. We shall also make a similar assumption for the regularization parameters η_α and η_ϕ, that is $\eta_\alpha = \eta_\phi = \eta$. In the numerical analysis, we shall study how the probability density (the probability here being that of the universe having a certain scale factor value) evolves differently with intrinsic time for various values of ζ and η.

The values for the constants a and b in equation (6.51) also remain to be determined. The constant a is negative, and although in the linear case we have $-a = b$ (see section 1.4 on the justification of the two ansatzes), in general we should have $-a \neq b$ for the nonlinear case. With these caveats in mind, we assume:

$$a = -1 - e\zeta, \tag{6.54}$$

$$b = 1 + f\zeta, \tag{6.55}$$

where,

$$e = 1, \tag{6.56}$$

$$f = 1.5. \tag{6.57}$$

Here $e \neq f$, since we want to ensure that $-a \neq b$ for all values of ζ. However we have chosen a value of f close to that of e, assuming that although the nonlinearities cause $-a$ to be not equal to b, the difference between both values is small. In fact it can clearly be seen that the difference $(-a - b)$ increases linearly as a function of ζ, since it is equal to $(f - e)\zeta = 0.5\zeta$, and that when $\zeta = 0$ (the linear case), the difference becomes zero, and $-a = b$, as expected.

Previously we only studied a difference equation in one dimension (the scale factor), that is for the case of a flat FLRW universe containing only a varying cosmological

constant. In that model we only needed to specify two initial values, before evolving the difference equation backward from these points explicitly, and forward from these points using Newton's method. However since we now have a two dimensional grid the problem is slightly more complicated. The full form of the difference equation is now

$$\begin{aligned} -a^2 + b^2 - \frac{1}{2\zeta^2\eta^2}\left[\ln\left(\frac{p}{(1-\eta)p+\eta p_+}\right) + \frac{\eta p_+}{(1-\eta)p+\eta p_+} - \frac{\eta p_-}{(1-\eta)p_- + \eta p}\right] \\ + \frac{1}{2\zeta^2\eta^2}\left[\ln\left(\frac{p}{(1-\eta)p+\eta p^+}\right) + \frac{\eta p^+}{(1-\eta)p+\eta p^+} - \frac{\eta p^-}{(1-\eta)p^- + \eta p}\right] = 0. \end{aligned} \tag{6.58}$$

We first notice that the difference equation now relates five lattice points; p_+, p_-, p^+, p^- and p, instead of just three. Also on further inspection of the equation, we notice that we are only able to obtain either p_- or p^- explicitly in terms of four other lattice points, and thus once again we are forced to resort to Newton's method for the forward evolution.

Now for the backward evolution, we once again need to make a change of variable to shift the lattice points by making the substitution $\phi \to \phi + \zeta$, which results in the following relabellings:

$$p^-(\alpha,\phi) \to p(\alpha,\phi) \tag{6.59}$$

$$p(\alpha,\phi) \to p^+(\alpha,\phi) \tag{6.60}$$

$$p^+(\alpha,\phi) \to p^{++}(\alpha,\phi) \tag{6.61}$$

$$p_-(\alpha,\phi) \to p^+_-(\alpha,\phi) \tag{6.62}$$

$$p_+(\alpha,\phi) \to p^+_+(\alpha,\phi) \tag{6.63}$$

where $p_\pm(\alpha,\phi) \equiv p(\alpha \pm \zeta, \phi)$, $p^\pm(\alpha,\phi) \equiv p(\alpha, \phi \pm \zeta)$ and $p^{++}(\alpha,\phi) \equiv p(\alpha, \phi + 2\zeta)$.

We then rearrange (6.58) to arrive at

$$p(\alpha,\phi) = \frac{\eta p^{+}(\alpha,\phi)}{(1-\eta)}\left[\frac{1}{1-(\frac{1-\eta}{\eta})D} - 1\right], \tag{6.64}$$

where

$$\begin{aligned} D = &\ln\left(\frac{p^{+}}{(1-\eta)p^{+}+\eta p^{++}}\right) + \frac{\eta p^{++}}{(1-\eta)p^{+}+\eta p^{++}} + 2\zeta^2\eta^2(b^2-a^2) \\ &- \left[\ln\left(\frac{p^{+}}{(1-\eta)p^{+}+\eta p^{+}_{+}}\right) + \frac{\eta p^{+}_{+}}{(1-\eta)p^{+}+\eta p^{+}_{+}} - \frac{\eta p^{+}_{-}}{(1-\eta)p^{+}_{-}+\eta p^{+}}\right] \end{aligned} \tag{6.65}$$

Ideally we would like to start with a particular value of ϕ, calculate all the lattice points for different α values at that value of ϕ, and then repeat the process for the next ϕ value, which is the previous ϕ value minus the step size ζ. However, from the difference equation, it is obvious that for each row of lattice points $p(\alpha,\phi)$, we need information from two other rows, that is $p(\alpha,\phi+\zeta)$ and $p(\alpha,\phi+2\zeta)$. Therefore, our initial values for the backward evolution has to be two rows of lattice points corresponding to two values of ϕ, which differ by ζ. For this we assume that at the two initial values of ϕ, the profile of the probability density is described by a Gaussian

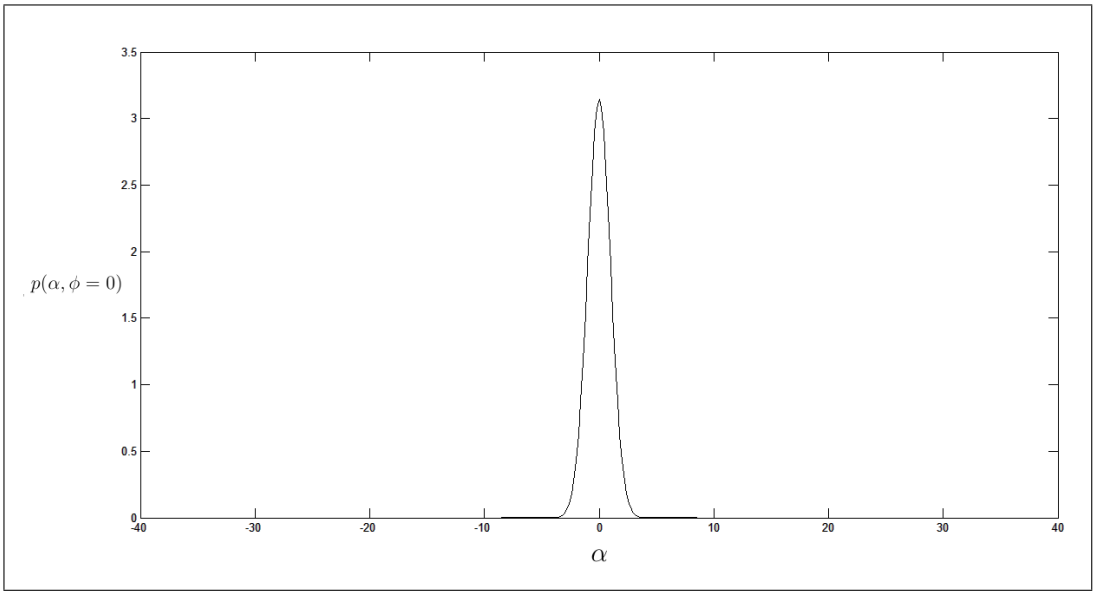

Figure 6.1: Initial Gaussian probability density distribution for $p(\alpha,0)$

wavepacket as in the linear case, equation (6.18). We shall always set the two initial rows to be at $p(\alpha, 0)$ (Figure 6.1) and $p(\alpha, -\zeta)$. From these two rows, we may generate the backward evolution of the difference equation.

For the forward evolution, we once again need to use Newton's method. We again use two rows of the linear solution as our initial probability density distributions, but this time for $p(\alpha, \phi)$ and $p(\alpha, \phi - \zeta)$, and use equation (6.58) as the function in Newton's method to obtain the values of $p(\alpha, \phi + \zeta)$, and then iterate the whole process to evolve the equation forward in intrinsic time.

It is also important to note that the two initial wavepackets set the hard boundaries within which we perform our calculations. In theory the Gaussian wavepacket solution (6.18) extends from $\alpha = -\infty$ to $\alpha = \infty$ for any value of ϕ, but due to the limitations of our numerical analysis using MATLAB, calculations are only performed within a limit of about $\alpha = -38.5$ to $\alpha = 38.5$. In doing this we have ensured that the Gaussian peak is far enough from the boundaries during the numerical evolution so as to not affect its dynamical evolution substantially.

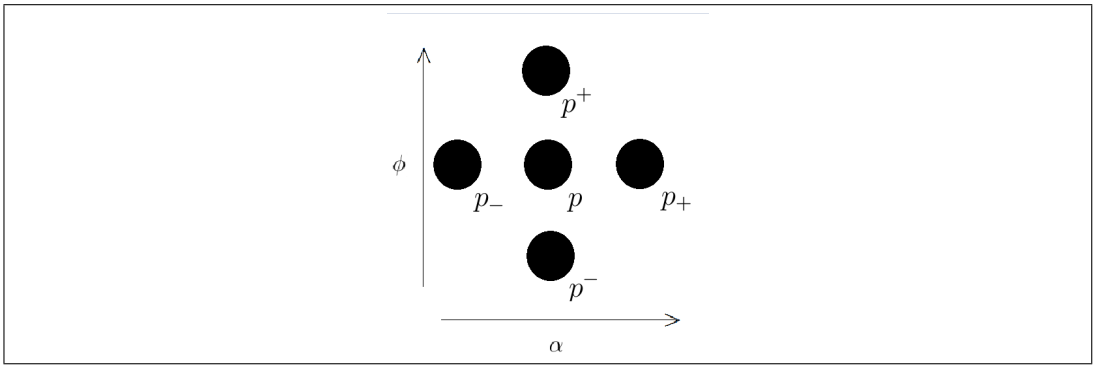

Figure 6.2: Lattice points related by the difference equation.

In the numerical analysis, several interesting characteristics are seen. First we shall see that at every step in the evolution of the equation backward or forward in intrinsic time, it seems that we lose information about two lattice points. The reason for this is that the difference equation (6.58) relates five lattice points for any particular value of ϕ and α, namely p, p^+, p^-, p_+ and p_-, as in Figure 6.2. This

forms the basic 'unit' of the lattice, and in the forward and backward evolutions there is loss of information due to the shape of this basic unit.

A pedagogical example of how this happens can be seen in Figure 6.3. We shall however consider this apparent loss of information as meaning that the probability density p is not defined at points where the loss of information occurs, and can therefore be considered to be zero at these points. In other words it is not actual loss of information, but rather a loss of range, since the difference equation is merely telling us that the range of scale factor values that the universe can have shrinks in both the forward and backward evolutions in time.

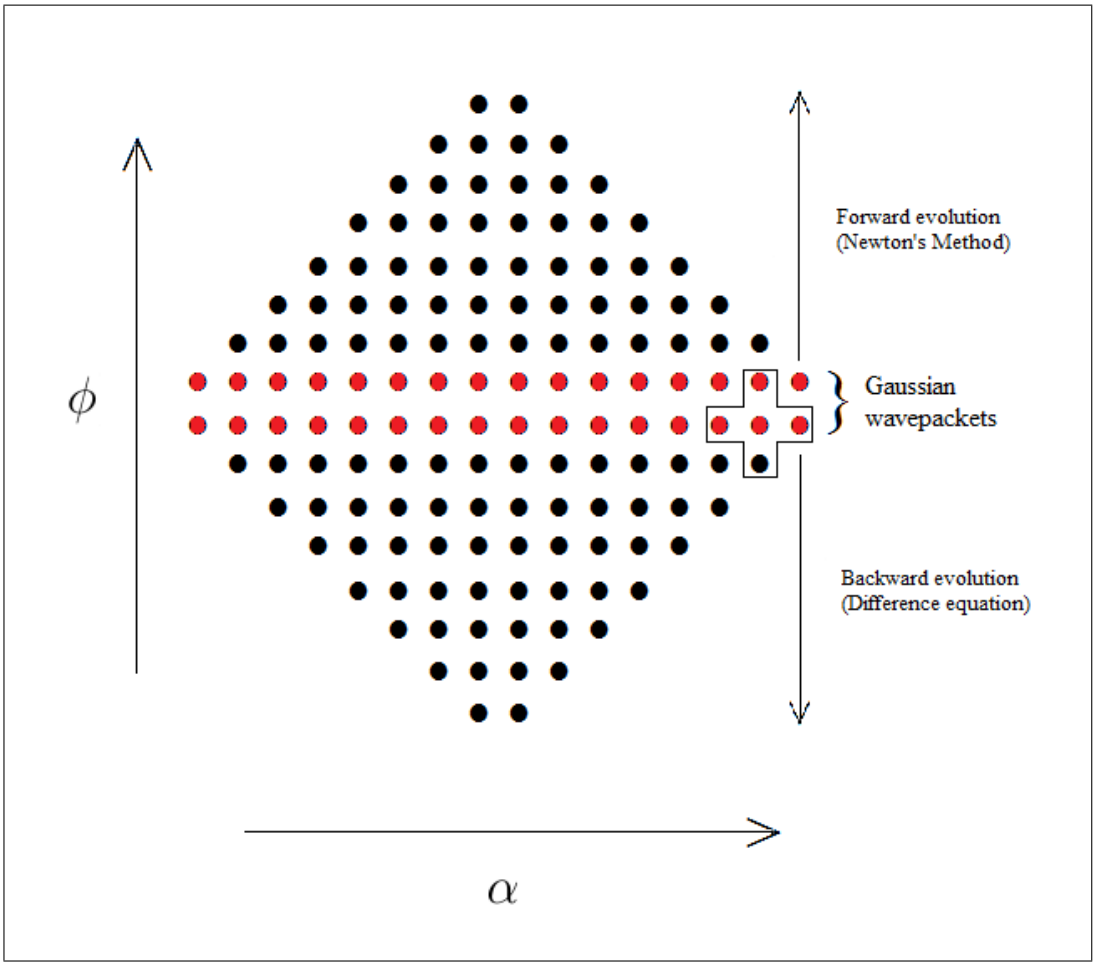

Figure 6.3: Loss of range in the two-dimensional lattice (Black dots represent lattice points with non-zero probability).

However Figure 6.3 does not address another important feature seen in our numerical analysis. In the case of Parwani and Tarih [4], a feature that was not previously seen was the occurrence of negative/complex probabilities after evolving beyond a certain value of the scale factor a, both when the difference equation was evolved using the difference equation and using Newton's method. As mentioned before these negative/complex probabilities are interpreted as being unphysical.

In our numerical analysis of the two-dimensional difference equation for our case of the free massless scalar field we find similar features, but in this case the negative/complex points occur for different scale factor (α) values at different points in intrinsic time (ϕ). Since we do not consider these points as being physical, wherever such points are encountered in the numerical work for a particular value of ϕ, we truncate the original boundaries to form new soft boundaries, and the lattice points for the next iteration at $\phi-\zeta$ (or $\phi+\zeta$ in the forward evolution) will only be calculated within these new soft boundaries. A pedagogical example of this is Figure 6.4.

It is also important to note that in the numerical analysis there are cases where the probability density becomes positive again after having previously become negative as we iterate along α. However, as in Parwani and Tarih [4] we do not consider these regions, as we require that the probability density at every point in intrinsic time must be continuous and positive definite.

It is thus obvious that all universes described by the difference equation (6.58) will begin and end at finite intrinsic times, since whenever we evolve the equation forward or backward in time, the wavepacket will eventually disappear at some value of ϕ.

We have performed the backward and forward evolution for three values of η, namely $\eta = 0.1$, $\eta = 0.5$, $\eta = 0.9$; and for various values of ζ, ranging from about $\zeta = 0.01$ to $\zeta = 0.9$. In doing so we have been able to deduce the dynamics of several types of universes.

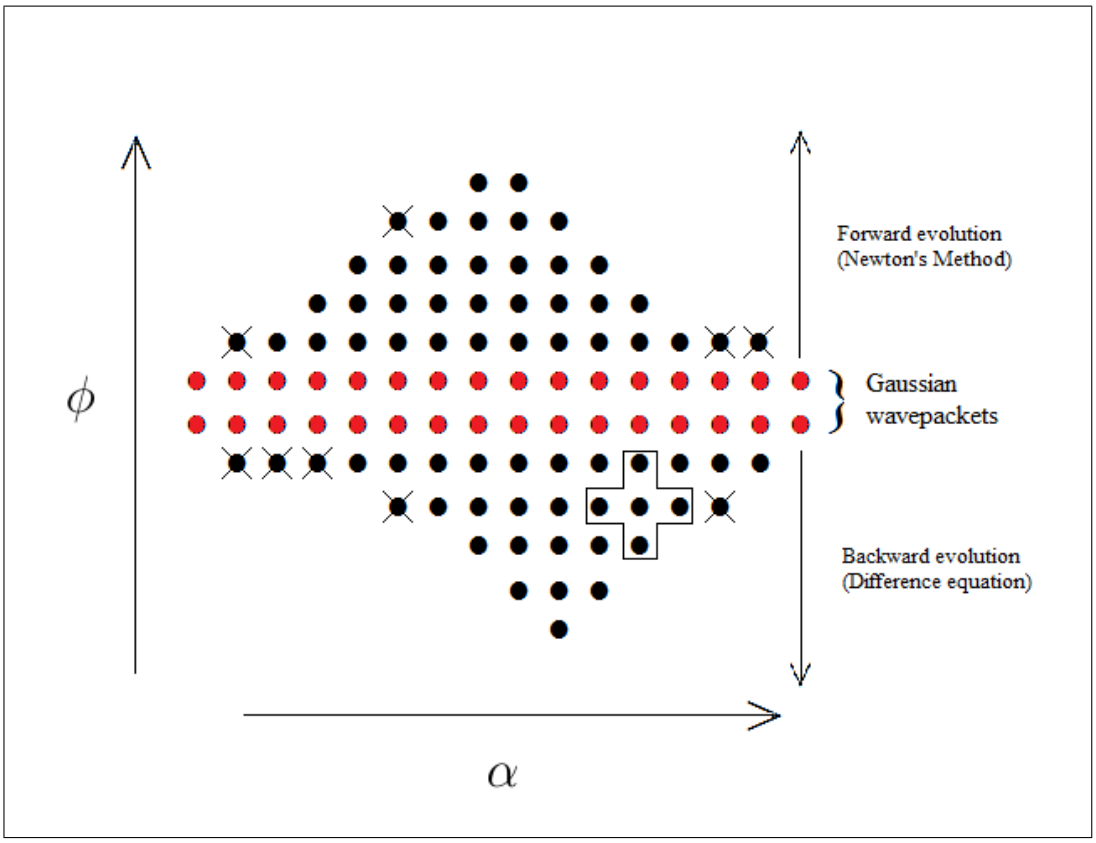

Figure 6.4: Occurrence of negative/complex probabilities in the two-dimensional lattice (Black dots with crosses represent lattice points with negative/complex probability).

6.6 Results

The easiest way of deducing the dynamics from the lattice of probability density points, is by studying how the peak of the wavepacket moves along the axis α as intrinsic time changes. In other words we are deducing a plot of the scale factor, α against ϕ, to give us an idea of how the universe expands or contracts as a function of intrinsic time. It should be noted that these are not the actual dynamics of the universe, since we are not able to deduce α as function of time, t. Nevertheless it does give us good insight into how the dynamical behaviour of the universe is affected as the nonlinear parameter ζ is varied.

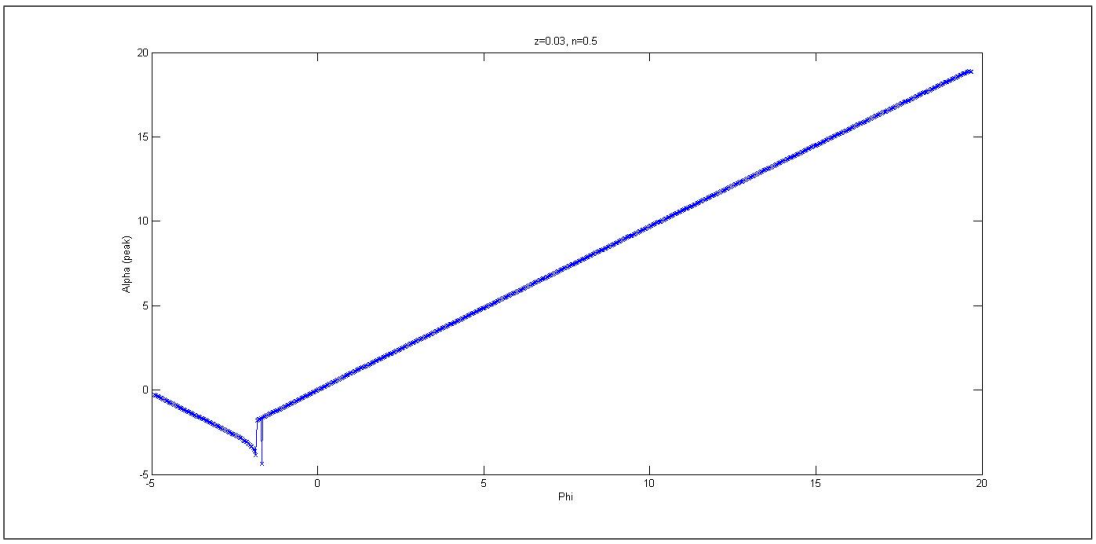

Figure 6.5: Plot of the scale factor (α) value at which the peak of the wavepacket occurs as a function of intrinsic time, ϕ for $\eta = 0.5$, $\zeta = 0.03$. The peaks of the initial Gaussian wavepackets are at $\phi = 0$, $\alpha = 0$ and $\phi = -\zeta$, $\alpha = -\zeta$.

6.6.1 η=0.5

For the $\eta = 0.5$ case we found a total of 4 distinct types of universes as we varied the parameter ζ. We shall start with the simplest case; that is for all universes with $\zeta \leq 0.03$. For this case we find that the scale factor (α) value at which the probability density is peaked increases linearly as a function of intrinsic time (ϕ) almost throughout the lifetime of the universe. In other words as we evolve the difference equation both forward and backward in intrinsic time, we find an almost complete linear dependence between the scale factor value of the probability density's peak and the intrinsic time. The only exceptions are at the end of the backward and forward evolutions. As we have mentioned before, due to the form of the difference equation, all universes we shall study begin and end at finite intrinsic time. In the present case these coincide with divergences from linear behaviour. Figure 6.5 shows the plot of the α value of the peak against the intrinsic time, ϕ, for the case of $\zeta = 0.03$.

At the end of the backward evolution we see what we shall henceforth refer to as a 'bounce'. As we evolve backwards from the two initial wavepackets peaked at $\alpha = 0$,

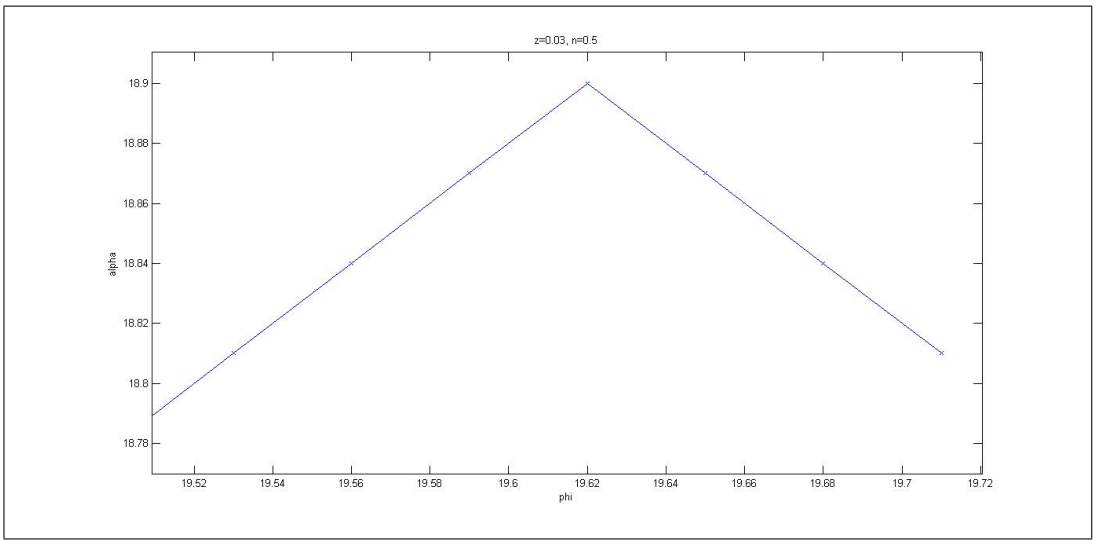

Figure 6.6: Contraction at the end of the forward evolution for $\eta = 0.5$, $\zeta = 0.03$.

$\phi = 0$ and $\alpha = -\zeta$, $\phi = -\zeta$, the scale factor value of the peak of the wavepacket, is seen to jump once to a lower value and back to a value that obeys the linear relationship, decreases linearly again, and then jumps to a lower value again. From there the scale factor value of the peak begins to increase gradually, before the peak finally disappears at a certain value of ϕ.

Near the end of the forward evolution, we also see non-linear behaviour which is less obvious. This behaviour is more clearly seen in Figure 6.6.

We can interpret the behaviour of the peak we have seen thus far as a universe that appears at a finite (non-zero) scale factor value, contracting up to a certain point in intrinsic time (ϕ), then undergoing inflation, some linear expansion, a sudden deflation and then a re-inflation, and then followed by linear expansion until a point near its death, where it suddenly begins to contract for a very short time, doing so until it vanishes at a finite, large size.

It is however important to note that so far we have only discussed the peak of the probability density curve, and at every point in intrinsic time, the universe can have a scale factor value other than that specified by the peak, as long as there is a non-zero probability density value at that scale factor value. Nevertheless the

probability density curves we find numerically are always highly localized and as such studying just their peaks gives us a good idea of the mean dynamics of the universe. It also should be noted that the difference equation is discrete in nature, and as such the actual location of the peak of a wavepacket could be in between lattice points. However as we are dealing with a small value of ζ in the current case, the peak we measure will not vary much from the actual peak. Later this effect of discreteness on the plots of α versus ϕ will be more noticeable for higher values of ζ.

We would like to further understand the evolution of the wavepacket and the dynamics of the bounces by studying how the form of the probability density distributions evolve. Figures 6.7 to 6.20 show the backward evolution for various values of ϕ, from $\phi = 0$ (the initial Gaussian wavepacket) to $\phi = -4.95$, when the wavepacket disappears.

It should be kept in mind that the various probability density distributions are deduced from a finite number of lattice points at every point in intrinsic time, ϕ. From the figures we clearly see the wavepacket traveling backwards (i.e. to lower scale factor values), which is then followed by oscillations occurring on the left tail of the profile (Figure 6.9 onwards). In Figure 6.10 we see one of the oscillatory peaks outgrowing the main Gaussian peak, and quickly shrinking again in Figure 6.11. This corresponds to the first jump from linear behaviour and back when evolving backwards

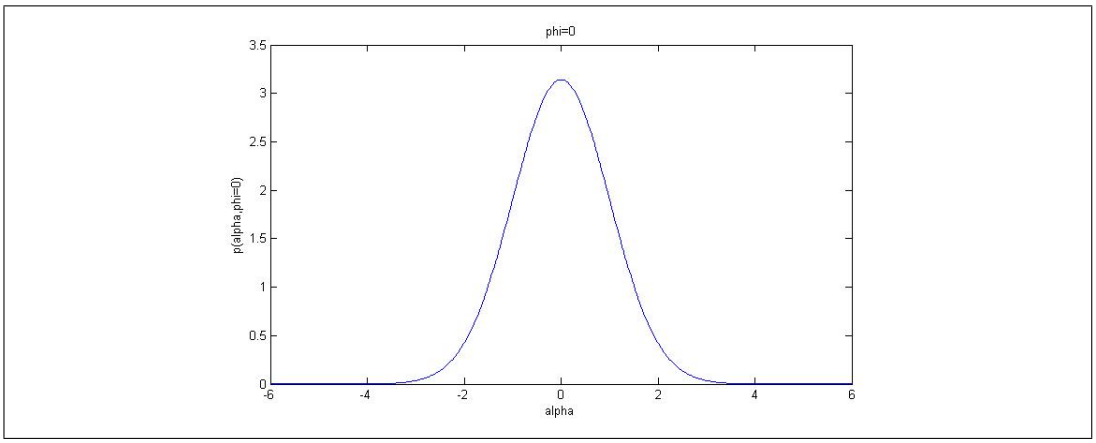

Figure 6.7: Probability density distribution at $\phi = 0$

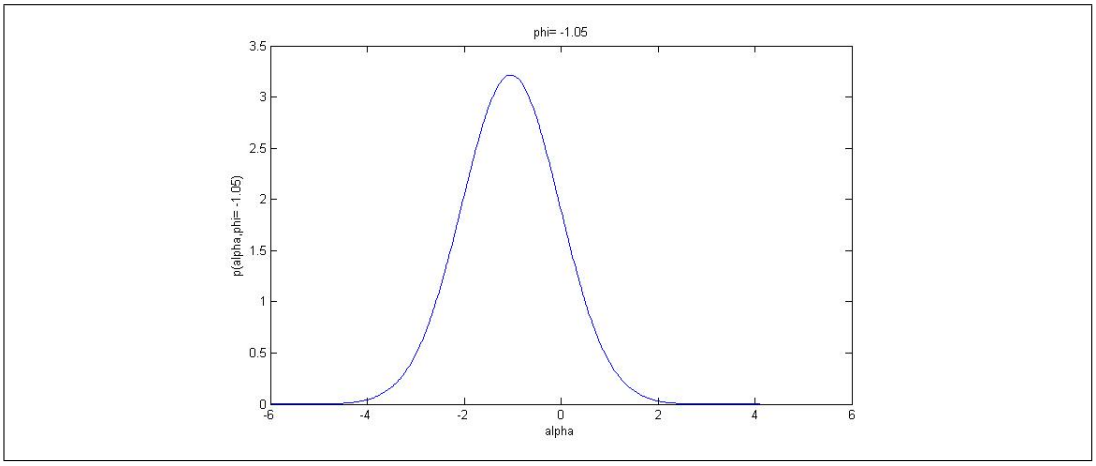

Figure 6.8: Probability density distribution at $\phi = -1.05$

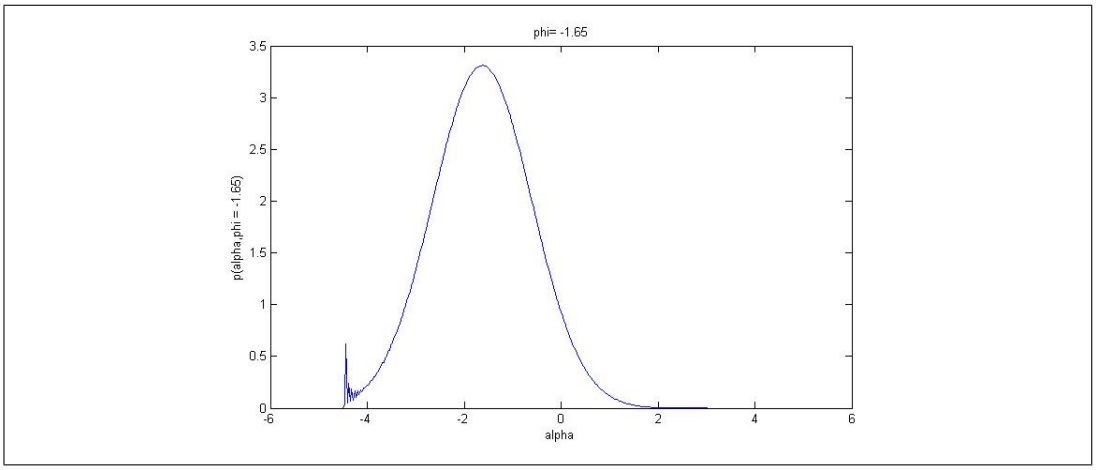

Figure 6.9: Probability density distribution at $\phi = -1.65$

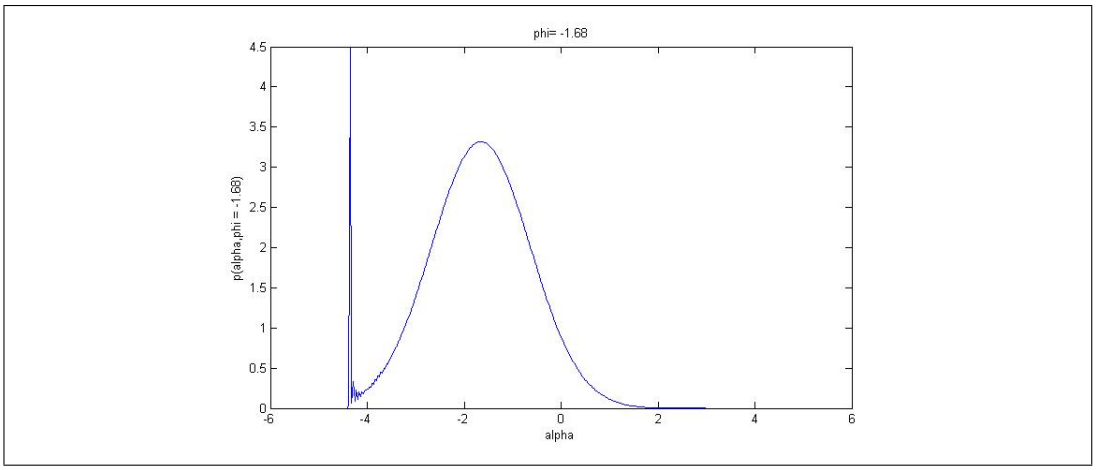

Figure 6.10: Probability density distribution at $\phi = -1.68$

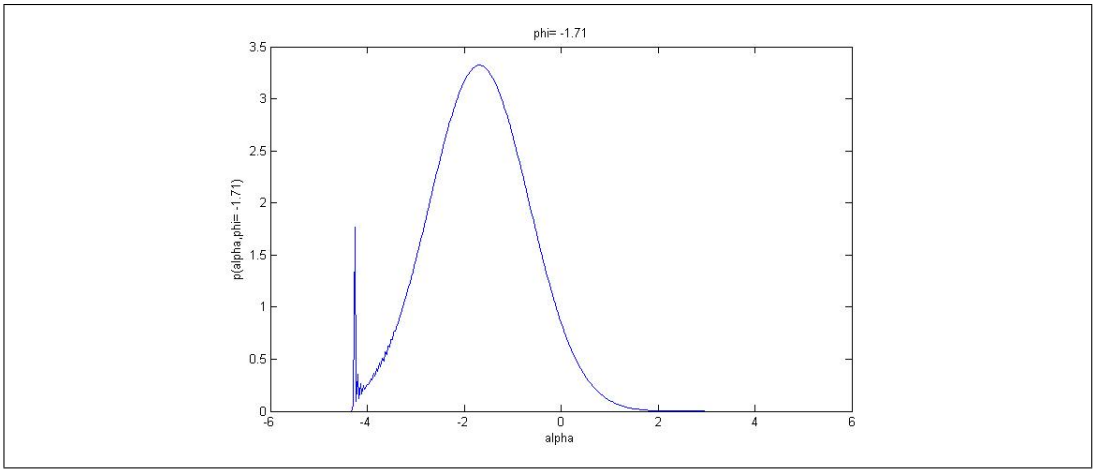

Figure 6.11: Probability density distribution at $\phi = -1.71$

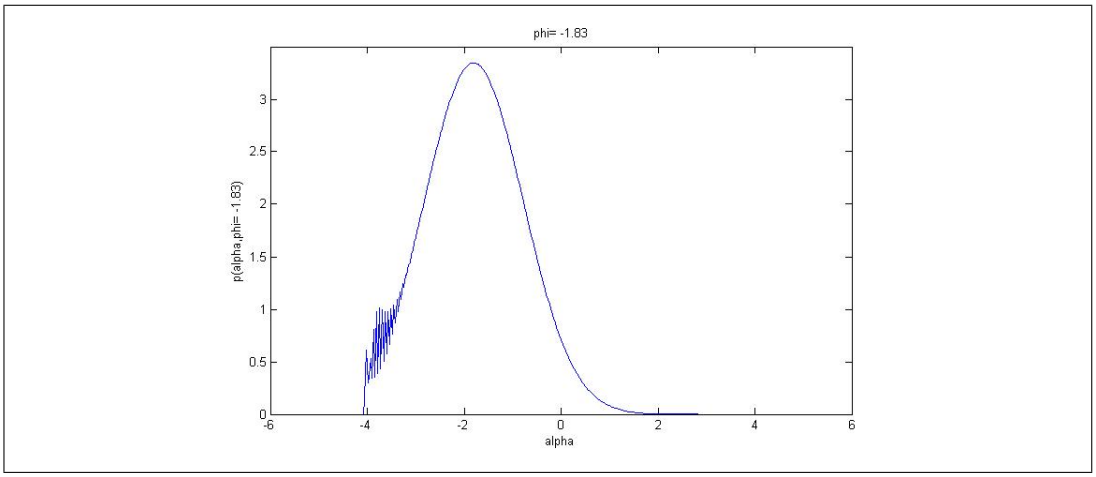

Figure 6.12: Probability density distribution at $\phi = -1.83$

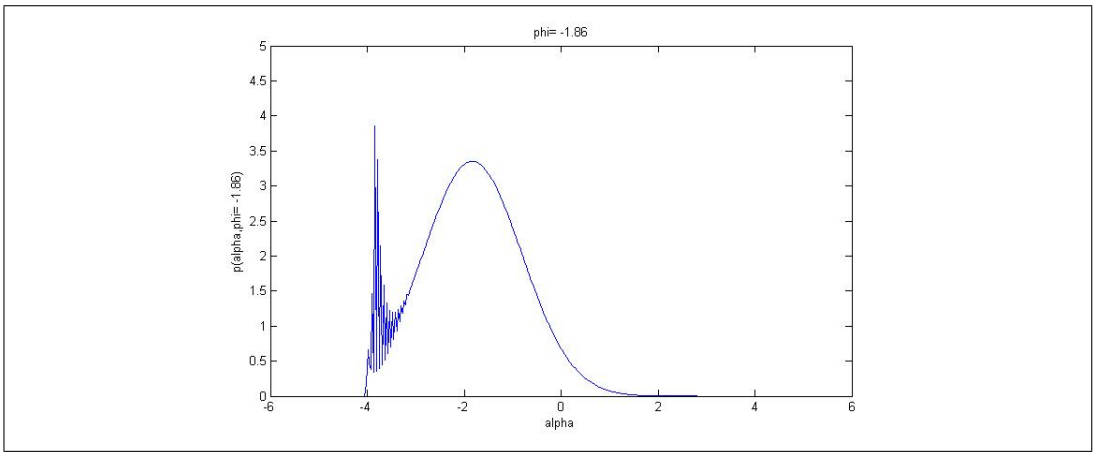

Figure 6.13: Probability density distribution at $\phi = -1.86$

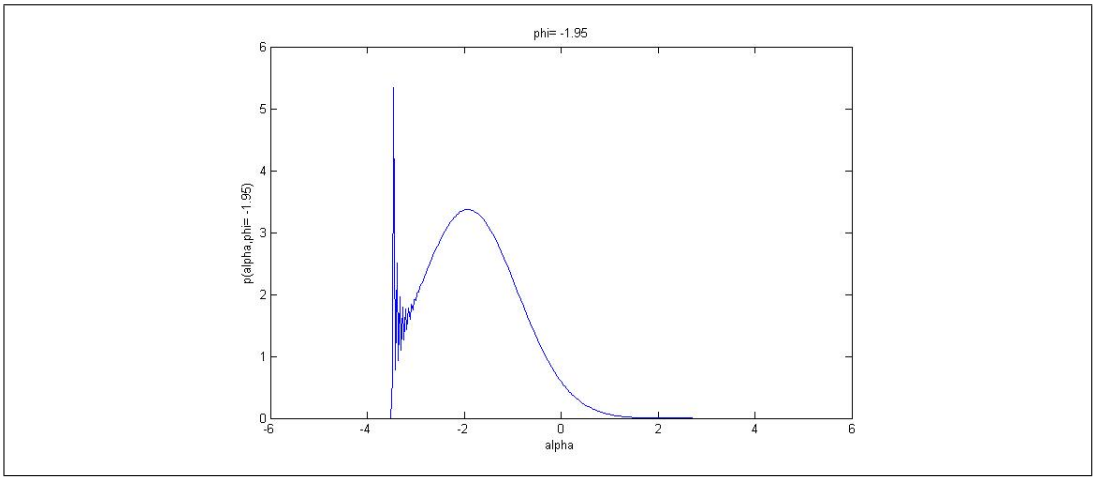

Figure 6.14: Probability density distribution at $\phi = -1.95$

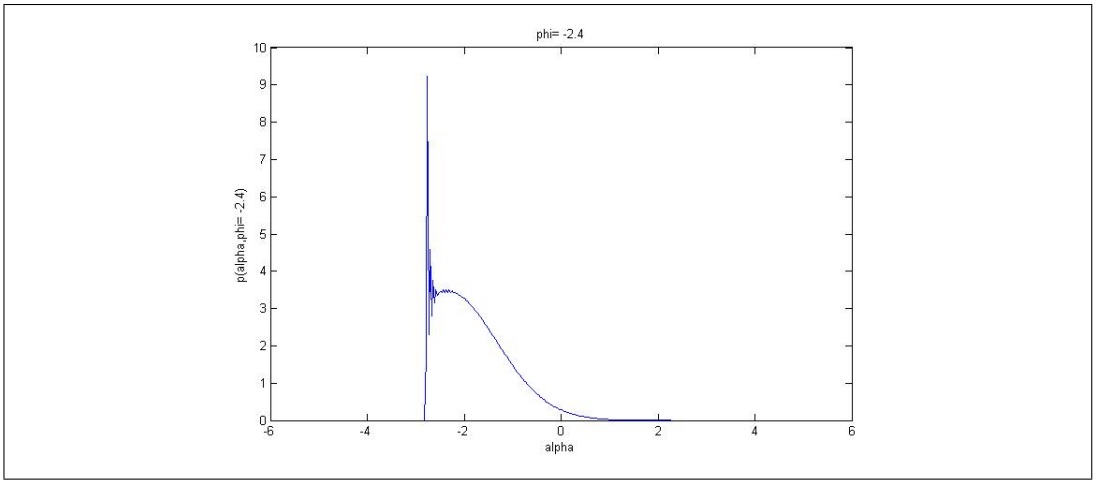

Figure 6.15: Probability density distribution at $\phi = -2.4$

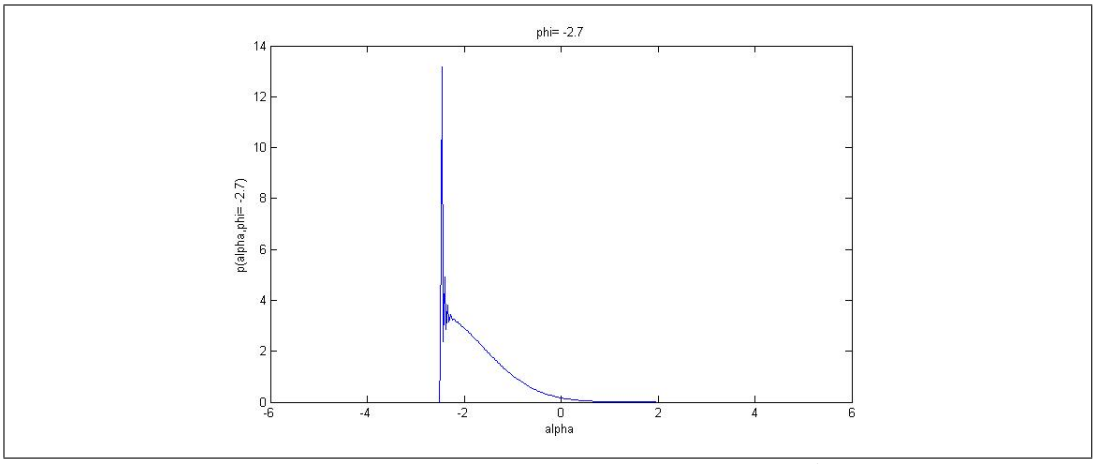

Figure 6.16: Probability density distribution at $\phi = -2.7$

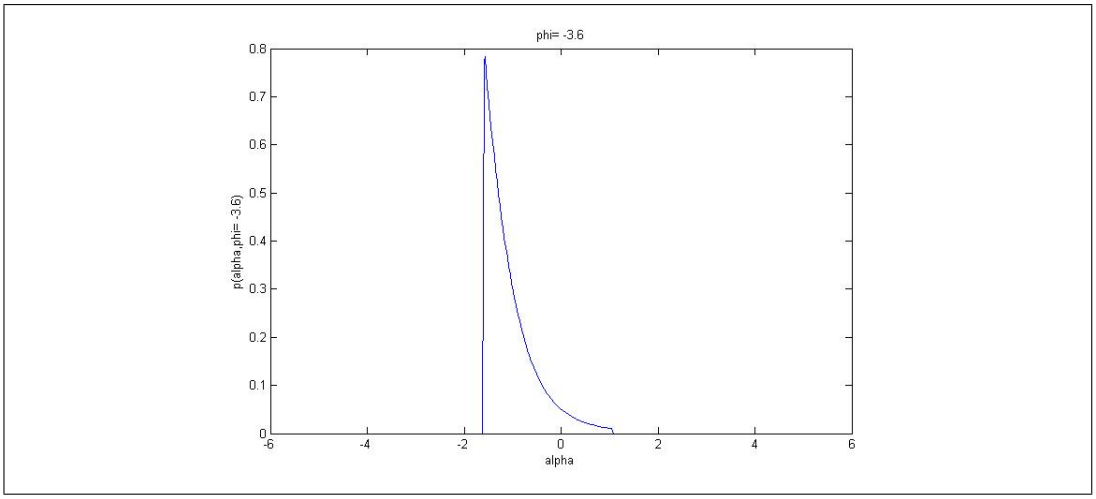

Figure 6.17: Probability density distribution at $\phi = -3.6$

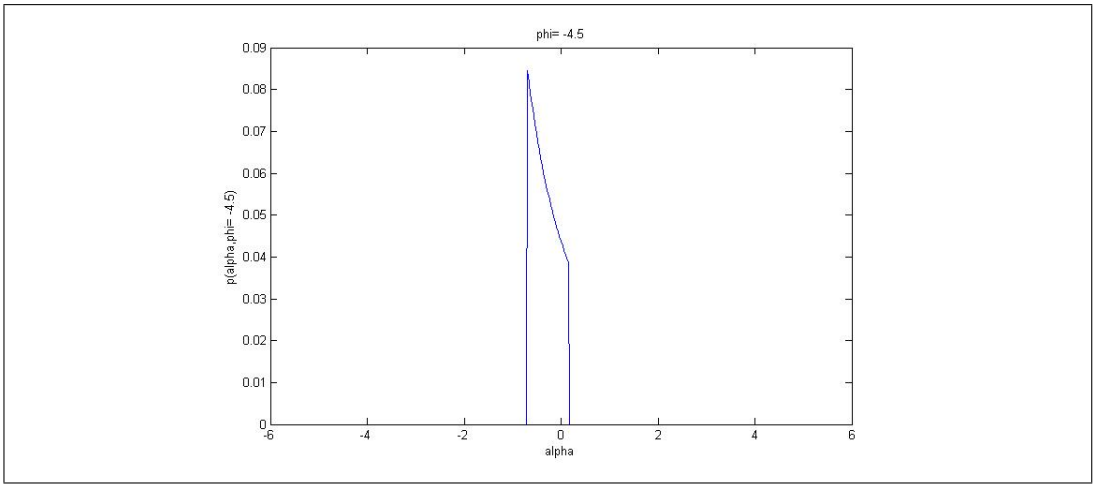

Figure 6.18: Probability density distribution at $\phi = -4.5$

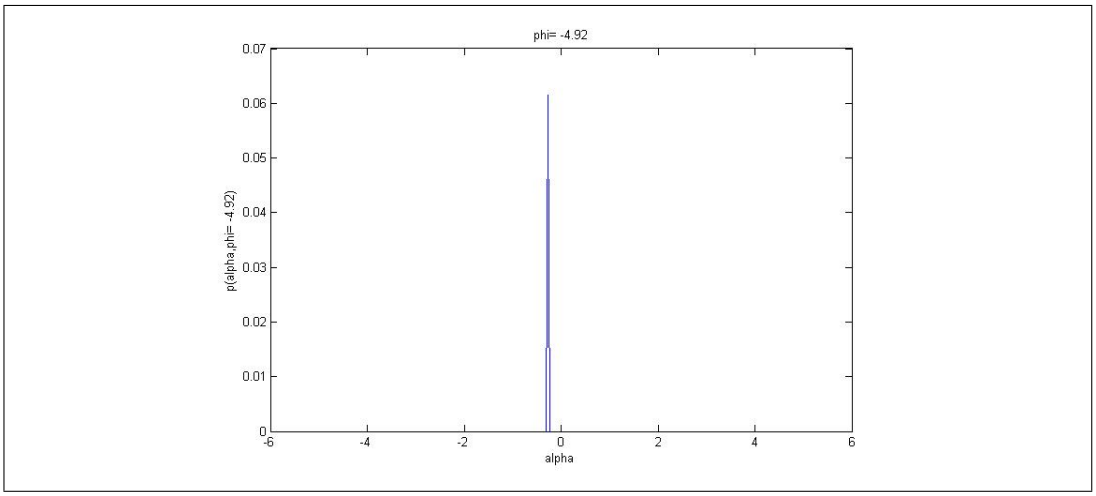

Figure 6.19: Probability density distribution at $\phi = -4.92$

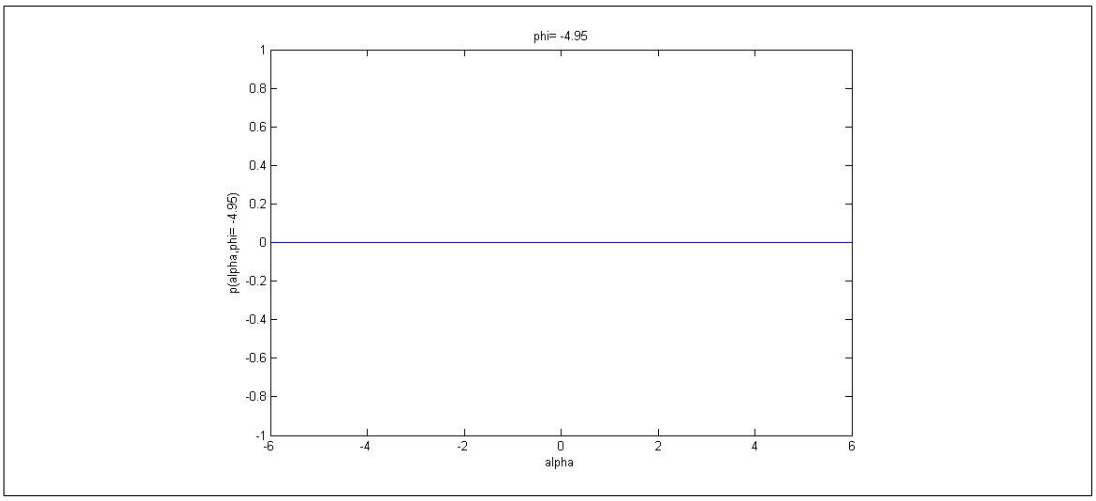

Figure 6.20: Probability density distribution at $\phi = -4.95$

from $\alpha = 0$, $\phi = 0$ that we saw in Figure 6.5.

The oscillations still persist even though we once again have linear behaviour due to the Gaussian peak being larger (Figure 6.12), and in Figure 6.13 we see that an oscillatory peak eventually outgrows the Gaussian peak again, and that oscillatory peak hereon remains the largest of the two peaks until the end of the evolution. This new peak moves forward (i.e. to higher scale factor values) throughout the rest of the backward evolution, eventually merging with the Gaussian peak (Figure 6.16). This behaviour corresponds to the jump to a lower scale factor value, and the subsequent movement of the peak to higher scale factor values for the rest of the backward evolution (the 'bounce') seen in Figure 6.5. Finally, the loss of range mentioned earlier causes the range of lattice points to shrink (Figures 6.17-6.19), and ultimately results in the wavepacket vanishing at $\phi = -4.95$ (Figure 6.20).

The bounce at the end of the forward evolution is much simpler, and occurs solely due to loss of range. Figures 6.21 to 6.36 show the forward evolution of the wavepacket, with Figures 6.27 to 6.36 showing the last few lattice steps in intrinsic time of the evolution to elucidate how the peak of the wavepacket moves backwards in space at the end of the evolution, as the range of positive probability density values becomes smaller. Here we see that the loss of range causes the original, linearly behaving

peak to be 'hidden', and the 'peak' of the wavepacket thereafter is just the highest probability density value that remains after the loss of range. In Figures 6.23 and 6.24 we also see a clear depiction of truncation of the wavepacket due to the occurrence of negative or complex numbers.

As mentioned before, for all ζ values below 0.03, we find similar behaviour to what we have seen thus far. However there are occasionally minute differences; for example if $\zeta = 0.00926$, the deflation-reinflation phase seen at the first bounce does not happen just once, but several times before the expansion continues. Such minute differences were rather common throughout the entire numerical analysis, especially

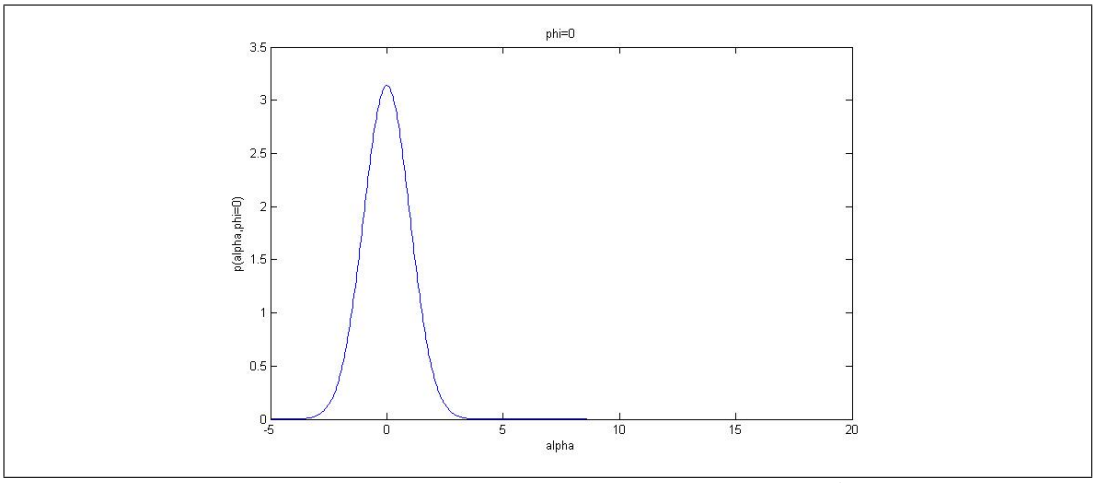

Figure 6.21: Probability density distribution at $\phi = 0$

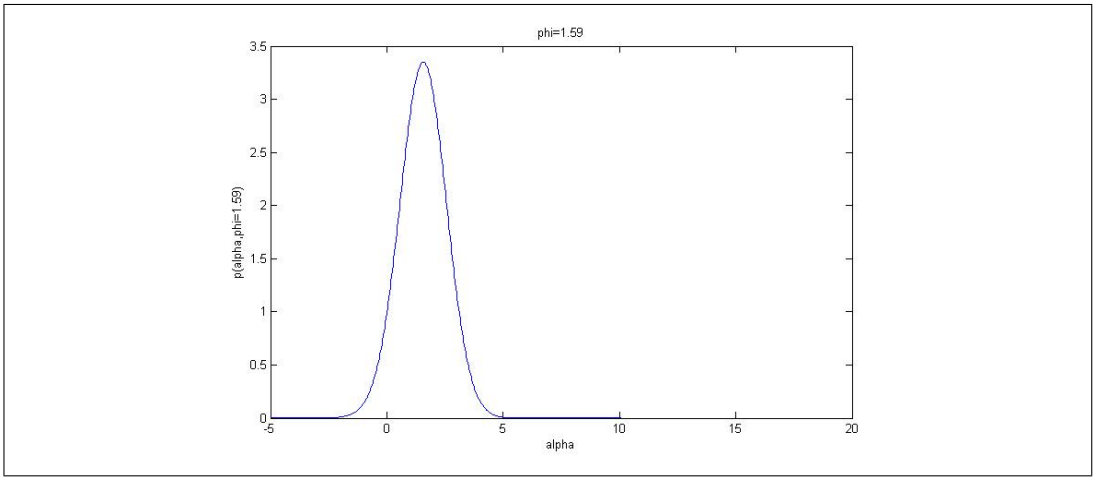

Figure 6.22: Probability density distribution at $\phi = 1.59$

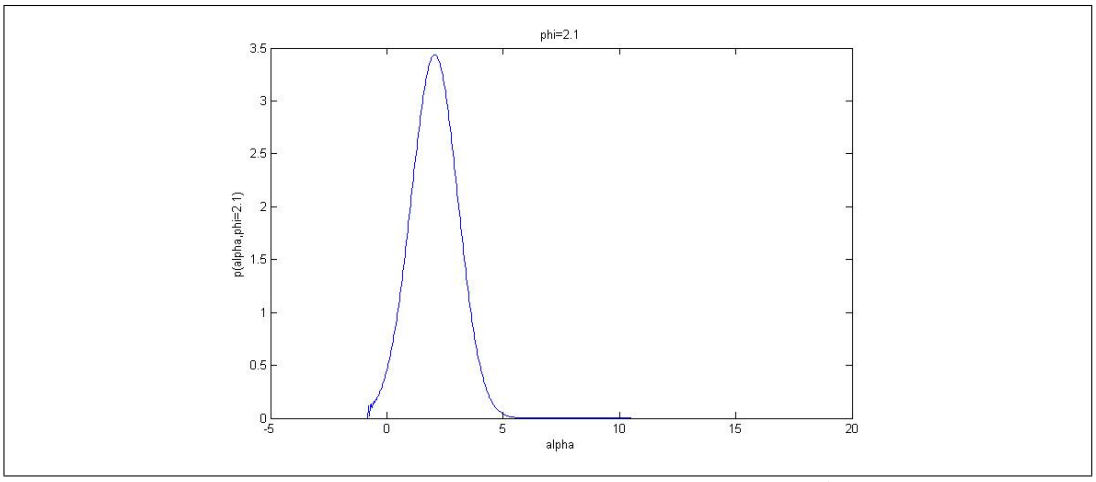

Figure 6.23: Probability density distribution at $\phi = 2.1$

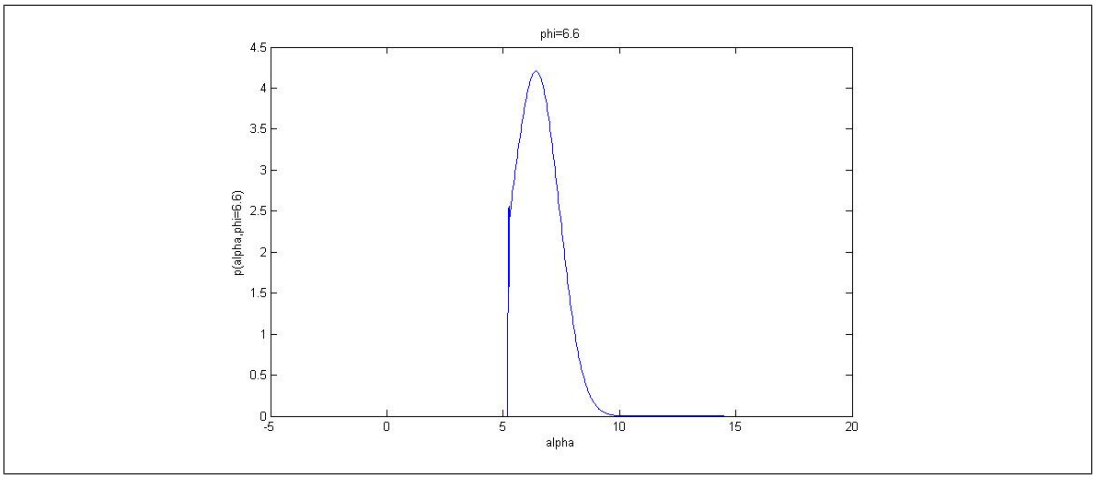

Figure 6.24: Probability density distribution at $\phi = 6.6$

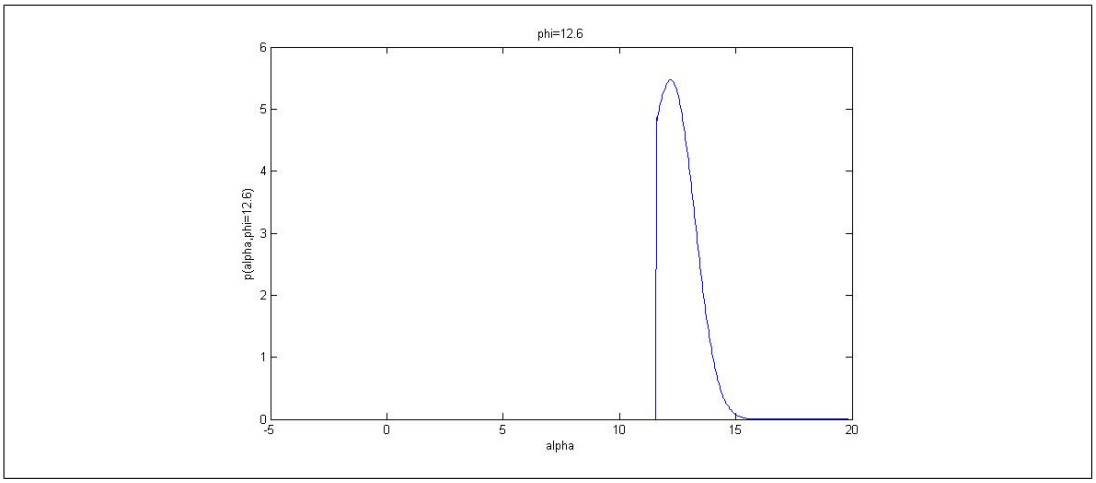

Figure 6.25: Probability density distribution at $\phi = 12.6$

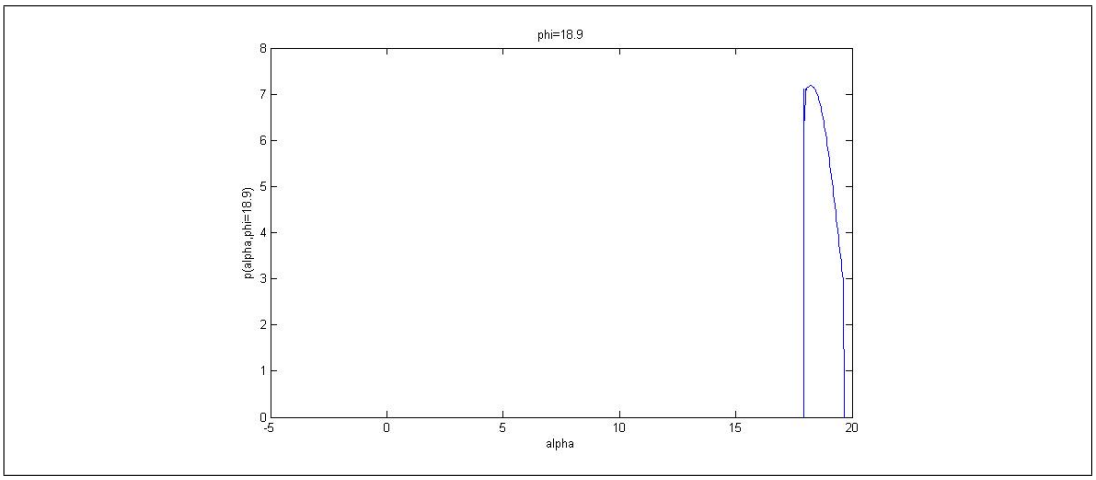

Figure 6.26: Probability density distribution at $\phi = 18.9$

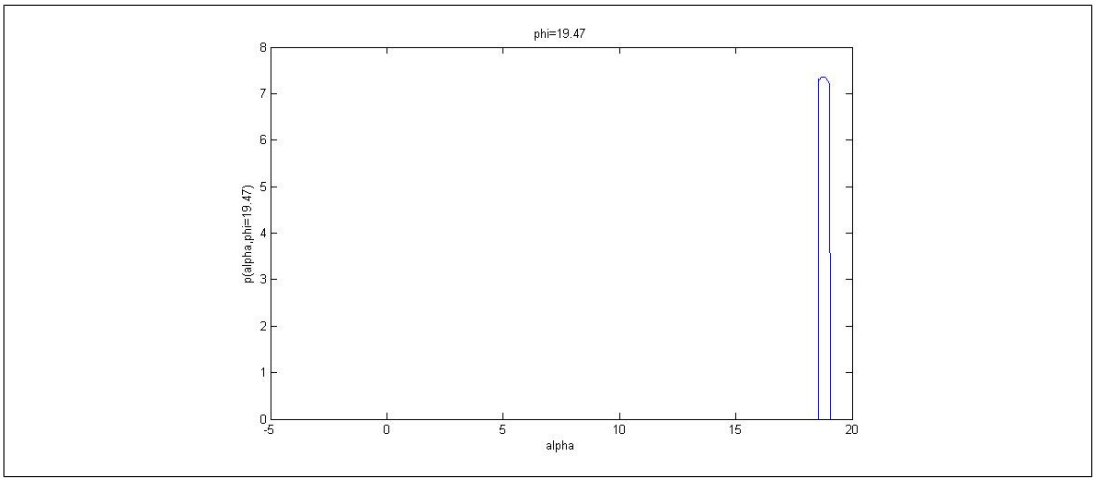

Figure 6.27: Probability density distribution at $\phi = 19.47$

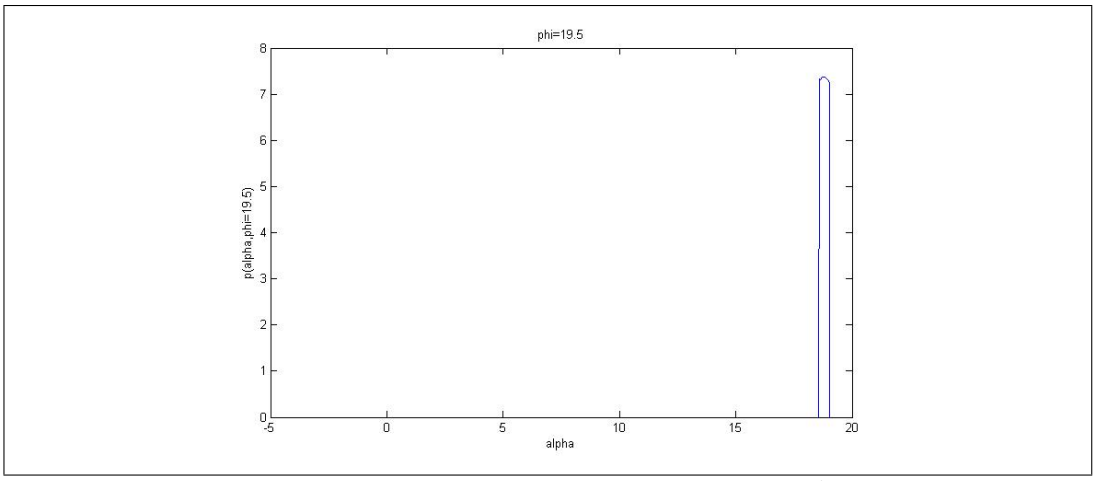

Figure 6.28: Probability density distribution at $\phi = 19.5$

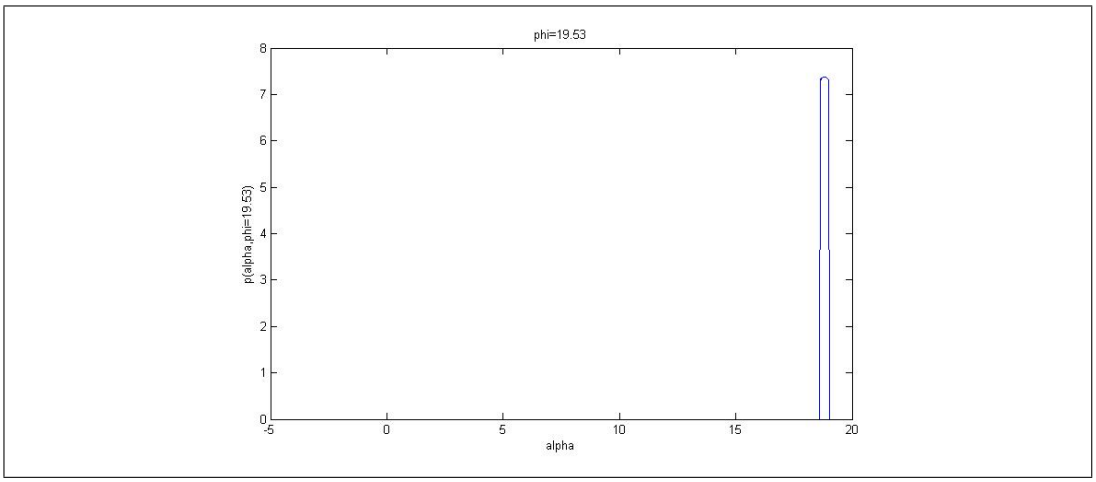

Figure 6.29: Probability density distribution at $\phi = 19.53$

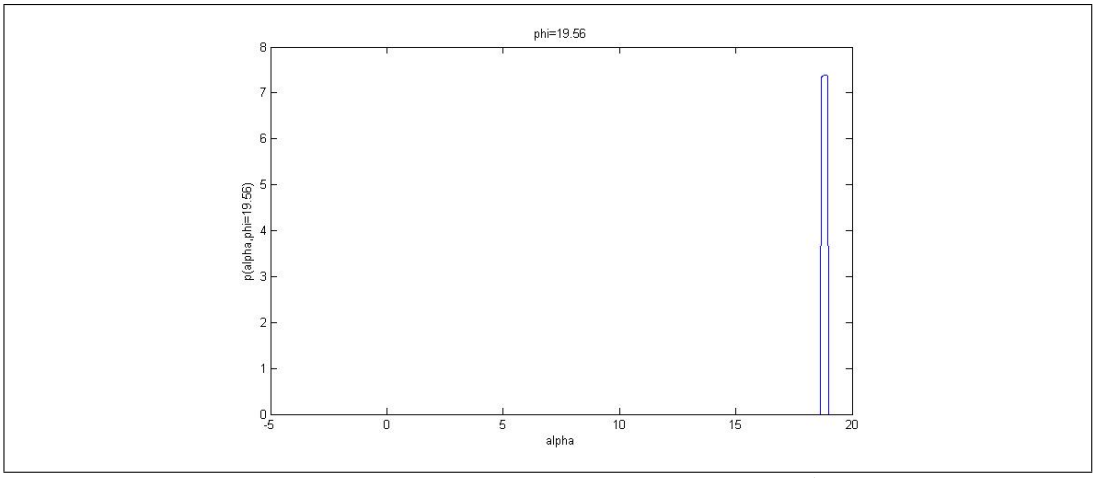

Figure 6.30: Probability density distribution at $\phi = 19.56$

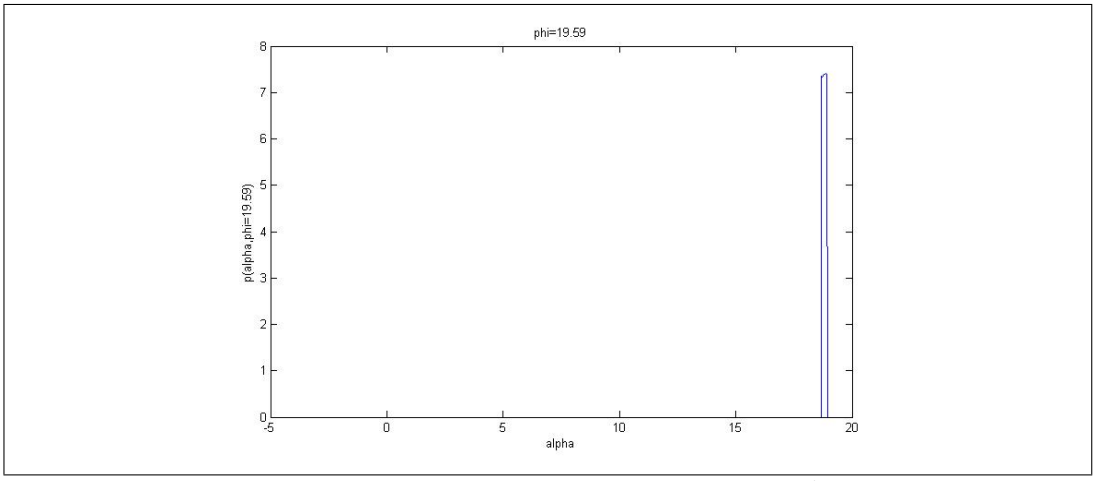

Figure 6.31: Probability density distribution at $\phi = 19.59$

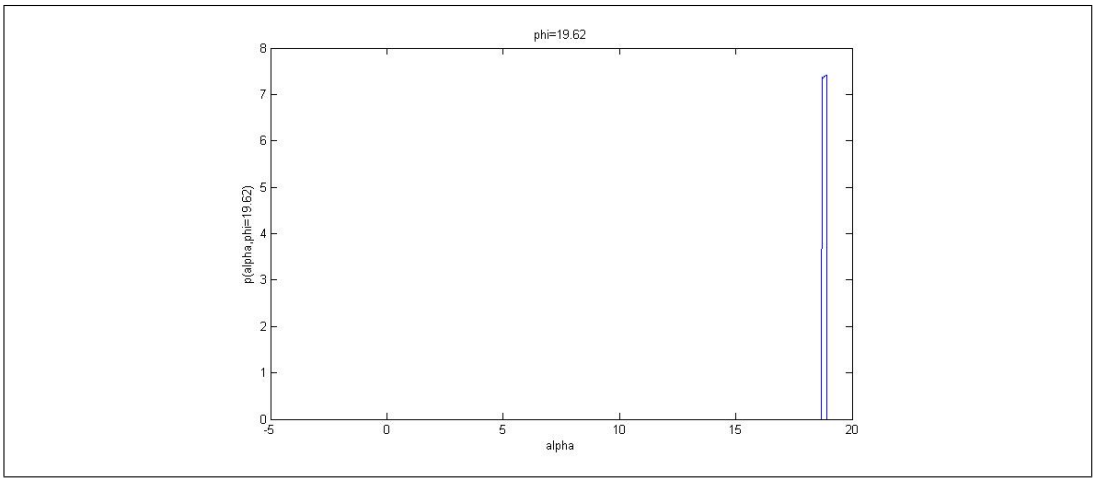

Figure 6.32: Probability density distribution at $\phi = 19.62$

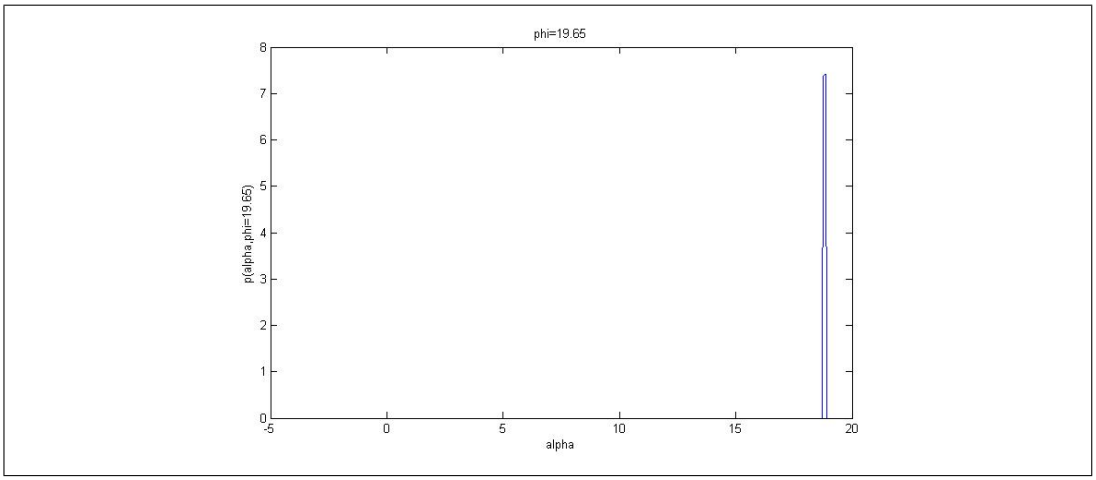

Figure 6.33: Probability density distribution at $\phi = 19.65$

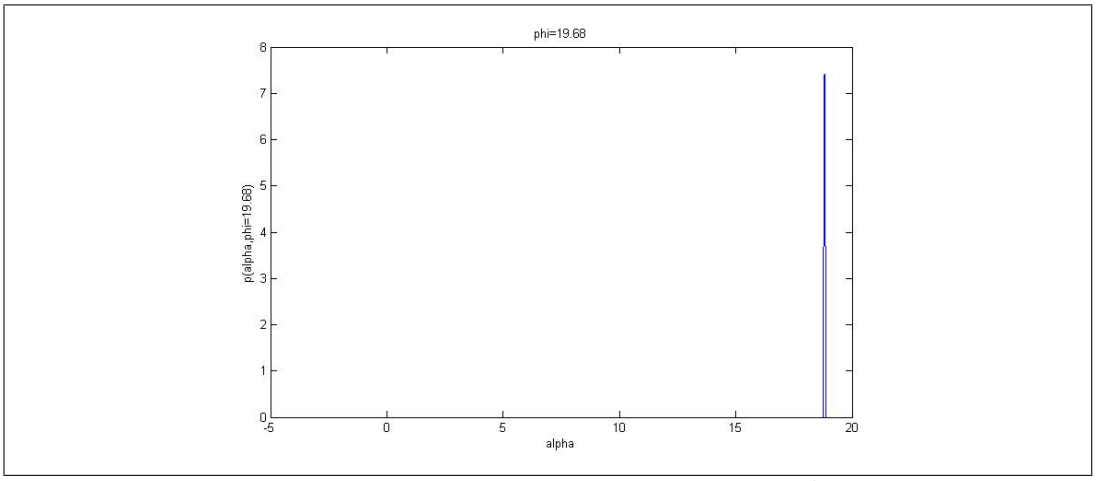

Figure 6.34: Probability density distribution at $\phi = 19.68$

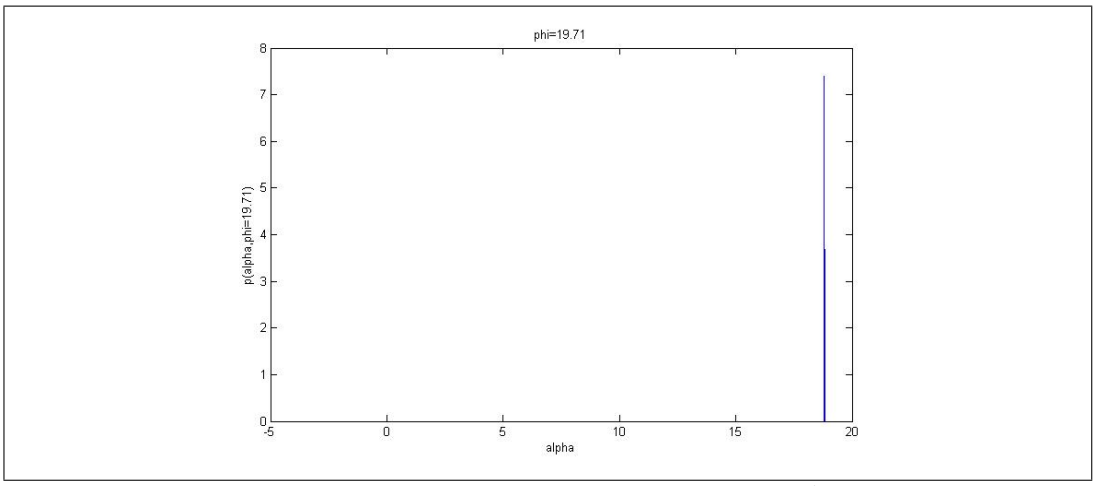

Figure 6.35: Probability density distribution at $\phi = 19.71$

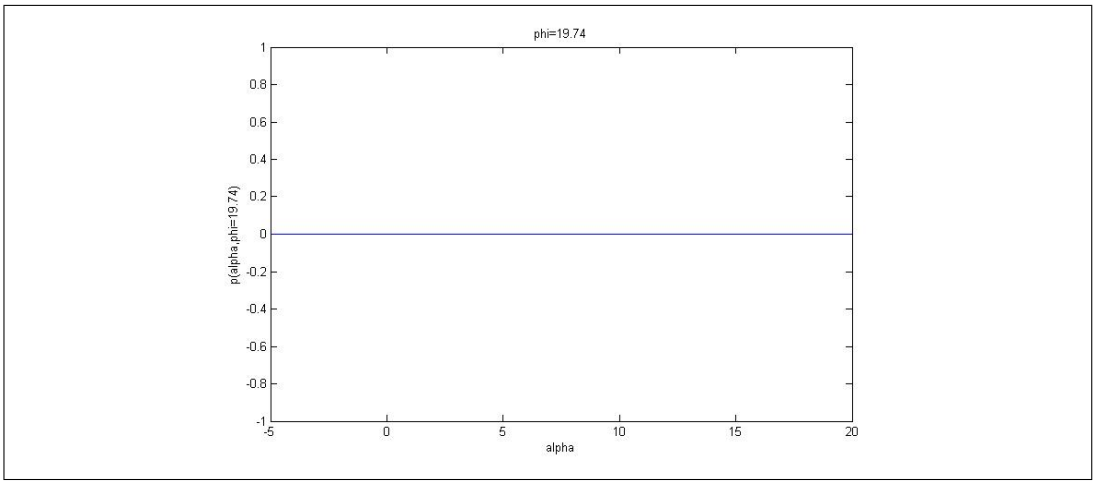

Figure 6.36: Probability density distribution at $\phi = 19.74$

at the end of the backward and forward evolutions, and here we shall not place much emphasis on them, instead focusing on how the general features of the peak behaviour change as the parameters ζ and η are varied.

For $0.04 \leq \zeta \leq 0.06$, the peak behaviour of the wavepacket is very similar to that of $\zeta \leq 0.03$, with the only difference being a rapid, extremely short period of contraction, or rather a deflation, followed quickly by reexpansion of the usual linear form, occurring when the universe is at a large size. This can be seen in Figure 6.37 which shows the plot of the α value of the peak against intrinsic time, ϕ, for the case of $\zeta = 0.06$. Once again we notice a minute difference in the backward

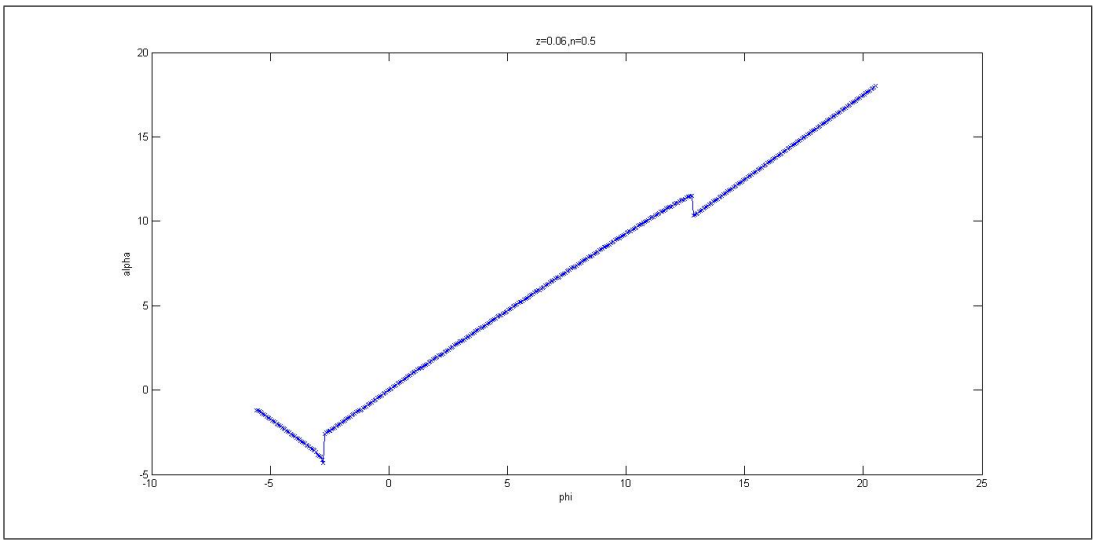

Figure 6.37: Plot of the scale factor (α) value at which the peak of the wavepacket occurs as a function of intrinsic time, ϕ for $\eta = 0.5$, $\zeta = 0.06$.

bounce compared to the previous cases; here there is no evidence of any deflation and reinflation occurring.

The deflation in the forward evolution occurs due to a secondary peak developing on the original Gaussian peak itself, instead of elsewhere in the profile. This can be seen in Figures 6.38 to 6.41. The evolution prior to that which is seen in these figures is similar to that seen in Figures 6.21 to 6.26.

For the cases of $0.07 \leq \zeta \leq 0.1$ we see a very different type of dynamics for the

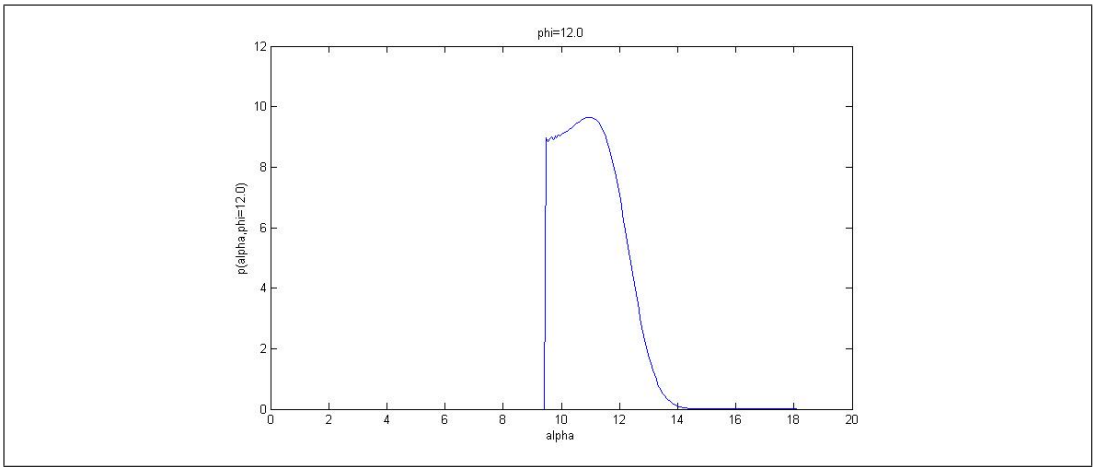

Figure 6.38: Probability density distribution at $\phi = 12.0$

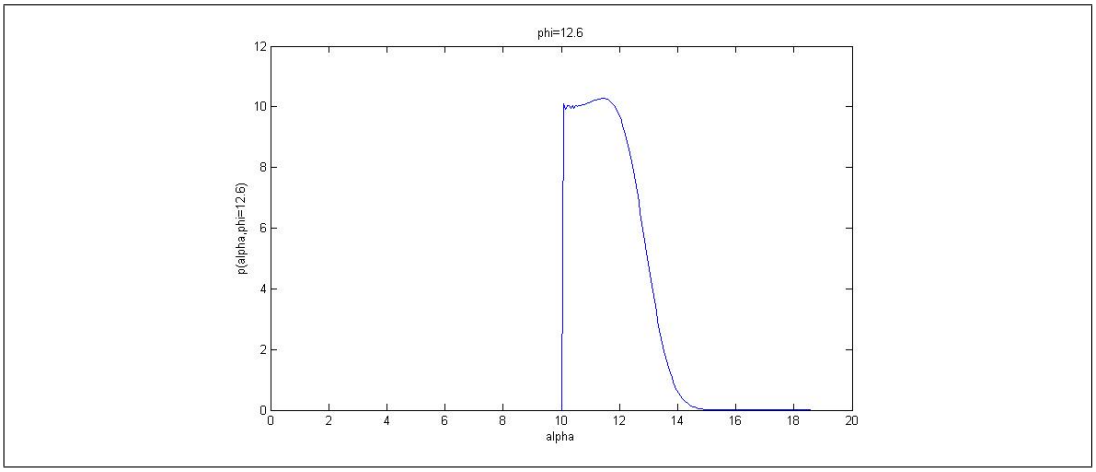

Figure 6.39: Probability density distribution at $\phi = 12.6$

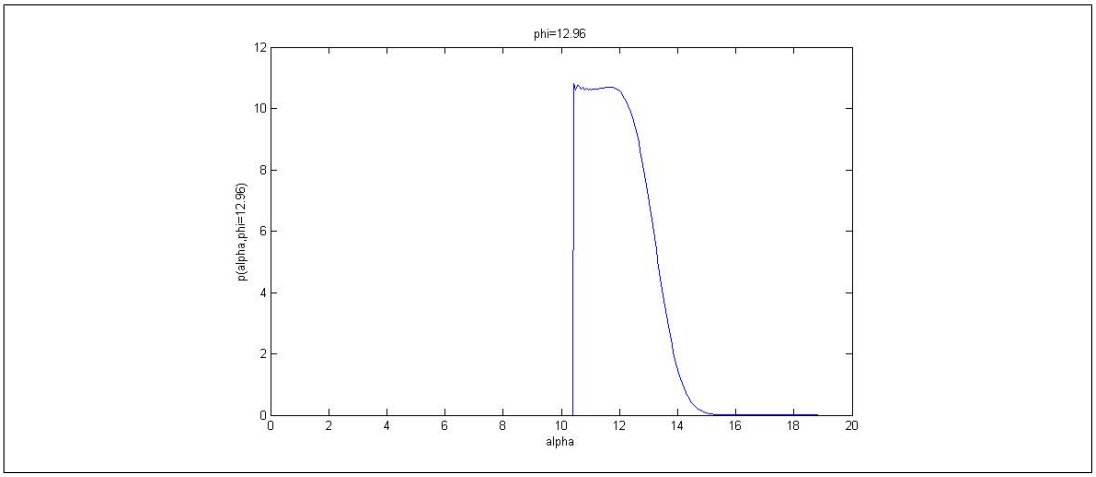

Figure 6.40: Probability density distribution at $\phi = 12.96$

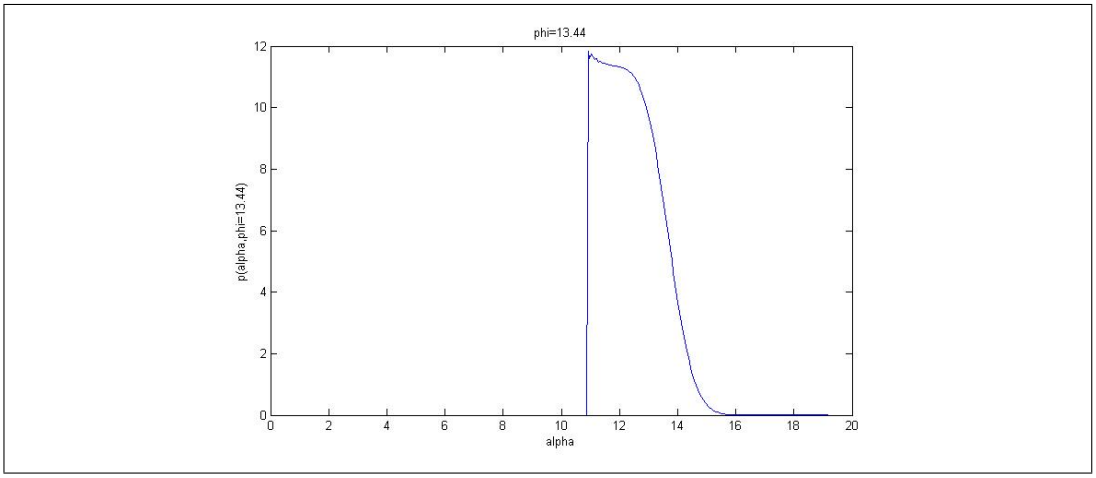

Figure 6.41: Probability density distribution at $\phi = 13.44$

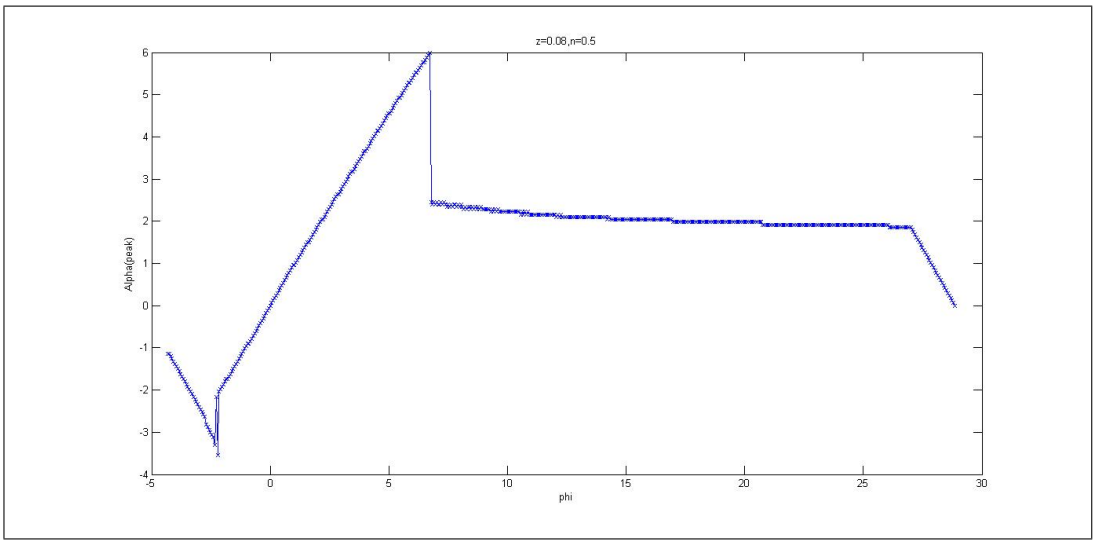

Figure 6.42: Plot of the scale factor (α) value at which the peak of the wavepacket occurs as a function of intrinsic time, ϕ for $\eta = 0.5$, $\zeta = 0.08$.

universe. Figure 6.42 shows the plot of the scale factor (α) value at which the peak of the wavepacket occurs as a function of intrinsic time, ϕ for $\zeta = 0.08$. The backward evolution for this case is similar to the previous cases seen, with a phase of inflation, deflation and reinflation present. However at $\phi = 6.7$, something unexpected happens, which is a sudden contraction of large magnitude, or deflation. This is followed by a period of further contraction. As forward evolution continues the contraction slows down, up until $\phi = 27$, when there is another sudden phase of rapid contraction, though not as rapid as the earlier one. The contraction continues until the wavepacket only has one lattice point with a non-zero value, that is when $\phi = 28.86$, and after this the wavepacket (and the universe) vanishes.

The period of contraction at the end of the forward evolution is due to the range of the probability density distribution becoming increasingly smaller, and is similar to the behaviour at the end of the forward evolution in the $\zeta = 0.03$ case. The more sudden jump from a large value of α to a smaller one that we see in the middle of the evolution however is a new type of bounce. Previously we saw bounces that occurred due to the emergence of another, non-Gaussian peak. However in this case, the bounce occurs because another Gaussian peak emerges, eventually outgrowing the

original one, and propagating in an opposite direction to it. This behaviour can be seen in Figures 6.43 to 6.46.

In Figure 6.42, one also notices upon closer inspection that the nonlinear contraction phase seems to be staccato, and consisting of sudden jumps. This however is just the effect of the discreteness of the difference equation mentioned earlier coming into play. The actual peak at any point in intrinsic time could be in between two lattice points, and the value we take as our peak value is merely the largest lattice point value. As such we should understand that the decelerating contraction phase seen in Figure 6.42 is actually continuous.

The fourth general type of universe found for $\eta = 0.5$, that is for the cases with $\zeta \geq 0.2$ has the form seen in Figure 6.47. Here, the large step size of $\zeta = 0.4$ causes the plot to be even more discontinuous than previously seen, and thus the possible, actual evolution of the peak approximately deduced through interpolation is also plotted in Figure 6.47. In this type of evolution the usual backward evolution is still seen, with the typical bounce followed by inflation as ϕ increases. However, in the forward evolution a new type of bounce occurs, which does not involve the growth of any secondary peak, but rather is only caused by the original wavepacket changing its direction of propagation. The contraction which occurs after the bounce is found

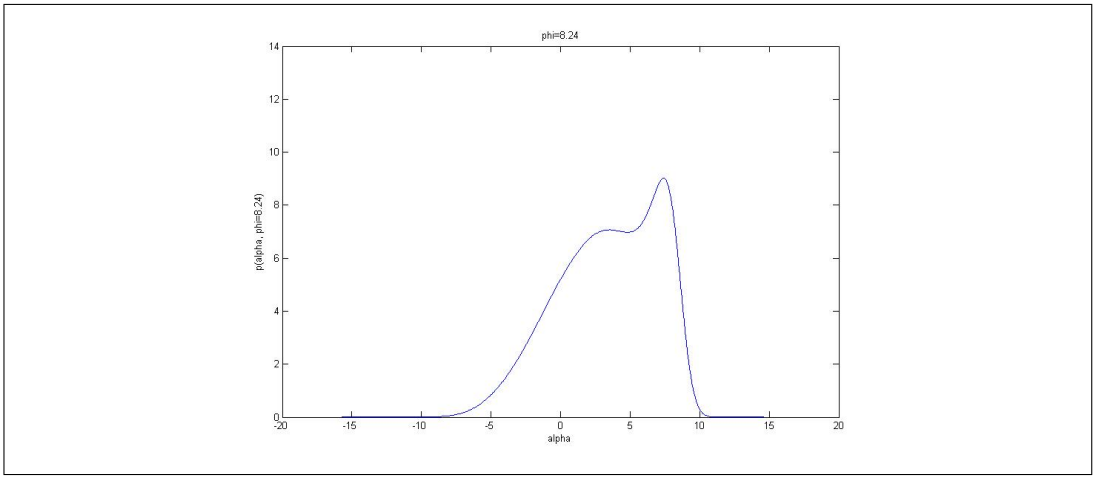

Figure 6.43: Probability density distribution at $\phi = 8.24$

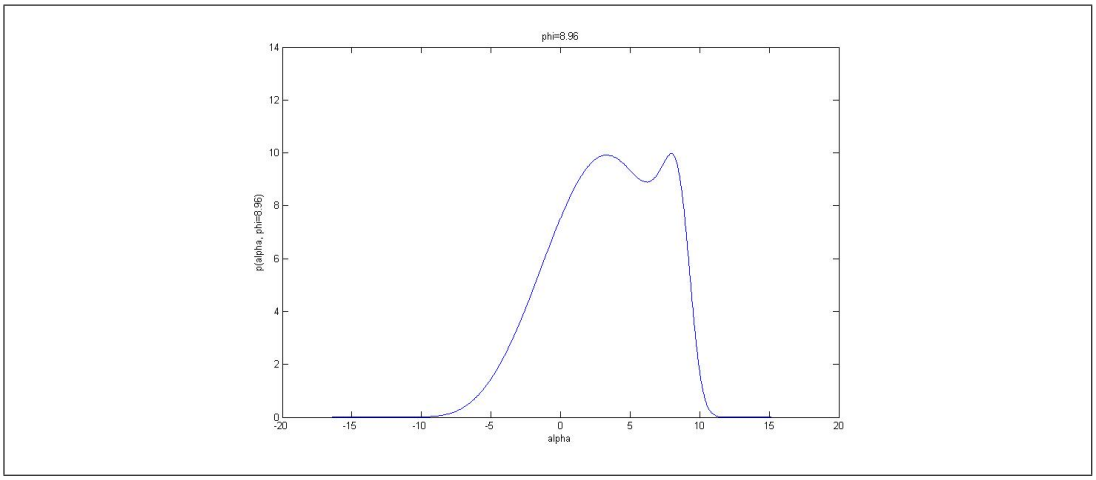

Figure 6.44: Probability density distribution at $\phi = 8.96$

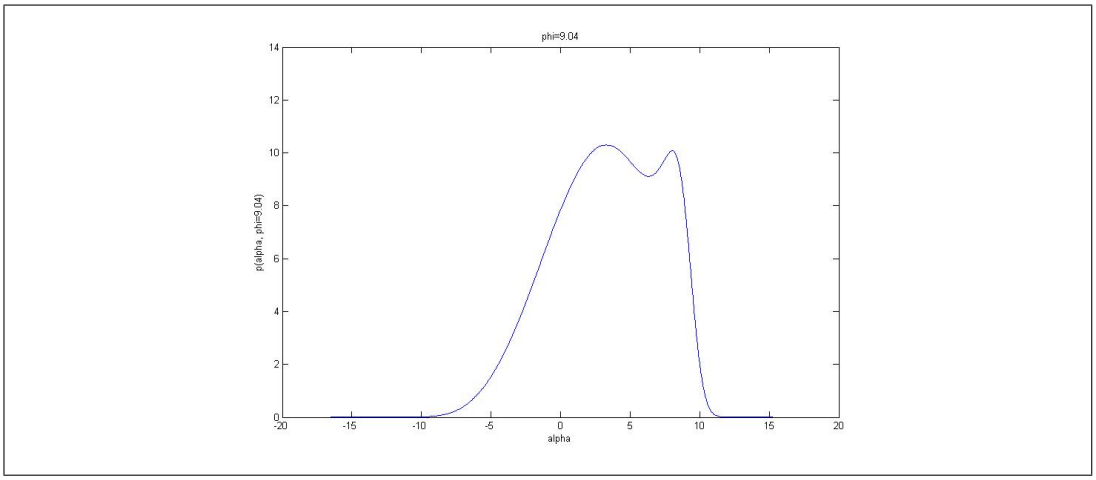

Figure 6.45: Probability density distribution at $\phi = 9.04$

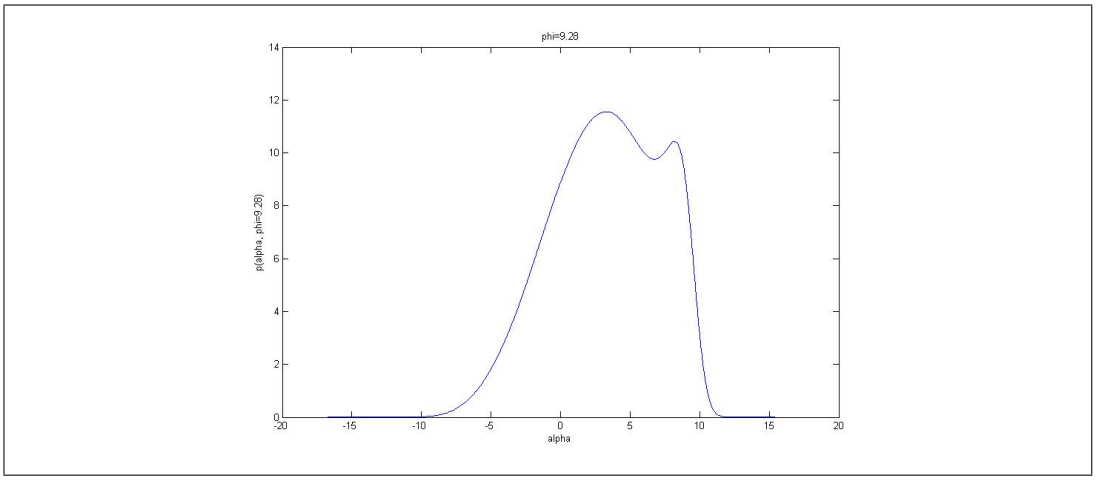

Figure 6.46: Probability density distribution at $\phi = 9.28$

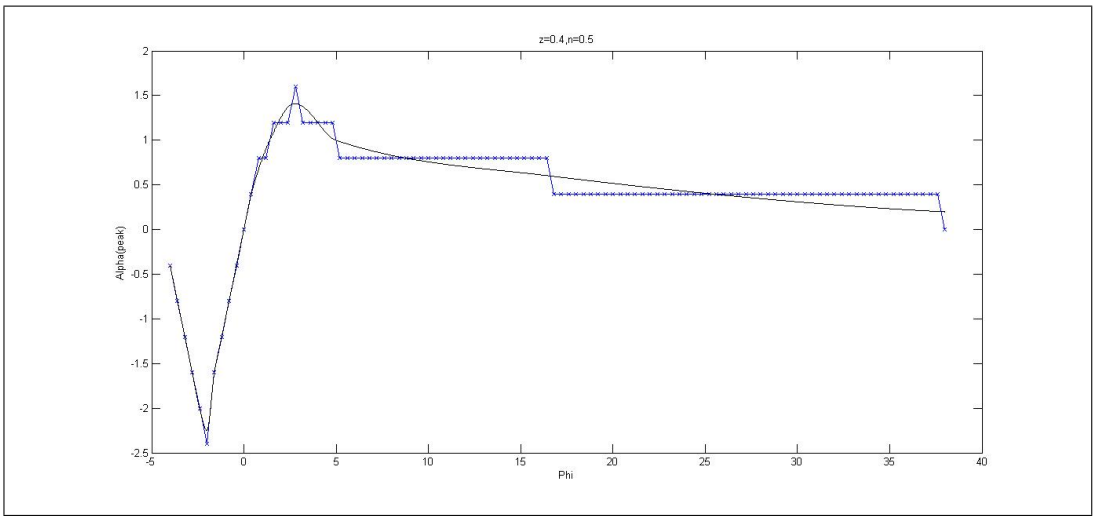

Figure 6.47: Plot of the scale factor (α) value at which the peak of the wavepacket occurs as a function of intrinsic time, ϕ for $\eta = 0.5$, $\zeta = 0.4$.

to slow down at first, and then settles to a constant speed. Finally at $\phi = 38$ there is only one non-zero lattice point in the profile, and for higher values of ϕ the wavepacket vanishes, signalling the end of the universe.

6.6.2 η=0.1

For the family of universes with $\eta = 0.1$ the results are very similar to that of $\eta = 0.5$. For $\zeta \leq 0.0095$ we find that the scale factor value of the peak of the wavepacket varies with intrinsic time, ϕ as in Figure 6.48, which has behaviour similar to that seen in Figure 6.5, with the minute difference that the contraction phase at the beginning of the evolution is much shorter. This extremely short contraction phase cannot be seen in Figure 6.48 due to the small lattice spacing, but is nevertheless present. If $0.01 \leq \zeta \leq 0.1$, then we find peak behaviour which is the same as that seen in Figure 6.37. Finally for universes with $\zeta \geq 0.2$, the peak behaviour is that seen in Figure 6.47. It should be noted that behaviour of the type seen in Figure 6.42 is absent for all universes which have $\eta = 0.1$.

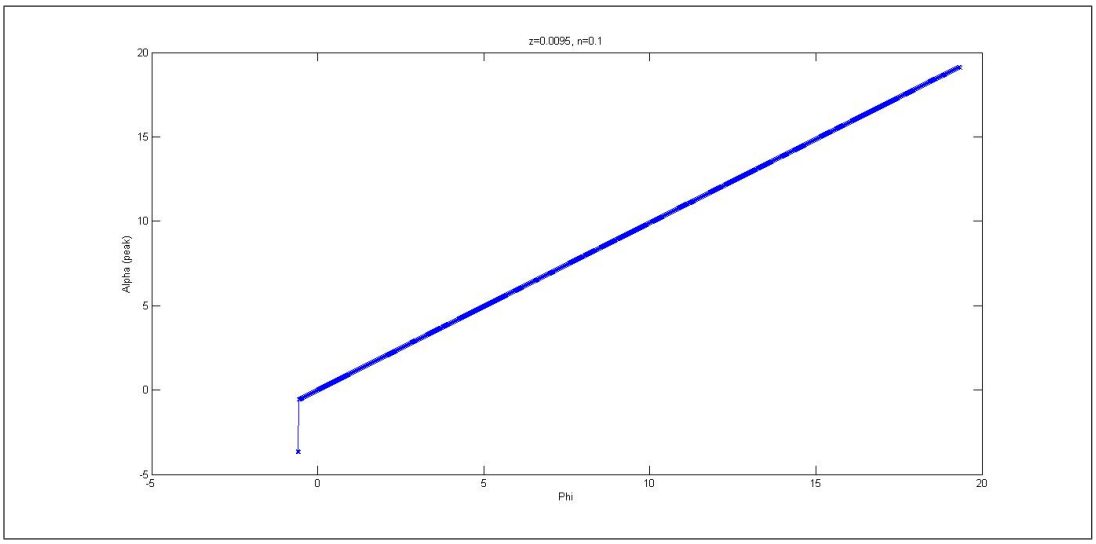

Figure 6.48: Plot of the scale factor (α) value at which the peak of the wavepacket occurs as a function of intrinsic time, ϕ for $\eta = 0.1$, $\zeta = 0.0095$.

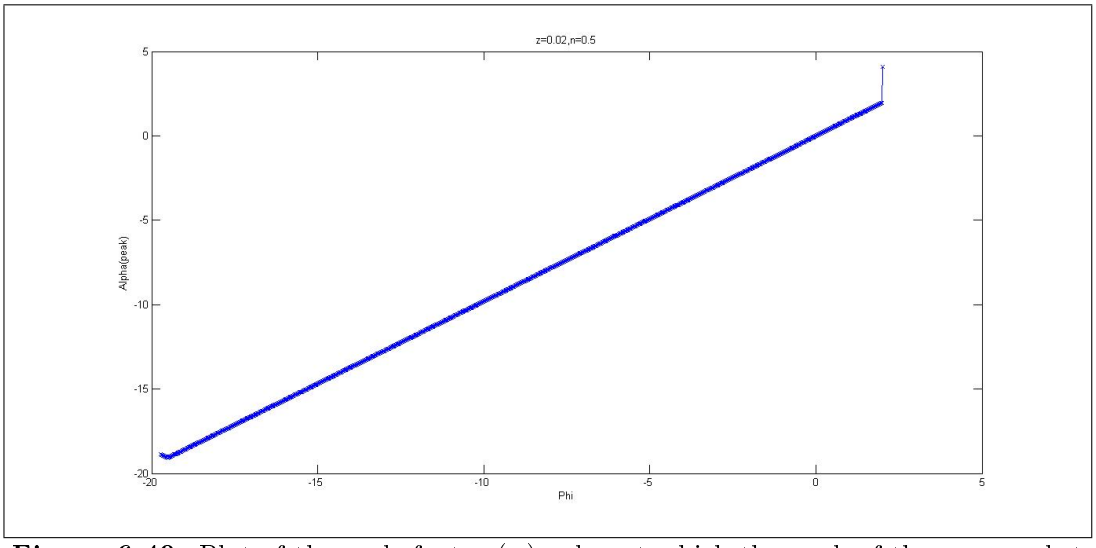

Figure 6.49: Plot of the scale factor (α) value at which the peak of the wavepacket occurs as a function of intrinsic time, ϕ for $\eta = 0.9$, $\zeta = 0.03$.

6.6.3 η=0.9

For $\eta = 0.9$ we find dynamics that we did not see previously for the other two η values. The first unique type of dynamics we see is in the range $0 < \zeta \leq 0.03$, an example of which is the evolution for $\zeta = 0.02$, as seen in Figure 6.49. In this range we have a bounce in the backward evolution. However this bounce is merely due to the range

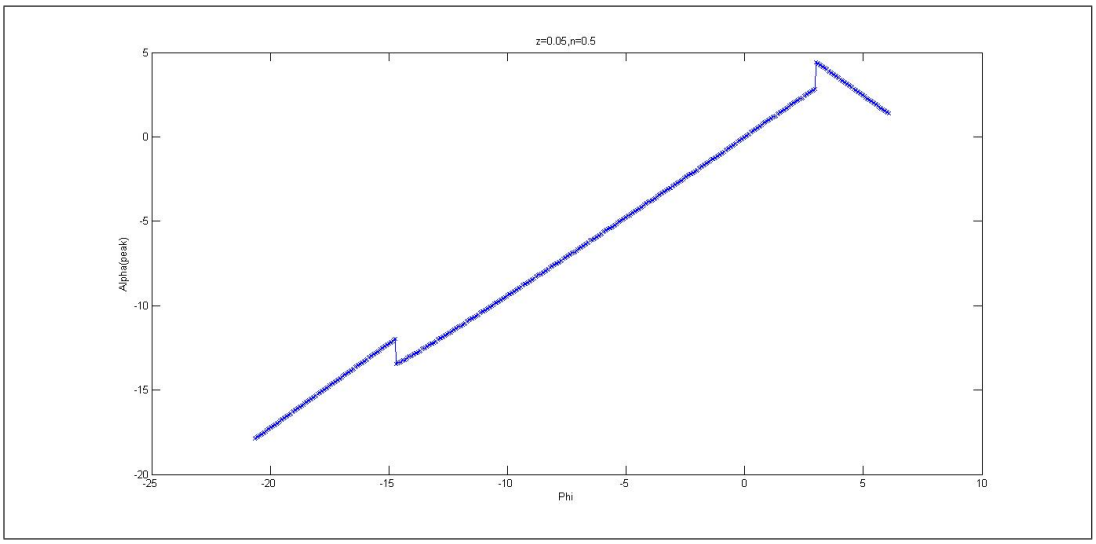

Figure 6.50: Plot of the scale factor (α) value at which the peak of the wavepacket occurs as a function of intrinsic time, ϕ for $\eta = 0.9$, $\zeta = 0.05$.

of the wavepacket becoming smaller as it evolves, causing the point where the peak is to change. There is also no inflation in the at the beginning of the evolution. The forward evolution on the other hand is mostly linear, except at the very end, where there is a sudden jump similar to the inflation previously seen. However right after this inflation, the wavepacket, and thus the universe, vanishes. It is not very difficult to see the similarity between these dynamics, and that seen in Figure 6.48. In fact the plot in Figure 6.49 looks just like the plot in Figure 6.48 but with the spatial and temporal axes reversed.

For $0.04 \leq \zeta \leq 0.05$, we find a slightly different evolution, as seen in Figure 6.50, which shows the dynamics for a universe with $\zeta = 0.05$. We see a universe that starts out at a finite size, expands linearly, up to a certain point, when there is a sudden contraction, followed quickly by linear expansion. Near the end of its life, it suddenly inflates, then begins to contract, finally vanishing at a finite size. Once again we find dynamics similar to that found previously, but with orientation reversal of the axes. Here we find that the plot in Figure 6.50 looks almost exactly like the plot in Figure 6.37 upside down. This is further confirmed by the fact that the wavepacket behaves similarly in both cases, except that now it is moving in the opposite directions in time

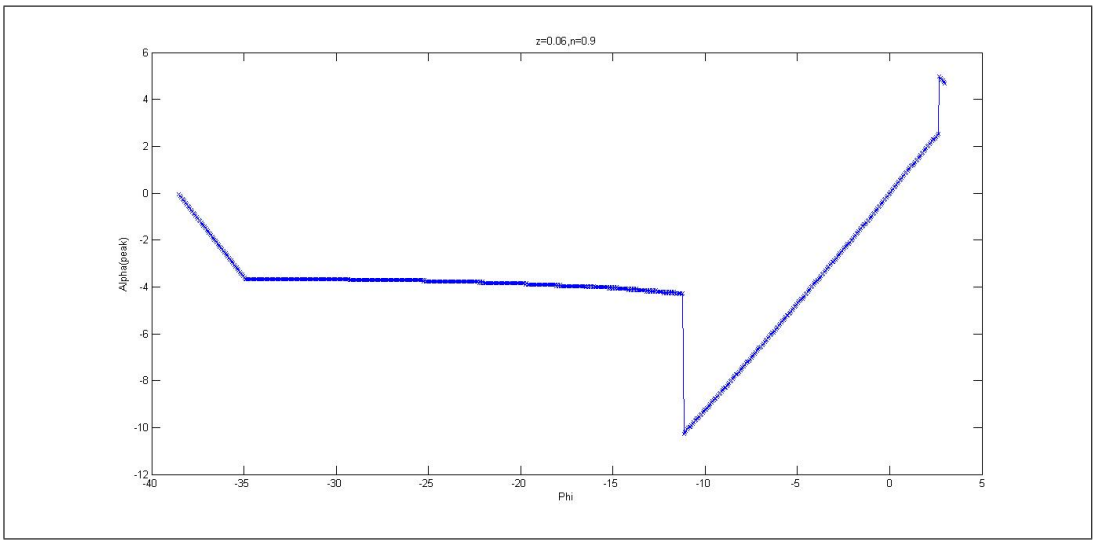

Figure 6.51: Plot of the scale factor (α) value at which the peak of the wavepacket occurs as a function of intrinsic time, ϕ for $\eta = 0.9$, $\zeta = 0.06$.

and space.

Behaviour which is opposite to that found in the $\eta = 0.5$ case can also be seen for the range $0.06 \leq \zeta \leq 0.1$, as seen in Figure 6.51. These dynamics are again just that seen in Figure 6.42, but with the spatial and temporal axes flipped. Here we see a universe that is born at a finite size, contracting rapidly at first, before suddenly entering a phase of very slow contraction. This contraction eventually speeds up, and it culminates with a sudden deflation. From here the universe expands linearly up until a point near its death, where it again inflates, but not with as large a magnitude as seen in the earlier deflation. After inflating it contracts for a short period of time, and then vanishes. The deflation of large magnitude that we see in the middle of the evolution, as expected, occurs due to the appearance of another Gaussian peak, which outgrows the original one.

For the range $0.1 \leq \zeta \leq 0.4$, we see dynamical behaviour as in Figure 6.52. Again, this is similar to the evolution seen in Figure 6.47, but with the spatial and temporal axes inverted. Here we see a universe that is born with finite size, which undergoes rapid contraction at first, which then abruptly slows down. The contraction continues, gradually speeding up, and suddenly we see a period of rapid contraction, followed

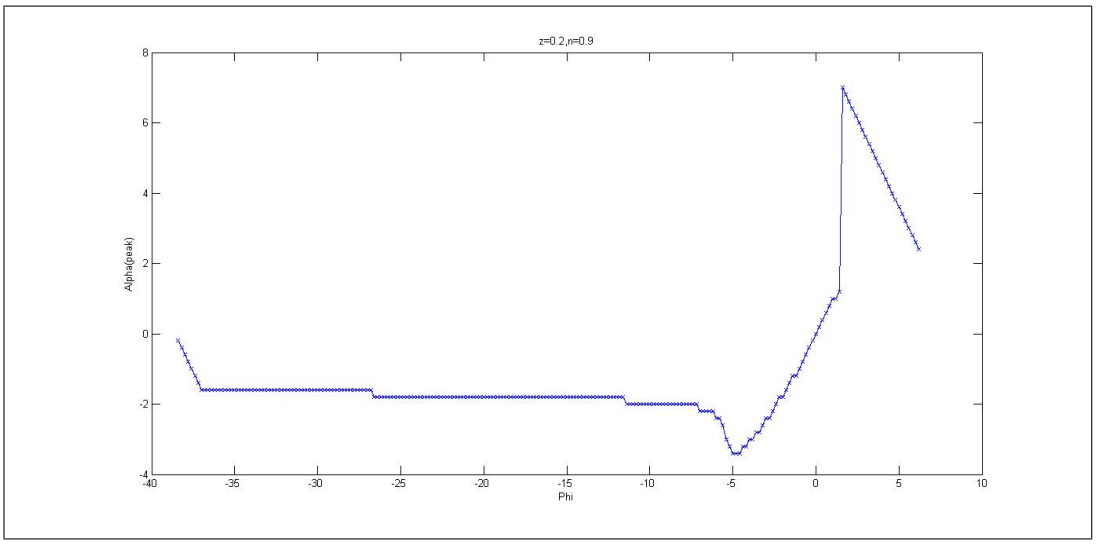

Figure 6.52: Plot of the scale factor (α) value at which the peak of the wavepacket occurs as a function of intrinsic time, ϕ for $\eta = 0.9$, $\zeta = 0.2$.

by expansion (a bounce). There seems to be a short period of slight acceleration in the expansion, which eventually vanishes to make the expansion linear, up to a point when there is sudden inflation. After the inflation the universe contracts, down to a certain ϕ value, at which the wavepacket vanishes.

For $\zeta \geq 0.5$, the dynamics of the universe become hard to discern, mainly because the large lattice step size obscures the actual locations of the peaks, and the behaviour is much more complicated when compared to previous η values for the same range of ζ, leaving us with an inaccurate description of the peak behaviour. However we will still attempt to understand the behaviour from the lattice points we have. For $\zeta = 0.5$ (Figure 6.53) the dynamics are rather unique when compared to others in the range. We see that there are two plateaus within a certain range of ϕ in the plot, however by studying the form of the probability denstiy functions in that range, we can deduce that the plateaus actually contain two bounces, one at a larger size followed by one at smaller size, with both bounces occurring around the centre of the plateaus. We do not actually see the bounces since they are obscured due to the large step size. After the bounces there seems to be linear expansion, which eventually slows down, and the evolution finally culminates with an inflation of high magnitude, after which

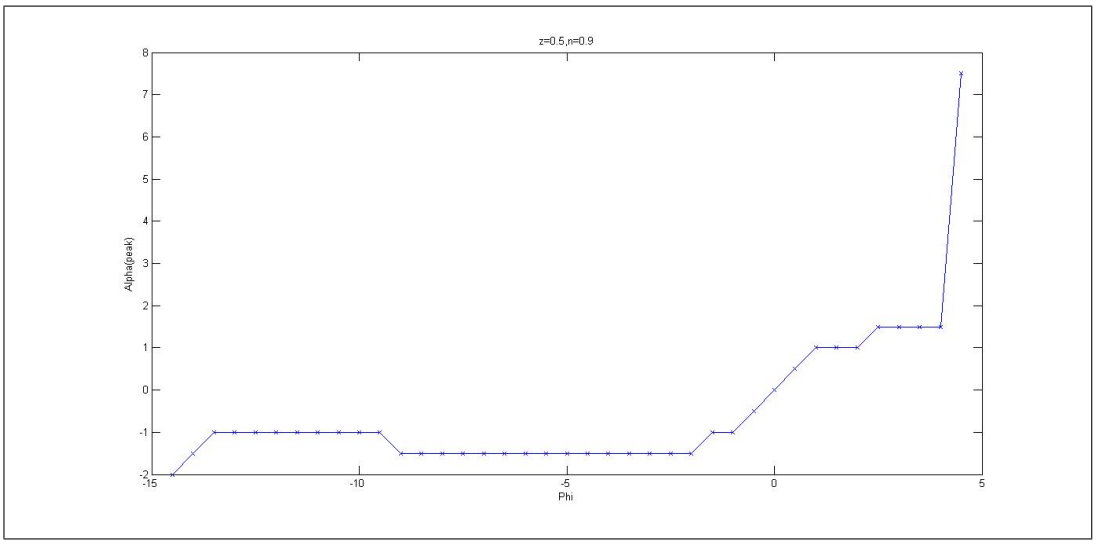

Figure 6.53: Plot of the scale factor (α) value at which the peak of the wavepacket occurs as a function of intrinsic time, ϕ for $\eta = 0.9$, $\zeta = 0.5$.

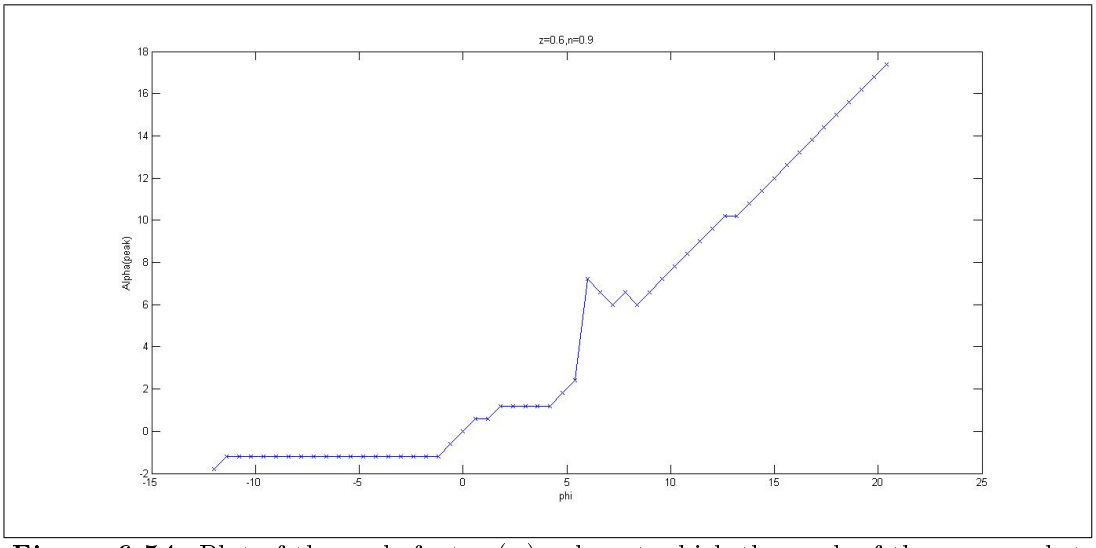

Figure 6.54: Plot of the scale factor (α) value at which the peak of the wavepacket occurs as a function of intrinsic time, ϕ for $\eta = 0.9$, $\zeta = 0.6$.

the wavepacket disappears.

Finally for $\zeta \geq 0.6$ we see dynamics as in Figure 6.54. As in the previous case this plot is difficult to interpret, due to the large step size. From studying the probability density distributions in its range, the plateau here does not seem to contain a bounce, but rather is a period of very slow expansion. We then see a period of erratic expansion, in which we see linear expansion at first, which then slows down, and then

speeds up again, followed by an inflation-like jump. We then see contraction, followed by slight fluctuations in size, before near linear expansion continues once again, before the wavepacket disappears at a finite time.

6.7 A Proof of Consistency

We shall now find an exact solution to the difference equation (6.58), using only 5 lattice points. We let p_- and p_+ to be equal to 0, and we let p be some positive number. For the values of p^+ and p^- we say that the peak of the wavepacket grows and the wavepacket itself becomes narrower in both the forward and backward evolution, and as such we choose both p^+ and p^- to be equal to $1.5p$.

Now the constant terms in the difference equation,

$$-a^2 + b^2 = \zeta + 1.25\zeta^2, \tag{6.66}$$

due to the forms (6.54) and (6.55) we have chosen for a and b respectively. The expression (6.66) is positive definite, as long as $\zeta > 0$. Thus it follows that the combination of the third and fourth terms in the difference equation (6.58) must be negative definite, which leads to the inequality

$$\begin{aligned} &\frac{1}{2\zeta^2\eta^2}\left[\ln\left(\frac{p}{(1-\eta)p+\eta p_+}\right)+\frac{\eta p_+}{(1-\eta)p+\eta p_+}-\frac{\eta p_-}{(1-\eta)p_-+\eta p}\right] > \\ &\frac{1}{2\zeta^2\eta^2}\left[\ln\left(\frac{p}{(1-\eta)p+\eta p^+}\right)+\frac{\eta p^+}{(1-\eta)p+\eta p^+}-\frac{\eta p^-}{(1-\eta)p^-+\eta p}\right]. \end{aligned} \tag{6.67}$$

Using the 5 lattice points we chose earlier, the inequality becomes,

$$\ln\left(\frac{p}{(1-\eta)p}\right) > \ln\left(\frac{p}{(1-\eta)p+\eta(1.5p)}\right)+\frac{\eta(1.5p)}{(1-\eta)p+\eta(1.5p)}-\frac{\eta(1.5p)}{(1-\eta)(1.5p)+\eta p}, \tag{6.68}$$

which can be simplified to become

$$\ln\left(\frac{1}{1-\eta}\right) > \ln\left(\frac{1}{1+0.5\eta}\right) + \frac{1.5\eta}{1+0.5\eta} - \frac{1.5\eta}{1.5-0.5\eta}. \tag{6.69}$$

After some further algebra, the inequality can be reduced to

$$\ln\left(\frac{1+\frac{\eta}{2}}{1-\eta}\right) > \frac{3-6\eta}{1-\eta+\frac{6}{\eta}}. \tag{6.70}$$

This expression is only satisfied for the range $0 < \eta \leq 1$, which is consistent with the range of values η can take. We can also find similar expressions consistent with the same range for other choices of p^+ and p^-, as long as $p^+ = p^- > p$.

6.8 Interpretation of results

We have seen that the non-pertubative study of the Wheeler-DeWitt difference equation for a flat FLRW universe containing a free massless scalar field gives us several types of dynamics for different values of the nonlinear parameters η and ζ. It may be somewhat strange that in all cases we see that the wavepacket that represents the uncertainty in scale factor value vanishes at a large size, which in all cases is larger than the size the universe was born with, and also larger than the minimum size the universe reaches during the evolution. Although mathematically it is not a surprising effect considering the form of the difference equation, it is not physically appealing to have a universe that vanishes at large size. We also see that the universe is born at a finite size, which can be interpreted as the universe having tunnelled into existence. Using this interpretation one may also postulate that at the end of its life the universe tunnels out of existence, perhaps into some higher dimension. However as discussed by Carugno et. al. [34], the tunnelling analogy could become problematic for the Klein-Gordon-type equation we are working with, which in turn makes our interpretation problematic as well.

We also see that in all cases, we have avoided a singularity at zero size, since the universe never reaches the minimum scale factor value $\alpha = -\infty$. This confirms what was found pertubatively by Nguyen and Parwani [3], as reviewed in section 6.2. However here, unlike the pertubative study where we study the modified classical equations (6.25)-(6.27), we are not able to obtain α explicitly in terms of the time variable, t, since the Wheeler-DeWitt equation is independent of time, and as such it should be noted that the actual form of the dynamics and bounces we have seen thus far will depend on the functional form of ϕ in terms of t. In fact, in Nguyen and Parwani [3], we see bounces that occur for α as a function of t even when $\alpha = \phi$, which would just be a straight line without a bounce in an α versus ϕ plot. Nevertheless if we assume that the functional form of ϕ in the classical case, which is

$$\phi = \frac{1}{3} \ln t \tag{6.71}$$

does not differ significantly when we quantize and introduce nonlinearities, then we can say (since $\alpha = \ln a$) that a plot of the scale factor, a versus t would not differ qualitatively from a plot of α versus ϕ. This would be a safe assumption for small values of the nonlinear term, however, for larger nonlinearity the deviation from the form (6.71) may be significant, and the dynamics of a as a function of t may be very different from that of α as a function of ϕ. For example, if ϕ became a monotonically decreasing function of t, then the dynamics we found numerically in the last section would be happening backwards in time. Indeed, in the numerical analysis of the $\eta = 0.9$ case we saw dynamics that seemed to be the same as that found for lower values of η, but with spatial and temporal axes flipped.

Another interesting feature seen in the numerical results is the occurrence of what seem to be inflationary epochs, in some cases early in the evolution of the universe (see for example Figures 6.5, 6.37 and 6.47). However a proper inflationary epoch, as that postulated to have taken place early in our own universe's history, should involve the

scale factor of the universe increasing by a factor of at least 10^{26} within approximately 10^{-32} seconds. In order to accurately determine whether such an increase could take place, we would have to determine the exact functional form for ϕ in terms of t, which is not possible. Thus our result that the quantum nonlinearities can induce inflation in the early universe is only speculative.

It is unfortunate that we do not see evidence for accelerating expansion in the numerical results, a feature present in our own universe, except for an extremely short period in the case of $\eta = 0.9$ and $0.1 \leq \zeta \leq 0.4$ (Figure 6.52). It is possible that if we instead use a massless scalar field that is not free, but rather has a constant potential, as in a cosmological constant, we might see periods of accelerated expansion in the dynamics of the universe.

As previously mentioned, the plots for $\eta = 0.9$, for $\zeta \leq 0.4$, all seem to be identical to plots seen for $\eta = 0.5$ and $\eta = 0.1$, except that there is reversal of the orientation of the spatial and temporal axes. To further understand this, we can refer to the pertubative treatment reviewed earlier, which is valid for low values of ζ, since $\zeta = \eta L$. If we expand the nonlinear term $F(p)$, we find that the nonlinear Wheeler-DeWitt equation is

$$\left[\frac{\partial^2}{\partial\alpha^2} - \frac{\partial^2}{\partial\phi^2} + V_{eff}\right]\psi(\alpha,\phi) = 0, \tag{6.72}$$

where

$$V_{eff} = u\left[\sigma^2(\phi-\alpha)^2 - 3\right](\phi-\alpha), \tag{6.73}$$

$$u \equiv \frac{\eta(3-4\eta)L\sigma^4}{6}, \tag{6.74}$$

to leading order in L. We can see that as we increase η from 0 to 1, when $\eta > 3/4$, the effective potential changes sign. Thus we can postulate that for low ζ, when η becomes greater that $3/4$, the effect of the nonlinearity 'reverses', and we begin to

see the orientation reversal in the plots of α versus ϕ. This is indeed found to be true numerically, and $\eta = 3/4$ is a turning point for dynamics similar to that seen for $\eta = 0.1$ and $\eta = 0.5$ to become dynamics similar to that seen for $\eta = 0.9$ in the plots of α versus ϕ, as long as ζ is low.

In loop quantum cosmology (LQC), the Wheeler-DeWitt equation is also a difference equation not only in its spatial coordinate but also its temporal one [35], with evolution occurring in discrete steps. The discreteness in this theory arises due to geometry being quantized in nature in loop quantum gravity, and at small scales this discreteness is most apparent. Also, it is worth noting that Ashtekar et. al. [30] found, by solving the LQC Wheeler-DeWitt equation numerically for the FLRW-ϕ model, with the scalar field as intrinsic time, that the Big Bang is replaced by a bounce at early intrinsic times, which is similar to what we have found for various parameter values in our model.

It is interesting to note that the wavepackets we have seen in our work are examples of intrinsic localized modes, also known as discrete breathers. Intrinsic localized modes are modes prevented from dispersion due to the nonlinearity and discreteness inherent in a certain physical system. Examples of such systems are certain solid-state materials, optical waveguide arrays, photonic crystals and possibly Bose-Einstein condensates and biopolymers [36].

Chapter 7

Summary and Conclusion

We have studied two different, contrasting models in nonlinear quantum cosmology non-pertubatively, namely the spatially flat, empty FLRW universe with a scale factor-varying cosmological constant, and the spatially flat FLRW universe containing a free massless scalar field.

For the case of the scale factor-varying cosmological constant, $\Lambda(a)$, we find results similar to that found previously for a non-varying cosmological constant. With the variation of Λ controlled by a new parameter m, we find a maximum size, a_{max}, and a minimum size, a_{min}, to the universe by studying the probability density curves generated numerically, though both features are not present in all cases. The main new feature we see is that for $m = 1$, and low ζ, a_{max} is approximately infinity, and thus the expansion of the universe will be unbounded for these parameter values. The presence of a minimum size, a_{min}, also allows us to avoid the problems associated with a zero-size universe. We also find evidence for cyclic universes with bounces at a_{max} and a_{min} when we study the effective classical dynamics, due to real barriers occurring close to these points. For universes without an a_{min}, cyclic evolution is still possible as long as we have a real barrier close to a_{max}, since we find a real potential barrier appearing close to $a = 0$ as long as the parameter $\eta < 3/4$.

The non-pertubative study of the FLRW-ϕ universe enabled us to study its quan-

tum dynamics using the scalar field, ϕ as intrinsic time. We find cyclic-type behaviour for some values of the nonlinear parameters η and ζ, with bounces occurring at small and large size. However we do not see periodic cycles, nor do we see everlasting universes, since all universes we found were born and vanished at a certain point in intrinsic time. The singularity of curvature invariants was also avoided for all values of the parameters η and ζ, since in all cases the universe is born and vanishes at a finite, non-zero size, possibly tunnelling into existence at its birth, and tunnelling out of existence at its death. We also find novel behaviour, including possible evidence for an inflationary epoch in many of the universes, although in some cases the epochs do not occur near the beginning of the universe.

Both the models we have studied can only be considered toy models, and in order to mirror our universe more closely one would have to include matter in these models, perhaps in the form of a perfect fluid that mimics radiation at early times and dust at later times. The first step to a more realistic model would however be to combine both models studied here into a single one, with both a massless scalar field and a cosmological constant. A simple further generalisation would then be to allow the scalar field to be massive. In the long term it would be ideal to prove that both cosmic acceleration and an inflationary epoch can be produced by adding information theoretically motivated nonlinearities to the Wheeler-DeWitt equation. Another alternative generalisation would be to let the nonlinear parameters η and ζ vary with the scale factor, and this could also possibly produce inflation in the early universe and acceleration at late times. Finally, we hope to fix the values of both the nonlinear parameters by calculating observables which depend on them, and then comparing these with experimentally obtained data.

Bibliography

[1] D. L. Wiltshire, "An Introduction to Quantum Cosmology," in *Cosmology: the Physics of the Universe* (Robson, B. A., Visvanathan, N., & Woolcock, W. S., ed.), p. 473, 1996.

[2] R. R. Parwani, "An information-theoretic link between spacetime symmetries and quantum linearity," *Annals of Physics*, vol. 315, pp. 419–452, Feb. 2005.

[3] L.-H. Nguyen and R. R. Parwani, "Nonlinear quantum cosmology," *General Relativity and Gravitation*, vol. 41, pp. 2543–2560, Nov. 2009.

[4] R. R. Parwani and S. Nursaba Tarih, "Nonlinear Quantum Cosmology: A Non-perturbative Study," *ArXiv e-prints*, July 2011.

[5] B. S. DeWitt, "Quantum theory of gravity. i. the canonical theory," *Phys. Rev.*, vol. 160, pp. 1113–1148, Aug 1967.

[6] J. A. Wheeler, "Superspace and the Nature of Quantum Geometrodynamics," in *Quantum Cosmology* (L. Z. Fang and R. Ruffini, eds.), p. 27, 1987.

[7] C. W. Misner, "Quantum cosmology. i," *Phys. Rev.*, vol. 186, pp. 1319–1327, Oct 1969.

[8] J. B. Hartle and S. W. Hawking, "Wave function of the universe," *Phys. Rev. D*, vol. 28, pp. 2960–2975, Dec 1983.

[9] A. Vilenkin, "Creation of universes from nothing," *Physics Letters B*, vol. 117, no. 1–2, pp. 25 – 28, 1982.

[10] G. W. Gibbons and S. W. Hawking, "Action integrals and partition functions in quantum gravity," *Phys. Rev. D*, vol. 15, pp. 2752–2756, May 1977.

[11] S. W. Hawking, "Quantum gravity and path integrals," *Phys. Rev. D*, vol. 18, pp. 1747–1753, Sep 1978.

[12] D. Atkatz, "Quantum cosmology for pedestrians," *American Journal of Physics*, vol. 62, pp. 619–627, July 1994.

[13] A. Macías and H. Quevedo, "Time Paradox in Quantum Gravity," in *Quantum Gravity: Mathematical Models and Experimental Bounds* (B. Fauser, J. Tolksdorf, and E. Zeidler, eds.), p. 41, 2007.

[14] J. J. Halliwell. (Personal communication), 2012.

[15] K. V. Kuchař and M. P. Ryan, "Is minisuperspace quantization valid?: Taub in mixmaster," *Phys. Rev. D*, vol. 40, pp. 3982–3996, Dec 1989.

[16] N. Pinto-Neto and E. S. Santini, "The accelerated expansion of the Universe as a quantum cosmological effect," *Physics Letters A*, vol. 315, pp. 36–50, Aug. 2003.

[17] R. Colistete, Jr., J. C. Fabris, and N. Pinto-Neto, "Gaussian superpositions in scalar-tensor quantum cosmological models," *Phys. Rev. D*, vol. 62, p. 083507, Oct. 2000.

[18] V. A. De Lorenci, J. Martin, N. Pinto-Neto, and I. D. a. Soares, "Topology change in canonical quantum cosmology," *Phys. Rev. D*, vol. 56, pp. 3329–3340, Sep 1997.

[19] M. Gell-Mann and J. B. Hartle, "Quantum mechanics in the light of quantum cosmology," in *Complexity, Entropy and the Physics of Information* (W. Zurek, ed.), p. 23, 1990.

[20] G. Svetlichny, "Nonlinear quantum mechanics at the planck scale," *International Journal of Theoretical Physics*, vol. 44, pp. 2051–2058, 2005. 10.1007/s10773-005-8983-1.

[21] C. E. Shannon and W. Weaver, *The mathematical theory of communication.* 1949.

[22] M. Reginatto, "Derivation of the equations of nonrelativistic quantum mechanics using the principle of minimum fisher information," *Phys. Rev. A*, vol. 58, pp. 1775–1778, Sep 1998.

[23] R. R. Parwani, "Information and Cosmological Physics," *ArXiv e-prints*, Mar. 2012.

[24] D. Atkatz and H. Pagels, "Origin of the Universe as a quantum tunneling event," *Phys. Rev. D*, vol. 25, pp. 2065–2073, Apr. 1982.

[25] A. Vilenkin, "Creation of universes from nothing," *Physics Letters B*, vol. 117, pp. 25–28, Nov. 1982.

[26] R. Parwani and G. Tabia, "Universality in an information-theoretic motivated nonlinear Schrodinger equation," *Journal of Physics A : Mathematical and General*, vol. 40, pp. 5621–5635, May 2007.

[27] J. J. Halliwell, "Correlations in the wave function of the Universe," *Phys. Rev. D*, vol. 36, pp. 3626–3640, Dec. 1987.

[28] J. Halliwell, "Introductory lectures on quantum cosmology.," in *Proceedings of the Jerusalem Winter School on Quantum Cosmology and Baby Universes*, 1990.

[29] C. Kiefer, *Quantum gravity.* 2007.

[30] A. Ashtekar, T. Pawlowski, and P. Singh, "Quantum nature of the big bang: An analytical and numerical investigation," *Phys. Rev. D*, vol. 73, p. 124038, June 2006.

[31] P. Singh and K. Vandersloot, "Semiclassical states, effective dynamics, and classical emergence in loop quantum cosmology," *Phys. Rev. D*, vol. 72, p. 084004, Oct. 2005.

[32] P. Singh, K. Vandersloot, and G. V. Vereshchagin, "Nonsingular bouncing universes in loop quantum cosmology," *Phys. Rev. D*, vol. 74, p. 043510, Aug. 2006.

[33] C. Kiefer, "Wave packets in minisuperspace," *Phys. Rev. D*, vol. 38, pp. 1761–1772, Sept. 1988.

[34] E. Carugno, M. Litterio, F. Occhionero, and G. Pollifrone, "Inflation in multidimensional quantum cosmology," *Phys. Rev. D*, vol. 53, pp. 6863–6874, Jun 1996.

[35] M. Bojowald, "Loop quantum cosmology: Iv. discrete time evolution," *Classical and Quantum Gravity*, vol. 18, p. 1071, 2001.

[36] D. Campbell, S. Flach, and Y. Kivshar, "Localizing energy through nonlinearity and discreteness," *Physics Today*, vol. 57, no. 1, pp. 43–49, 2004.

Appendix A

Derivation of the difference equation for a FLRW-Λ universe

The nonlinear Wheeler-DeWitt equation for a spatially flat universe with a cosmological constant is,

$$\left[-\frac{\partial^2}{\partial a^2} - \frac{a^4}{a_0^2} + F(p)\right]\psi(a) = 0. \tag{A.1}$$

Making the Madelung transformation,

$$\psi = \sqrt{p}e^{iS}. \tag{A.2}$$

we find that

$$\frac{\partial\psi}{\partial a} = \frac{\partial\sqrt{p}}{\partial a}e^{iS} + i\sqrt{p}e^{iS}\frac{\partial S}{\partial a}, \tag{A.3}$$

and

$$\frac{\partial^2\psi}{\partial a^2} = \frac{\partial^2\sqrt{p}}{\partial a^2}e^{iS} + i\frac{\partial\sqrt{p}}{\partial a}e^{iS}\frac{\partial S}{\partial a} + i\frac{\partial\sqrt{p}}{\partial a}e^{iS}\frac{\partial S}{\partial a} - \sqrt{p}e^{iS}\left(\frac{\partial S}{\partial a}\right)^2 + i\sqrt{p}e^{iS}\frac{\partial^2 S}{\partial a^2}. \tag{A.4}$$

Replacing equation (A.4) into the Wheeler-DeWitt equation (A.1), gives us an equation with a real and an imaginary part. The imaginary part is

$$2\frac{\partial\sqrt{p}}{\partial a}\frac{\partial S}{\partial a}+\sqrt{p}\frac{\partial^2 S}{\partial a^2}=0, \tag{A.5}$$

or

$$\frac{1}{\sqrt{p}}\frac{\partial}{\partial a}\left(\frac{\partial S}{\partial a}(\sqrt{p})^2\right)=0. \tag{A.6}$$

The real part is

$$-\frac{\partial^2\sqrt{p}}{\partial a^2}+\sqrt{p}\left(\frac{\partial S}{\partial a}\right)^2-\frac{a^4}{a_0^2}\sqrt{p}+F(p)\sqrt{p}=0. \tag{A.7}$$

Since $F(p)=Q_{NL}-Q$ and

$$Q=-\frac{1}{\sqrt{p}}\frac{\partial^2\sqrt{p}}{\partial a^2}, \tag{A.8}$$

equation (A.7) then becomes

$$\left(\frac{\partial S}{\partial a}\right)^2-\frac{a^4}{a_0^2}+Q_{NL}=0. \tag{A.9}$$

Also (A.6) is equivalent to

$$\frac{\partial}{\partial a}\left(p\frac{\partial S}{\partial a}\right)=0, \tag{A.10}$$

which implies

$$p\frac{\partial S}{\partial a}=\sigma, \tag{A.11}$$

where σ is the conserved probability current. Using equation (A.11) in equation (A.9), we transform the latter into a form devoid of differentials,

$$\left(\frac{\sigma}{p}\right)^2=\frac{a^4}{a_0^2}-Q_{NL} \tag{A.12}$$

or

$$\left(\frac{\sigma}{p}\right)^2 = \frac{a^4}{a_0^2} - \frac{1}{2\zeta^2\eta^2}\left[\ln\left(\frac{p}{(1-\eta)p+\eta p_+}\right) + \frac{\eta p_+}{(1-\eta)p+\eta p_+} - \frac{\eta p_-}{(1-\eta)p_- + \eta p}\right] \tag{A.13}$$

which is the difference equation for a spatially flat FLRW universe with a cosmological constant.

Appendix B

Derivation of the difference equation for a FLRW-ϕ universe

The nonlinear Wheeler-DeWitt equation for a spatially flat universe with a free massless scalar field is,

$$\left[\frac{\partial^2}{\partial\alpha^2} - \frac{\partial^2}{\partial\phi^2} - F_\alpha(p) + F_\phi(p)\right]\psi(\alpha,\phi) = 0. \tag{B.1}$$

Writing the wavefunction in terms of its amplitude and phase,

$$\psi(\alpha,\phi) = A(\alpha,\phi)e^{iS(\alpha,\phi)}, \tag{B.2}$$

we see that

$$\frac{\partial\psi}{\partial\phi} = \frac{\partial A}{\partial\phi}e^{iS} + iAe^{iS}\frac{\partial S}{\partial\phi}, \tag{B.3}$$

and

$$\frac{\partial^2\psi}{\partial\phi^2} = \frac{\partial^2 A}{\partial\phi^2}e^{iS} + i\frac{\partial A}{\partial\phi}e^{iS}\frac{\partial S}{\partial\phi} + i\frac{\partial A}{\partial\phi}e^{iS}\frac{\partial S}{\partial\phi} - Ae^{iS}\left(\frac{\partial S}{\partial\phi}\right)^2 + iAe^{iS}\frac{\partial^2 S}{\partial\phi^2}. \tag{B.4}$$

Likewise,

$$\frac{\partial^2\psi}{\partial\alpha^2} = \frac{\partial^2 A}{\partial\alpha^2}e^{iS} + i\frac{\partial A}{\partial\alpha}e^{iS}\frac{\partial S}{\partial\alpha} + i\frac{\partial A}{\partial\alpha}e^{iS}\frac{\partial S}{\partial\alpha} - Ae^{iS}\left(\frac{\partial S}{\partial\alpha}\right)^2 + iAe^{iS}\frac{\partial^2 S}{\partial\alpha^2}. \tag{B.5}$$

Replacing equations (B.4) and (B.5) into equation (B.1) gives us an equation with two parts, one real and one imaginary. The imaginary part is

$$2\frac{\partial A}{\partial\phi}\frac{\partial S}{\partial\phi} + A\frac{\partial^2 S}{\partial\phi^2} - 2\frac{\partial A}{\partial\alpha}\frac{\partial S}{\partial\alpha} + A\frac{\partial^2 S}{\partial\alpha^2} = 0, \tag{B.6}$$

or

$$\frac{\partial}{\partial\phi}\left(A^2\frac{\partial S}{\partial\phi}\right) - \frac{\partial}{\partial\alpha}\left(A^2\frac{\partial S}{\partial\alpha}\right) = 0. \tag{B.7}$$

We do not need this equation in deriving the difference equation. It is however required to derive constraint (6.45).The real part of the equation is,

$$\frac{\partial^2 A}{\partial\phi^2} - A\left(\frac{\partial S}{\partial\phi}\right)^2 - F_\phi(p)A - \frac{\partial^2 A}{\partial\alpha^2} + A\left(\frac{\partial S}{\partial\alpha}\right)^2 + F_\alpha(p)A = 0. \tag{B.8}$$

Since $F_\phi(p) = Q^\phi_{NL} - Q^\phi$ and $F_\alpha(p) = Q^\alpha_{NL} - Q^\alpha$; with

$$Q^\phi = -\frac{1}{A}\frac{\partial^2 A}{\partial\phi^2} \tag{B.9}$$

and

$$Q^\alpha = -\frac{1}{A}\frac{\partial^2 A}{\partial\alpha^2} \tag{B.10}$$

equation (B.8) then becomes

$$-\left(\frac{\partial S}{\partial\phi}\right)^2 + \left(\frac{\partial S}{\partial\alpha}\right)^2 - Q^\alpha_{NL} + Q^\phi_{NL} = 0. \tag{B.11}$$

If we now assume that

$$S(\alpha,\phi) = a\phi + b\alpha, \tag{B.12}$$

where a and b are constants, we obtain

$$-a^2 + b^2 - Q^{\alpha}_{NL} + Q^{\phi}_{NL} = 0, \tag{B.13}$$

or,

$$-a^2 + b^2 - \frac{1}{2\zeta_\alpha^2\eta_\alpha^2}\left[\ln\left(\frac{p}{(1-\eta_\alpha)p + \eta_\alpha p_+}\right) + \frac{\eta_\alpha p_+}{(1-\eta_\alpha)p + \eta_\alpha p_+} - \frac{\eta_\alpha p_-}{(1-\eta_\alpha)p_- + \eta_\alpha p}\right] + \frac{1}{2\zeta_\phi^2\eta_\phi^2}\left[\ln\left(\frac{p}{(1-\eta_\phi)p + \eta_\phi p^+}\right) + \frac{\eta_\phi p^+}{(1-\eta_\phi)p + \eta_\phi p^+} - \frac{\eta_\phi p^-}{(1-\eta_\phi)p^- + \eta_\phi p}\right] = 0, \tag{B.14}$$

which is the difference equation for a spatially FLRW flat universe with a free massless scalar field.